12-13-2017 2:00 PM

Thermo-Hydro-Mechanical analysis of evaporation from unsaturated soils

Seyed Morteza Mousavi, *The University of Western Ontario*

Supervisor: Ernest K. Yanful, *The University of Western Ontario*
Joint Supervisor: M. H. El Naggar, *The University of Western Ontario*
A thesis submitted in partial fulfillment of the requirements for the Doctor of Philosophy degree in Civil and Environmental Engineering

ABSTRACT

Estimating evaporation from unsaturated soil is important for many applications including agriculture, climate, hydrology, water resources, saturated and unsaturated groundwater flow, slope stability, and soil covers. As an example, the long term performance of soil covers, which are widely used in mining and landfill applications to protect the environment, strongly depends on evaporation from their surfaces.

Evaporation depends on both moisture flow within an unsaturated soil mass, which is generally coupled with heat flow, and void ratio and hydraulic and air conductivities, which are in turn affected by stress and strain and resulting soil settlement. This makes thermo-hydro-mechanical (THM) analysis of evaporation necessary. Evaporation also depends on environmental parameters, including air temperature, humidity, net radiation and wind speed. Therefore, considering atmospheric coupling in predicting evaporation is also necessary.

The stress-strain behavior of the soil affects its settlement, which changes void ratio and porosity, and in turn permeability of the soil. This can alter the evaporation characteristics significantly and should be accounted for in any reliable evaluation of the actual evaporation and the performance of soil covers. However, existing soil-atmospheric models such as SOILCOVER (1994) and VADOSE/W (2002), which attempt to represent the soil-atmosphere continuum by linking the subsurface and the atmosphere, do not couple the equilibrium equation. Therefore, they can estimate evaporation but cannot estimate stress, strain and soil settlement. In fact, they perform thermo-hydraulic (TH) analysis.

On the other hand, thermo-hydro-mechanical models such as 2D finite element program θ-Stock (Gatmiri et al., 1999) can perform THM analysis of unsaturated soil by coupling equilibrium equation with moisture and heat flow equations, but only work under soil surface, and do not have

the capability to consider the environment and to incorporate atmospheric parameters. Therefore, they cannot estimate evaporation.

The purpose of this study is to bring together the advantages of the above-mentioned programs by using an approach including both ideas and employing a formulation coupling THM analysis with soil-atmosphere modeling. Therefore, the resulting program EVAP1 numerically estimates evaporation from unsaturated soil using THM analysis and at the same time estimates stress, strain and soil settlement. In other words, the program can estimate evaporation considering soil settlement, which occurs in real world.

The program EVAP1 was verified with published experimental and numerical studies on evaporation, including Wilson (1990) and Yang & Yanful (2002). Then, it was used to compare evaporation with and without considering soil settlement. The results showed that soil settlement alters the evaporation characteristics significantly and should be accounted for in any reliable evaluation of the evaporation from unsaturated soil. Neglecting settlement causes an overestimation of evaporation.

A parametric study was also performed to evaluate the effects of environmental parameters on evaporation, in order to identify the parameter that affects evaporation the most. It was found that the most important parameters, in order, are humidity, net radiation, temperature and wind speed. The sensitivity of evaporation to these parameters was also evaluated, and the trend of the change in evaporation due to the change in each of the parameters was noted. The results showed that the effects of these parameters on evaporation are mostly nonlinear.

Keywords: unsaturated soil, THM, evaporation, environment, geotechnics, θ-Stock, numerical, finite element

Copyright

ACKNOWLEDGEMENTS

First of all, I should thank Great God for His very kind help in enabling me to finish this research. Everything belongs to Him and comes from Him and I am totally in debt of Him.

Words can only fail in expressing my love and gratitude for my late parents who supported and encouraged me to finish this study, till the last minute of their lives. I am in debt of them for all that I have. I also really appreciate my dear brothers, sisters, wife and son for their great support.

I acknowledge with sincerity the contributions of many people who have helped me with this research. I am grateful to all my teachers, past and present. In particular, l owe a debt of gratitude to my great supervisors Professor Ernest K. Yanful and Professor M. Hesham El Naggar for supporting me kindly and continuously. I really appreciate their knowledge, experience, patience, and consideration. They were by my side whenever I faced a problem and needed them.

I also wish to thank my great advisor Professor B. Gatmiri who sincerely and generously granted me the results of over 20 years of his research. He helped me with my first Ph. D. too, that I did under supervision of Professor Shamsai. In fact, Professor Yanful and Professor Gatmiri opened windows in front of my eyes to the interesting worlds of environmental science and unsaturated soil, respectively.

Also, my sincere appreciation goes to Professor V. Khonsari and my other great advisor Professor A. Pak for their sincere and great support by all means and helping me every step of the way.

I also appreciate Western University and K. N. Toosi University of Technology for their long-term support during the lengthy period of doing this study. Meanwhile sincere thanks go to my colleagues and friends at both universities.

To:

My dear late parents,

who wished (and wish) for my success with this research.

PUBLICATIONS

1. Ernest K. Yanful, S. Morteza Mousavi, Lin-Pei De Souza. **"A numerical study of soil cover performance"**, Journal of Environmental Management, 81 (2006) pp. 72–92.

2. Ernest K. Yanful, S. Morteza Mousavi, and Mingdi Yang. **"Modeling and measurement of evaporation in moisture retaining soil covers"**, Advances in Environmental research, 7 (2003) pp.783-801.

3. Ernest K. Yanful, and S. Morteza Mousavi, **"Estimating falling rate evaporation from finite soil columns"**, The Science of the Total Environment, 313 (2003) pp.141-152.

4. E K Yanful, and S. M Mousavi, **"Quantifying Evaporation From Soils Using Experimental and Mathematical Methods",** Proceedings of 6th International Conference ICARD, Australia, 2003, 1185-1193.

5. S. Morteza Mousavi, Abolfazl Shamsai, M. Hesham El Naggar, and Mashaallah Khamehchian. **"A GPS-based monitoring program of land subsidence due to groundwater withdrawal in Iran",** Canadian Journal of Civil Engineering, 28 (2001) pp.452-464.

6. S. Morteza Mousavi, Behrouz Gatmiri, Ali Pak, M. Hesham El Naggar, "Analysis of land subsidence due to groundwater withdrawal considering unsaturated layers", **Proceedings of 53rd Canadian Geotechnical Conference, Montreal, Quebec, Oct. 15-18, 2000, Vol. 2, 1153-1160.**

7. S. Morteza Mousavi, M Hesham El Naggar, and Abolfazl Shamsai, **"Application of GPS**

to evaluate land subsidence in Iran", Proceedings of The Sixth International Symposium on Land Subsidence", Ravenna, Italy, September 2000, pp. 107-112.

8. S. Morteza Mousavi, M Hesham El Naggar, Abolfazl Shamsai, **"Evaluation of land subsidence using GPS",** 28th Annual Conference of Canadian Society for Civil Engineering, London, Canada, June 2000, pp. 440-447.

9. S. Morteza Mousavi, Abolfazl Shamsai, Mashalah Khamehchian, **"Land Subsidence in Rafsanjan Plain, Iran",** Proceedings of Eighth International Congress, International Association for Engineering Geology and Environment, Vancouver, Canada, 1999, pp. 2395-2400.

10. S. Morteza Mousavi, Abolfazl Shamsai, Mashalah Khamehchian **"Land Subsidence Due to Ground Water Withdrawal in Rafsanjan, Iran",** IWRE Symposium on Groundwater, The University of Memphis, USA, 1998, (Accepted for presentation).

TABLE OF CONTENTS PAGE

LIST OF FIGURES PAGE

LIST OF TABLES PAGE

NOTATIONS

$\alpha =$ scaling factor to water pressure

$\alpha_a =$ a constant at the equation for hydraulic conductivity of soil relative to air

$\alpha_w =$ a constant at the equation for hydraulic conductivity of soil relative to water

$\alpha_{ij} =$ weighting factor at the sampling point (r_i, s_j)

$\beta =$ scaling factor to air pressure

$\nu =$ Poisson's ratio

$\theta =$ indicator for the type of interpolation

(for forward interpolation or fully explicit $\theta = 0$,

for linear interpolation or Crank-Nicholson $\theta = 1/2$,

and for backward interpolation or fully implicit, $\theta = 1$)

$\phi =$ internal friction angle degree

$\mu_a =$ air viscosity at the equation of hydraulic conductivity of soil relative to air

$\gamma_a =$ specific weight of air

$\gamma_s =$ specific weight of soil

$\gamma_w =$ specific weight of water

$\gamma_{xy} =$ shear strain at x-y plane

$\delta_{ij} =$ Kronecker delta

σ = total stress

$\sigma - u_a$ = mean net normal stress

σ_e = swelling pressure at the equation of bulk modulus

σ_1 = total axial normal stress (major principal stress)

σ_3 = total confining pressure (minor principal stress)

$(\sigma_1 - \sigma_3)_f$ = deviator stress at failure condition

$(\sigma_1 - \sigma_3)_u$ = ultimate deviator stress

σ' = effective normal stress

ε_{xx} = strain tensor at x direction

ε_{yy} = strain tensor at y direction

ε_{zz} = strain tensor at z direction

σ_{xx} = stress tensor at x direction

σ_{yy} = stress tensor at y direction

σ_{zz} = stress tensor at z direction

τ_{xy} = shear stress at x-y plane

ρ_a = air density

ρ_w = water density

$\Delta h =$ element height

$\Delta t =$ time step

$a =$ a constant at the equation of bulk modulus

$a_1 =$ a constant at the equation of hydraulic conductivity of soil relative to water

$a_e =$ coefficient "a" at the equation of state surface of void ratio (e)

$a_s =$ coefficient "a" at the equation of state surface of saturation degree (s_r)

$B_{ij} =$ a member of strain-displacement matrix (B-matrix) at the sampling point (r_i, s_j)

$b =$ a constant at the equation of bulk modulus

$b_i =$ body force at i direction

$b_e =$ coefficient "b" at the equation of state surface of void ratio (e)

$b_s =$ coefficient "b" at the equation of state surface of saturation degree (s_r)

C_{ijkl} = nonlinear elasticity matrix

$c =$ cohesion coefficient

$c_e =$ coefficient "c" at the equation of state surface of void ratio (e)

$comp =$ compressibility of water

$c_h =$ coefficient of consolidation (horizontal drainage)

$c_v =$ coefficient of consolidation (vertical drainage)

$D =$ stress-strain matrix (material matrix)

D_1 = a constant at the equation of hydraulic conductivity of soil relative to air

d_e = coefficient "d" at the equation of state surface of void ratio (e)

d_s = coefficient "d" at the equation of state surface of saturation degree (s_r)

E = elastic modulus

E_1 = a constant at the equation of hydraulic conductivity of soil relative to air

E_e = initial elastic modulus

E_s = representative of the effect of suction on the elastic modulus

E_t = tangent elastic modulus

e = void ratio

e_0 = void ratio with a suction and stress equal to zero

e_f = minimum elastic coefficient

F_{ij} = suction modulus matrix

H = Henry constant

H' = layer thickness

J_{ij} = Jacobian at the sampling point (r_i, s_j)

K = stiffness matrix of element

K_0 = bulk modulus

K_0' = coefficient of earth pressure at rest

$K_1 =$ dimensionless parameter at the equation of initial elastic modulus

$\underline{\underline{K}}_a =$ hydraulic conductivity of soil relative to air

$K_{a\max} =$ maximum hydraulic conductivity of soil relative to air

$K_b =$ number of volume module (a constant at the equation of bulk modulus)

$K_l =$ number of elastic coefficient in loading stage

$K_u =$ number of elastic coefficient in unloading stage

$\underline{\underline{K}}_w =$ hydraulic conductivity of soil relative to water

$K_{w\max} =$ maximum hydraulic conductivity of soil relative to water

$K_{wx} =$ hydraulic conductivity of soil relative to water at horizontal direction

$K_{wz} =$ hydraulic conductivity of soil relative to water at vertical direction

$\frac{K_{wx}}{K_{wz}} =$ relation of horizontal hydraulic conductivity to vertical hydraulic conductivity

$m =$ a constant at the equation of bulk modulus

$m_1 =$ a constant at the equation of E_s

$(msuc)_c =$ constant of cohesion-suction ($m2$)

$(msuc)_e =$ constant of elastic coefficient-suction ($m1$)

$(msuc)_{p1} = \phi_\infty$, minimum ϕ at $S = S_\infty$

$(msuc)_{p2} =$ S_{∞}, maximum suction

$m_v =$ coefficient of volume compressibility

$N =$ shape function

$n =$ porosity

$n_1 =$ dimensionless parameter at the equation of initial elastic modulus

$P_{atm} =$ atmospheric pressure

$R_f =$ rupture relation

$S =$ suction at the equation of bulk modulus

$S_{ini} =$ initial saturation degree

$S_r =$ degree of saturation

$S_{ru} =$ residual degree of saturation

$t_{ij} =$ thickness of the element at the sampling point (r_i, s_j)

$(ten)_{st} =$ tensile strength

$u_a =$ pore-air pressure

$u_w =$ pore-water pressure

$u_a - u_w =$ matric suction

$\underline{v}_a =$ velocity of air

$\underline{v}_w =$ velocity of water

CHAPTER 1

INTORDUCTION

1.1 BACKGROUND

The critical role of unsaturated zone near the soil surface, during groundwater recharge, surface runoff and evapotranspiration, was the center of attention in earlier investigations. However, more recently, major attention has been focused on geothermal energy extraction, contaminant transport analysis, safe disposal of high-level radioactive waste, and the design of engineered clay barriers.

Engineered clay barriers have been used in many geotechnical projects including filling and sealing of underground nuclear waste repositories and other waste containment systems, such as soil covers. Engineered clay barriers are used in the mining industry as soil cover for mine waste that includes sulfide minerals, common components of ores. These minerals can react with oxygen and water to produce sulfuric acid, which can dissolve heavy metals in the mine waste and produce acid rock drainage (ARD), a solution potentially toxic to humans, animals and plants (Yanful et al., 2006).

Because of the important role of moisture and heat transport in soil cover performance, and since the soil is continuously under the effects of temperature changes in its natural environment, a great deal of attention has been paid to the phenomenon of moisture transport due to thermal gradient, and evaporation.

Estimating evaporation is important in many fields including geo-environmental engineering. For example, evaporation has a definitive role in the performance of soil covers

widely used for environmental protection. The ability to estimate evaporation from different soils is useful, especially during the initial stages of soil cover design in order to ensure its satisfactory long-term performance (Yanful and Mousavi, 2003). To achieve a realistic result, it is necessary to consider any real change in soil including the settlement at the soil surface.

Soil settlement decreases void ratio and porosity, which in turn decreases hydraulic conductivity. Consequently, evaporation from the soil surface decreases. Therefore, there is an absolute need to consider the deformation of unsaturated soil to properly evaluate the coupling effects of moisture, heat, air, and soil deformation, which can be achieved by performing a thermo-hydro-mechanical (THM) analysis.

THM analysis is required to analyze the subsurface flow system, which is generally coupled with heat flow, and is also coupled to the atmosphere through the evaporation/infiltration process at the soil surface. In general, this process is dominated by three important factors. Firstly, atmospheric conditions, which control the supply of water and in turn demand for water. Secondly, permeability and storage characteristics of the soil, which govern the ability of the surface to transmit water. Thirdly, the vegetation which determines the consumption of water through root uptake (Wilson, 1990).

To deal with this process, in the most general case, solving the coupled nonlinear governing partial differential equations of heat and mass transfer at the soil surface is required. This is a complex task and analytical solutions are possible only for the very simple cases, and numerical methods must be used. Among the numerical approaches, the Finite Element method is most popular because of its ability to accurately simulate complex phenomena encountered in a variety of engineering problems. It can easily handle irregular geometry and varying properties and different types of boundary conditions.

A number of attempts have been made to solve the coupled heat and mass transfer equations using finite element techniques. However, there exists a need for a numerical model that calculates evaporation using THM analysis. This study entitled as "Thermo-hydro-mechanical analysis of evaporation from unsaturated soils" is focused on this issue.

1.2 OBJECTIVES

The main objective of this study is to develop a THM methodology for calculating evaporation from unsaturated soil. The 2D finite element program, θ-Stock, uses THM analysis in unsaturated soil, but works only within the soil. The developed methodology couples a soil-atmosphere model with THM analysis to account for soil equilibrium along with coupling atmospheric phenomena with the equations of water, vapor, air and heat flows. The developed computer program, EVAP1, can estimate evaporation from unsaturated soil using THM methodology.

The main contribution of this study is to estimate actual evaporation from engineered geotechnical structures such as soil covers, which are used to protect environment, considering soil settlement, and clarifying the importance of this consideration in estimating the correct amount of evaporation. A more accurate estimation of evaporation is very important in long-term performance of environmental geotechnical structures such as soil covers, and in many other fields including – but not limited to- agriculture, water resources management, hydrology, saturated and unsaturated groundwater flow, and slope stability.

1.3 ORGANIZATION OF THE THESIS

Chapter 2 includes an extensive literature review covering both thermo-hydro-mechanical analysis, and atmospheric coupling.

Chapter 3 presents the theory used in this study, including the development of the relevant

equations for the coupled equilibrium, atmospheric, water flow, vapor flow, air flow and heat flow processes. It describes the details of the numerical model, including a flowchart for the model, and a brief explanation of the functioning of its modules.

Chapter 4 presents the validation of the developed model through a comparison of its predictions with measured evaporation of some well documented studies available in the literature. The influence of considering the effect of soil settlement on evaporation is investigated next. Also, the results of a parametric study and a sensitivity analysis considering all main environmental parameters affecting evaporation are presented in this chapter.

Chapter 5 includes summary, conclusions, and recommendations for future research.

CHAPTER 2

LITERATURE REVIEW

2.1 INTRODUCTION

The first three sections of literature review are devoted to evaporation, unsaturated soil, and thermo-hydro-mechanical (THM) analysis. The evaporation section discusses the importance and mechanism of evaporation and presents methods used for its estimation as well as mutual effects of evaporation and soil property and atmospheric parameters, and their modeling. The section of unsaturated soil explains the isothermal and non-isothermal behavior, deformation, evaporation from unsaturated soil, and their modeling. The THM section highlights the importance of the coupled THM phenomenon, and the analysis of evaporation from unsaturated soil using this approach, and its modeling. Finally, the application of THM for estimating evaporation from soil covers is addressed. The literature review in each section is presented in a chronological order.

2.2 EVAPORATION

2.2.1 The importance of evaporation and need for continued research

Prediction of the flux boundary condition with respect to water flow across the soil-atmosphere boundary is an important consideration in many problems in geotechnical engineering. The problems include long term performance of soil covers, saturated-unsaturated groundwater flow, and the prediction of heave for shallow foundations built on expansive soils (Wilson et al., 1994).

Blight (2002) emphasized that from the environmental and geotechnical viewpoints, it is often important to determine the rate of evaporation of water from a soil surface, a waste deposit

or a soil-covered waste deposit. This is particularly important in arid or semi-arid climates with shortage of water, or where seasonal cycles of precipitation and evaporation can lead to damage to shallow foundations. Similarly, Kebede et al. (2006) stated that evaporation is a crucial factor between land and the atmosphere, and in semi-arid regions it assumes even greater importance.

Evaporation is a major component of the hydrologic cycle. The estimation of evaporation is widely used in hydrologic and irrigation engineering applications. The accurate estimation of evaporation is required for many studies, such as hydrologic water balance, water resources planning and management, and irrigation scheduling (Valiantzas, 2006).

Bare soil evaporation has been found to be very difficult to estimate in modeling studies (Seager et al., 2007). In spite of decades of research, which have improved our understanding, many knowledge gaps still exist in the current science on how the soil water in the shallow subsurface close to the land surface interacts with the air in the atmosphere. Understanding this interaction is paramount to our understanding of many emerging problems, including climate change, water and food supply, the accurate detection of buried objects such as landmines (Das et al., 2001), and the remediation of contaminated soil in the shallow subsurface (Weaver and Tillman, 2005).

More than half of the land surface on the globe is arid or semiarid. Understanding the water cycle on the basis of heat and water exchanges between air and the soil surface is necessary. In bare soils evaporation at the soil atmosphere interface is the dominant process for water vapour exchange. Evaporation process has a large impact on the heat and water exchange between the atmosphere and land surface and is necessary to accurately predict it. (Katata et al., 2007).

Soil water evaporation is a key process for water exchange between soil and atmosphere. Bare soil evaporation and plant-soil-atmospheric interactions are important components of the water balance. Drying and evaporation processes are also of interest for many engineering and industrial applications and numerous construction activities (Lehmann et al., 2008).

Furthermore, evaporation is a key process in the hydrologic cycle. It affects mass exchange between land and atmosphere and the energy balance of terrestrial surfaces. Evaporation involves simultaneous heat and mass transfer, phase changes, and interfacial liquid and vapor transfer at pore scales. This results in a complex phenomenon that is difficult to predict (Shokri et al., 2010).

Despite a long history of application to bare soils drying by evaporation, the implications of the coupled heat and moisture transfer theory of Philip and de Vries (1957) for temperature and moisture regimes near the soil surface have not been fully described (Novak, 2010)

Evaporation from porous media is a highly dynamic process. It may vary considerably in space and time reflecting the interplay between internal flow processes (capillary liquid flow to vaporization surface and vapour diffusion) and atmospheric conditions (air temperature, relative humidity, energy input, and wind speed). Prediction of drying rates from porous media has remained a challenge due to complex integrations between ambient conditions and the properties of porous media (Shahraeeni et al., 2012).

Vapor diffusion in porous media is of interest for many natural and engineering applications including hydrology, geothermal reservoir performance, thermally enhanced oil recovery, and drying of textiles, grains, and food. The diversity of disciplines and applications has led to confusion in formulation and treatment of coupled heat and mass transport through porous media. Recent theoretical and experimental studies of vapor transport through porous media question the

existence and significance of the mechanisms of vapor transport enhancement postulated by Philip and de Vries (Shahraeeni et al., 2012).

Accurate estimates of water losses by evaporation from shallow water tables are important for hydrological, agricultural, and climatic purposes (Assouline et al., 2013). The complexity of soil evaporation, depending on the atmospheric conditions, emphasizes the importance of its quantification under potential changes in ambient air temperature and relative humidity (Neriah et al., 2014).

Assessment of evaporation from soil surface is critical for design of soil cover systems for hazardous waste sites (Teng et al., 2014) and forecasting its long-term performance (Wilson, 1994; Yanful and Mousavi, 2003). In addition, it is critical for many other engineering, environmental and hydrological applications such as hydrological modeling (Shokri and Or, 2011). Also, understanding the dynamics of soil water content during evaporation is required for the management of soil water practices (Blight, 1997; Fredlund et al., 2011).

Evaporation from bare sandy soils is the core component of the hydrologic cycle in arid environments, where vertical water movement dominates. Although extensive measurement and modeling studies have been conducted and reported in existing literature, the physics of drying soil and evaporation from bare soil is still a challenging topic and there are still significant remaining issues (Wang, 2015). Trautz (2016) stated that “bare soil evaporation is one of the governing processes responsible for controlling heat and water exchanges between the land and lower part of the atmospheric boundary layer with direct implications in meteorology and climatology, waste isolation and storage, vadose zone remediation, and water management. Despite its obvious importance to a wide range of scientific and industry disciplines, this process

remains poorly understood. This is due in part to evaporation being a complex multiphase phenomenon that must be described and understood in terms of a variety of processes that occur simultaneously at different scales".

2.2.2 The mechanism of evaporation

The flow of moisture between soil and atmosphere is a complex process in which three factors dominate and function as a closely coupled system, not as independent variables. The first factor is the supply of water at soil surface, and demand for water imposed at the soil surface by atmospheric conditions, which are air humidity, net radiation, wind speed, and air temperature. The second factor is the ability of the soil to transmit water, and the associated water regime. Soil moisture flow is controlled by both hydraulic conductivity and storage characteristics of the soil. The final factor involves the influence of vegetation. The type and density of vegetation influences evaporation through the consumption of water (Wilson, 1990).

The rate of evaporation is influenced by both atmospheric demand, and soil pore space and transport properties. This complexity leads to highly dynamic interactions between media properties, transport processes and boundary conditions, which in turn, results in a broad range of evaporation behaviors as discussed by Prat (2002).

Evaporation is a complex dynamic process affected by many environmental factors including air temperature, relative humidity, water vapor pressure deficit, solar irradiance, wind speed, and soil moisture (Liu et al., 2004; Xu et al., 2006; Wang and Liang, 2008; Wang et al., 2010a, 2010b, Su et al., 2015).

Evaporation from soil surfaces involves mass and energy transfer including phase change, vapor diffusion, and liquid flow resulting in complex displacement patterns, which causes the drying rate to vary with time (Sakai et al., 2011).

All of the factors affecting the rate of soil evaporation are strongly coupled, which leads to highly dynamic interactions between the atmosphere and soil resulting in dynamic evaporative behaviors (Sakai et al., 2011). However, the atmospheric coupling to the soil at the land-atmospheric interface is rarely considered in most current models or practical application, due to complexity of the problem, and the scarcity of field or laboratory data (Davarzani et al., 2014).

With supporting experimental evidence from three separate field studies of daily mean evaporation from bare soil with vastly different physical characteristics, it was shown that evaporation process can be described as isothermal linear diffusion in a finite depth domain. It appears that in many situations the soil layer which contributes to evaporation is shallow with a thickness of only a few tens of centimeters (Brutsaert, 2013).

Water loss through evaporation is one of the major components of the hydrological cycle affecting water resources availability. Most precipitation is lost in the form of evaporation and evapotranspiration with the percentage varying globally in different regions (Abtew & Melesse, 2013).

The heat that is required to evaporate water from the surface of the earth is provided by the sun in radiation form. As Figure 2.1 shows a portion of sun radiation is adsorbed by the atmosphere and converted into heat. Two other portions are reflected back into space, and reflected towards the earth surface. Almost 48% of the incoming solar radiation reaches the ground surface. A portion of this energy is reflected back to the sky through the albedo effect; a portion is absorbed

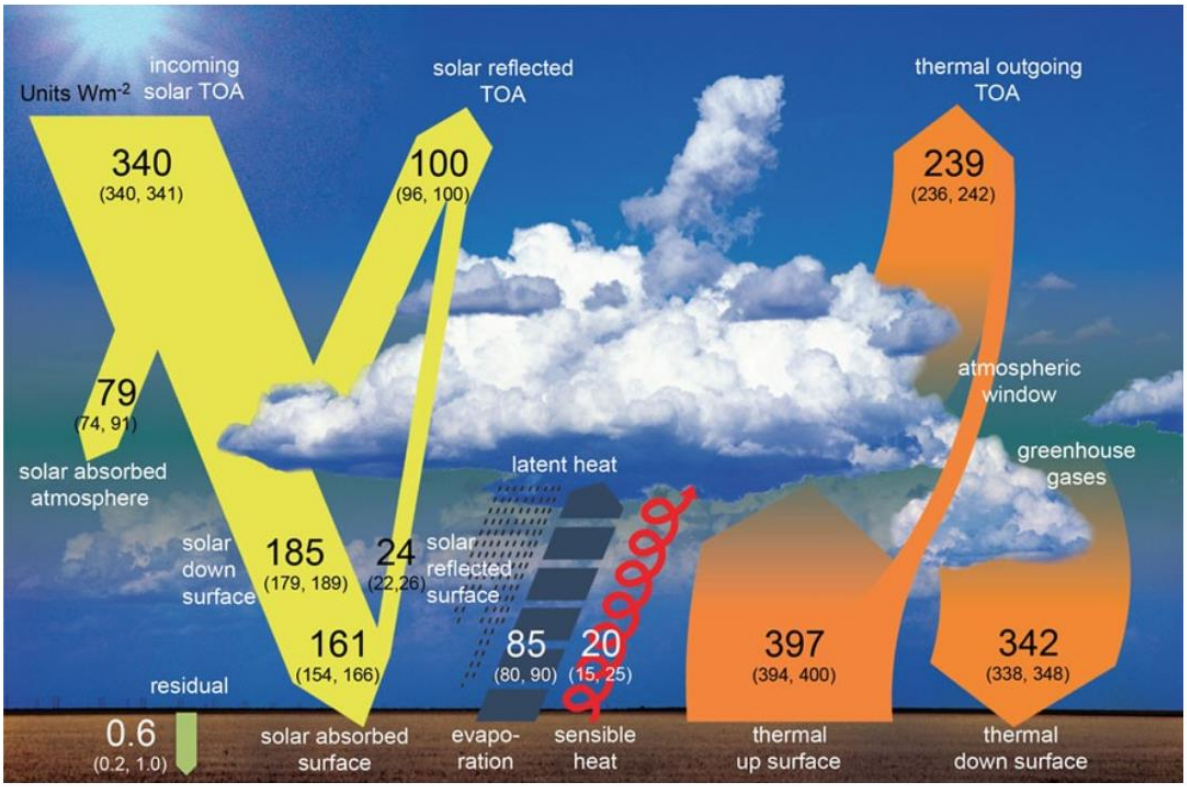

Figure 2.1 Global energy balance (Pontius, 2012).

into the soil as heat; a portion heats the air right above the ground surface; and a portion is used to vaporize pore water as quantified by the mass rate of evaporation and the latent heat of vaporization (Djalal, 2014).

"Bare soil evaporation involves the strong coupling of phase change kinematics, internal transport mechanisms, soil hydraulics and thermal properties, and atmospheric demand." (Trautz, 2016).

2.2.3 Evaporation stages

The drying process occurs in two distinct stages of "constant rate stage or stage I" and "falling rate stage". The falling rate stage itself consists of two parts: very important part of "stage

I", and almost negligible part of "stage III" (Figure 1) (Yanful & Mousavi, 2003).

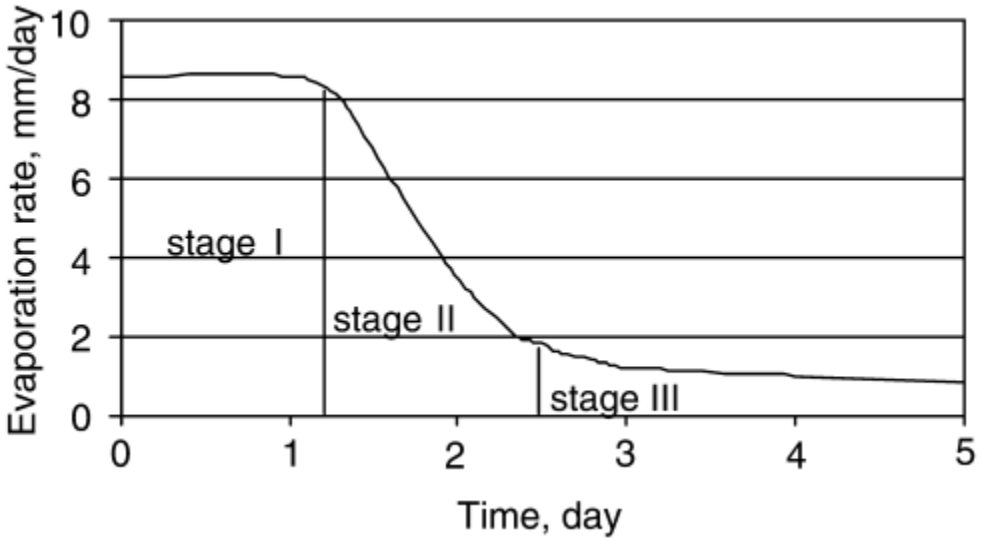

Figure 2.2 Schematic of the three stages of evaporation from soil (Yanful & Mousavi, 2003).

Initially, evaporation rate from saturated porous media is high and almost constant. It is called stage I evaporation and is limited mostly by atmospheric condition. This is followed by a lower (stage II) evaporation, which is limited by hydraulic conductivity of porous media (Lehmann et al., 2008; Shokri et al., 2009). Finally, within stage III, evaporation continues with a small magnitude corresponding to residual moisture in the soil.

In other words, evaporation rate from porous media often exhibits an abrupt transition from a high and almost constant rate supplied by capillary-induced liquid flow (stage I) to lower values supported by vapour diffusion (Shokri et al., 2009). The evaporation process in tight sandstone can be divided into three stages based on the water evaporation behavior in pores of different sizes (Wang et al., 2015).

2.2.4 Potential and actual evaporations

All of the climatological methods for estimating evaporation provide or rely on the potential rate of evaporation. The term 'Potential Evaporation' has been used by engineers and hydrologists for tens of years (Thornthwaite, 1948; Penman, 1948; among others). In general terms, it may be considered as an upper limit to evaporation.

The simplest definition is equating potential evaporation to evaporation from a free water surface. The International Glossary of Hydrology WMO (1974) defines potential evaporation as "The quantity of water vapor which could be emitted by a surface of pure water per unit surface area and unit time under the existing atmospheric conditions."

Calculation of the actual evaporation rate from an unsaturated soil is more difficult than the calculation of potential evaporation. The problem becomes more indeterminate because the vapor pressure at the surface is less than the saturation vapor pressure. Both the temperature and the relative humidity of the soil surface are unknown.

Generally, evaporation occurs in two forms; one form is evaporation from free water surface (potential evaporation) and another form from the soil surface (actual evaporation) (Yanful & Mousavi, 2003). There is only a partial understanding about the link between actual evaporation and potential evaporation (Van Heerwaarden et al., 2010).

2.2.5 Methods to estimate evaporation

Climatological methods to predict evaporation are more acceptable for many applications in geotechnical engineering. This may be mainly attributed to the fact that these methods require only routine climate data such as temperature and relative humidity (Wilson, 1990).

Standardized measurement and estimation of evaporation is challenging. The lack of uniformity in input data collection and quality control is another factor that causes variation in estimates of evaporation. However, it has relatively smaller variation for a definite time and

location. Moreover, estimation error is relatively low if appropriate equation and reliable input data is used (Abtew & Melesse, 2013).

Estimating evaporation from standard meteorological data has been an active area of research and practical application. Peel & McMahon (2014) reported on recent progress in using standard meteorological data to estimate potential and actual evaporations from both terrestrial landscapes and lakes and reservoirs. They observed that remote sensing offers significant potential for mapping spatial variations in evaporation. However, there has been limited progress in estimating actual evaporation using the complementary relationship. A brief explanation of the most known evaporation estimation methods will follow. The details and equations will be presented in the Theory part (Ch. 3).

2.2.5.1 Gardner solution

One of the earliest and probably the most influential solutions of the soil-controlled daily mean evaporation problem was the one proposed by Gardner (1958) to estimate the steady state upward flow from a shallow water table toward the soil surface.

Gardner and Hillel (1962) developed an equation to calculate evaporation from finite soil columns involving the soil moisture diffusivity. They assumed infinite evaporativity, constant diffusivity with depth, and uniform wetness. They neglected gravity and obtained a solution for the falling rate stage evaporation in a finite system.

Yanful & Mousavi (2003) studied the capability of Gardner and Hillel (1962) equation to predict falling rate evaporation from finite coarse sand and fine sand. They also modeled the studied cases using the finite element model SOILCOVER (1994). They compared the results from the equation and the model with experimental data and found them to agree reasonably. The capability

of the equation to predict falling rate evaporation from finite coarse sand and fine sand was studied and confirmed.

2.2.5.2 Thornthwaite method

Thornthwaite (1948) developed a method to estimate potential evapotranspiration. His method is an "air temperature-based" formula which provides monthly estimates of potential evapotranspiration. He considered meteorological conditions, i.e. solar radiation, temperature, relative humidity and wind speed, as the dominant factors controlling evapotranspiration, compared with vegetation and soil factors (Thornthwaite and Mather, 1955).

2.2.5.3 Penman method

The Penman (1948) approach provides an estimate of potential evaporation for a saturated surface under specific atmospheric and energy supply conditions (Granger, 1989a). Rosenberg et al. (1983) reported that Penman's method was popular and was widely used for estimating potential evapotranspiration. This popularity is attributed to its simplicity and ease of application. The Penman formula requires only the measurement of routine weather parameters such as air temperature, relative humidity and wind speed.

The application of the Penman (1948) method to water limiting problems requires adjustment or correction for aridity. The corrective coefficients may be based on factors such as soil moisture, but generally they are empirical in nature. The Penman method has been found suitable for the estimation of evaporation under any climate conditions (Jensen et al., 1990). The Penman approach considers the fact that evaporation is a diffusive process and that energy can be expressed in terms of mass (Kebede et al., 2006).

2.2.5.4 Wilson method

The soil evaporative flux is a function of the vapor pressure gradient between the soil surface and the atmosphere. The solution to the problem of evaluating evaporation from unsaturated soil surface relies on the ability to provide more physical relationships to make the calculation determinant. Wilson (1990) proposed a relationship to do this. He proposed a modified Penman (1948) approach to estimate evaporation from unsaturated soil surface. He combined vapor transfer equation with heat transfer equation to determine actual evaporation from soil surface. His method was used in this study to estimate actual evaporation, and will be explained in detail in Chapter 3.

The method proposed by Wilson (1990) requires atmospheric data such as air temperature, wind speed, humidity and net radiation, and has a new parameter, compared to Penman (1948) equation, for relative humidity of the evaporating surface. Machibroda (1994) implemented the modified Penman formulation proposed by Wilson (1990) in the 1D finite element program SOILCOVER to estimate actual evaporation (1994).

2.2.6 The effect of evaporating soil on evaporation

The ability of the soil to transmit water, and the associated water regime is an important factor in the evaporation process. Figure 2.3 shows typical drying curves for sand and clay versus moisture availability.

Soil moisture flow is controlled by both hydraulic conductivity and storage characteristics of the soil. Some of the controlling factors are briefly discussed in the following subsections.

2.2.6.1 The effect of hydraulic properties of soil

The hydraulic properties of the layer at the vicinity of the soil surface have significant impact on evaporation and could be harnessed to decrease water losses.

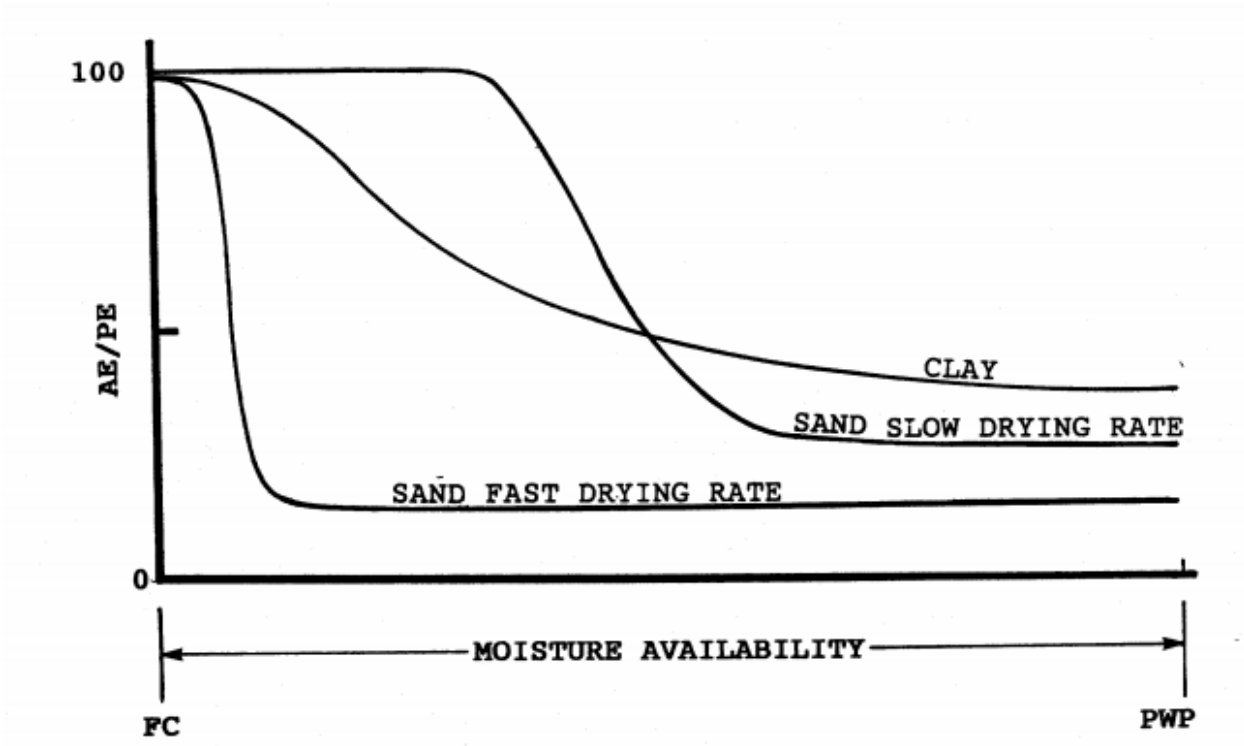

Figure 2.3 Typical drying curves for sand and clay showing actual evaporation as a percentage of potential evaporation versus moisture availability (Wilson 1990). PWP: permanent wilting point, FC: field capacity

Assouline et al. (2014) used pore network simulations to illustrate the structure of phase distribution during evaporation for the various systems considered. The simulated results and the experimental data confirmed that adding a narrow layer of porous media with different properties from the underlying main soil is a simple means of controlling evaporation losses.

2.2.6.2 The effect of the depth of the evaporating surface

Yamanaka et al. (1997) conducted five different wind tunnel experiments, and developed a simple energy-balance model in which surface moisture availability was represented by

evaporating surface depth. The model could estimate not only the latent heat flux but also the depth of the evaporating surface. They verified the model by experiments under steady state atmospheric conditions. They demonstrated the significance of the depth of the evaporating surface as a determining factor for surface moisture availability.

2.2.6.3 The effect of surface roughness, crack and deformation

Sattler and Fredlund (1989) demonstrated how heave and settlement in expansive clay soils are affected by evaporation. Silvestri et al. (1990) showed settlement problems in lightweight structures founded on Champlain clays in Montreal to be strongly controlled by potential evapotranspiration.

Moisture-induced suction changes in expansive soils due to infiltration and evaporation result in failure of civil infrastructures. Deformations in expansive soils closely match cyclical suction changes corresponding to seasonal weather variations. Volume changes fluctuated close to the ground surface and gradually decreased with depth (overburden pressure) due to isolation from meteorological effects. The top 2 m depth was found to be the active zone susceptible to moisture variations (Ito et al., 2014).

Crack development in soils and the associated potential for higher evaporation rates are pertinent to many agricultural and engineering applications. Many researchers have attempted to model crack formation though none have succeeded to comprehensively capture it (Djalal, 2014).

2.2.6.4 The effect of water retention or soil water characteristic curve (SWCC)

Soil water characteristic curve (SWCC) or water retention curve presents the relation between volumetric water content and suction. As Figure 2.4 shows, in coarse sands volumetric water

content decreases at lower suctions than in find sands. Similarly, in sands, volumetric water content decreases at lower suctions than in fine grained soils, such as clay. The suction beyond which a sharp decrease in volumetric water content occurs is called the air entry value (AEV). This value is lower for coarse grained soils than for fine grained soils. Figure 2.4 shows SWCCs for coarse and fine sands (Yanful & Mousavi, 2003).

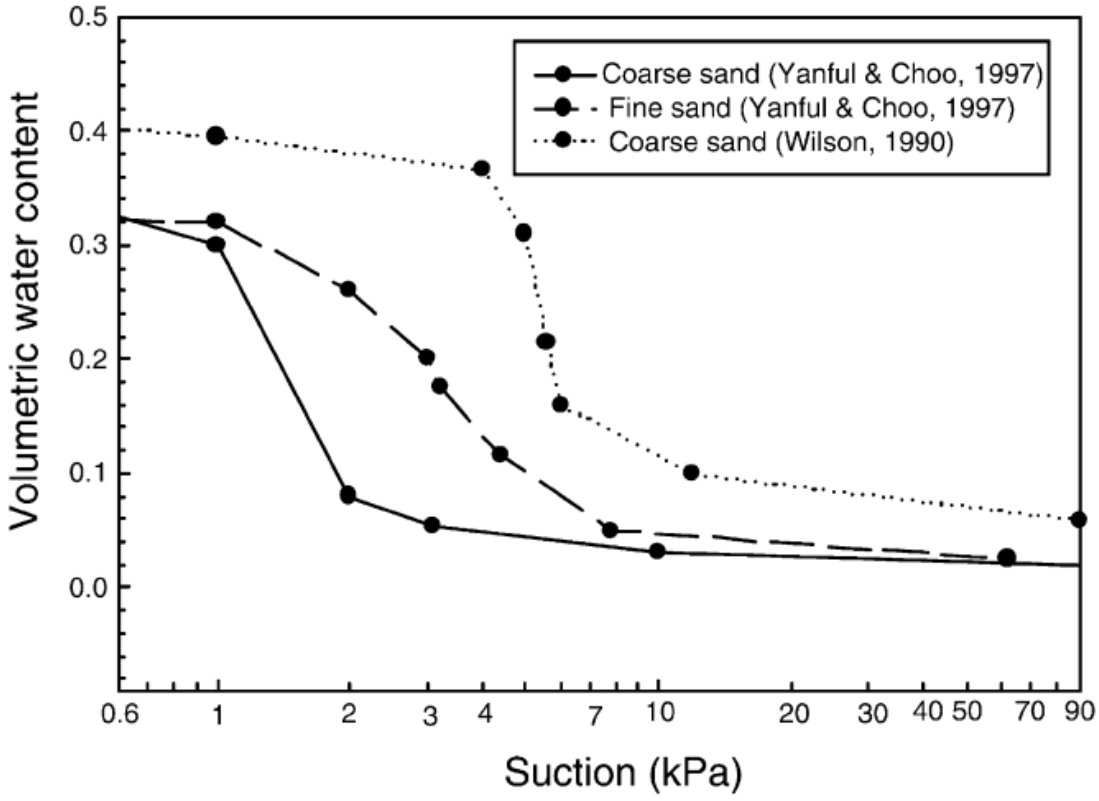

Figure 2.4 Soil water characteristic curves for the studies soils (Yanful & Mousavi, 2003).

To model soil moisture dynamics, water retention curves approaching infinitely negative matric potentials at residual water content are widely employed. Regarding numerical simulations, these retention curves fail to satisfactorily describe evaporation from arid soil because they do not allow the soil to dry below residual water content. Ciocca et al. (2016) introduced simple modification to prevent unrealistic water retention at residual water content. This might reduce the

need to introduce empirical enhancement factors. This may also improve the capability of modeling evaporation into the atmosphere in arid regions.

2.2.6.5 The effect of layered soils

Evaporation in layered porous media is influenced by the thickness and sequence of layers and capillary characteristics of each layer. Shokri et al. (2010) proposed a composite characteristic length to predict drying front depth at the end of a period with a high and constant drying rate (stage I evaporation) from layered porous media. The model was tested in laboratory experiments with alternating layers of coarse and fine sands. Different combinations of thicknesses and positions were considered. The results showed that air invasion at the interface between fine and coarse layers leads to a capillary pressure jump, and this in turn, causes relaxation, which significantly modifies the liquid phase distribution, compared to evaporation from homogeneous porous media. Insights from this study are useful for designing capillary barriers for reducing evaporative losses (Shokri et al., 2010).

2.2.6.6 The effect of soil air pressure gradient

Zeng et al. (2011) developed a vertical 1D two-phase heat and mass flow model that fully considers diffusion, advection, and dispersion. The proposed model was calibrated and used to investigate the advective effect in low permeability and high permeability soils. The results of the study showed that there is an underestimation of evaporation when airflow is neglected. This is more evident in low-permeability soils.

2.2.7 The effect of atmospheric parameters on evaporation

In order to predict evaporation, the heat and moisture flow equations should be coupled with the atmosphere through the evaporation, precipitation and heat flux. This could be performed by

evaluating the boundary conditions at the soil-atmosphere interface for the heat and moisture flow equations. Atmospheric coupling is achieved by calculating the soil evaporative flux. This flux is a function of vapor pressure gradient between the soil surface and the atmosphere (MEND, 1996).

Rianna et al. (2012) investigated the interaction between soil and atmosphere in pyroclastic soils to understand the influence of meteorological factors on soil variables (essentially water content and suction). Because particular interest of the work lied in the influence of evaporation, a physical model was set to quantify evaporation fluxes and the influence they have on fluctuations in soil water content and suction. Their results indicated that soil variables, which typically control stability conditions (suction and water contents) may be related not only to precipitation and drainage as traditionally found in the literature, but also to other atmospheric variables including temperature, humidity, wind speed, and solar radiation. Also, according to this study, evaporation exerts a significant influence on suction fluctuation and cannot be neglected in interpreting or predicting groundwater and slope behavior.

Atmospheric conditions control the rate of evaporation as long as the moisture content near the surface is sufficiently close to saturation. However, the atmospheric effect decreases drastically and evaporation is controlled mostly by the conductivity properties of the soil, as soon as the surface is drying, referred to as the falling rate stage or stage II (Brutsaert, 2013).

2.2.7.1 The effect of temperature and radiation

Experiments under non-steady state atmospheric conditions indicated that the transient phase transition of soil water in the drying soil layer can occur with dramatic change in radiation conditions. Therefore, to exactly simulate the diurnal variation of surface energy balance, the

transient phase transition must be accounted for in the energy balance model (Yamanaka et al., 1997).

2.2.7.2 The effect of air velocity and wind speed

Evaporation exhibits nonlinear behavior due to enhanced diffusive fluxes from increasingly isolated active pores. Wind tunnel experiments showed that in contrast with nearly constant evaporation rates obtained at low atmospheric demand (typically <5 mm/day), evaporation fluxes under high atmospheric demand (high air velocities) exhibit a continuous decrease with surface drying even in the absence of internal capillary flow limitations (Shahraeeni et al., 2012).

Turbulent airflows near the Earth's surface introduce complex boundary conditions that affect vapor, heat, and momentum exchange rates with the atmosphere (Haghighi & Or, 2013).

In an effort to develop methods based on integrating the subsurface boundary layer to estimate evaporation, Davarzani et al. (2014) developed a model and tested it using experimental data to study the effect of wind speed on evaporation. Their results demonstrated that increasing the wind speed increases the first stage evaporation rate and decreases transition time between stages I and II of evaporation.

Smits et al. (2015) developed an experimental apparatus, whichconsisted of a soil tank and a small climate controlled wind tunnel both with sensors for the continuous in situ measurement of pertinent soil and atmospheric variables, including wind speed, relative humidity, soil and air temperature, to study the effects of atmospheric forcing on evaporation. They aimed to experimentally study evaporation under various surface boundary conditions to improve the current understanding of this multiphase phenomenon.

Based on the results of their study, Smits et al. (2015) emphasized that evaporation is directly influenced by the interactions between the atmosphere, land surface and soil subsurface, and increasing wind speed leads to an increased evaporation rate and shortened stage I evaporation duration. However, increasing wind speed beyond 3 m/s shows little additional impact on stage I evaporation. Meanwhile, stage II evaporation was governed primarily by properties of the porous medium, and is independent of or only slightly influenced by wind speed (Smits et al., 2015).

2.2.7.3 The effect of air relative humidity

Relative humidity is the ratio of the current humidity of the air to the maximum amount of vapor air can hold at a given temperature. The rate of evaporation at a given place is always dependent on the humidity of that place because if the air is already filled with water vapor, it will not have any place to hold excess vapor and therefore, evaporation will occur at an extremely slow rate (FAO website, 2017; Gupta & Cosmato, 2011; among others). Relative humidity of the evaporating soil is a different issue, which affects evaporation from soil and is discussed in "Wilson method" in subsection 2.2.5.4 of this review, and "Atmospheric coupling and estimating evaporation" in section 3.3 of Chapter 3.

2.2.8 The effect of climate change on evaporation

Global warming may affect rainfall and surface evaporation, both of which, in turn, affect the ground's moisture content. Measuring evaporation from a land surface is not easy. It can readily be inferred only over large areas and long periods of time. Actual rates of evaporation from land surfaces are decreasing in 'wet' areas but in the more prevalent 'damp' areas, the increase of evaporation is associated with slightly more soil moisture (Linacre E. T., 2004).

Oceans are the source of 86% of the global evaporation and the receiver of 78% of global precipitation (Lagerloef et al., 2010). Evaporation is a key component of the global water cycle and an enhanced global oceanic evaporation implies a changing global water cycle. A hydrographic data-based study by Curry et al. (2003) presented evidence of a 5%-10% increase in evaporation (Yu, 2007). Thus, the study of the effects of environmental parameters on evaporation paves the way to study the effect of climate change (Douville et al., 2013; Stocker et al., 2013).

Climate change has the potential to affect all of these parameters in a combined way. Therefore, any change in climatic parameters due to climate warming will affect the potential for evaporation. There remains a considerable amount of uncertainty concerning the magnitude and spatial distribution of evaporation in response to a changing climate. Thus, the study of the possible effects of climate warming on evaporation is an attracting considerable interest (Su et al., 2015).

2.2.9 The effect of suction on evaporation

Figure 2.5 shows the effect of total suction on evaporation and the proportion of actual evaporation to potential evaporation. As the figure shows, actual evaporation is almost equal to potential evaporation for suctions less than or equal to 100 kPa with Regina clay and Beaver Creek sand, and for suctions less than or equal to 30 kPa for Custom Silt. Actual evaporation is still more than 90 to 95% of potential evaporation for suctions less than or equal to 1000 kPa for the sand, silt and clay. For more suctions, actual evaporation decreases with a higher slope relative to potential evaporation. The slope becomes higher for suctions greater than approximately 20,000 kPa.

2.2.10 Modeling evaporation

The lowest atmospheric layer is characterized by large vertical gradients of temperature,

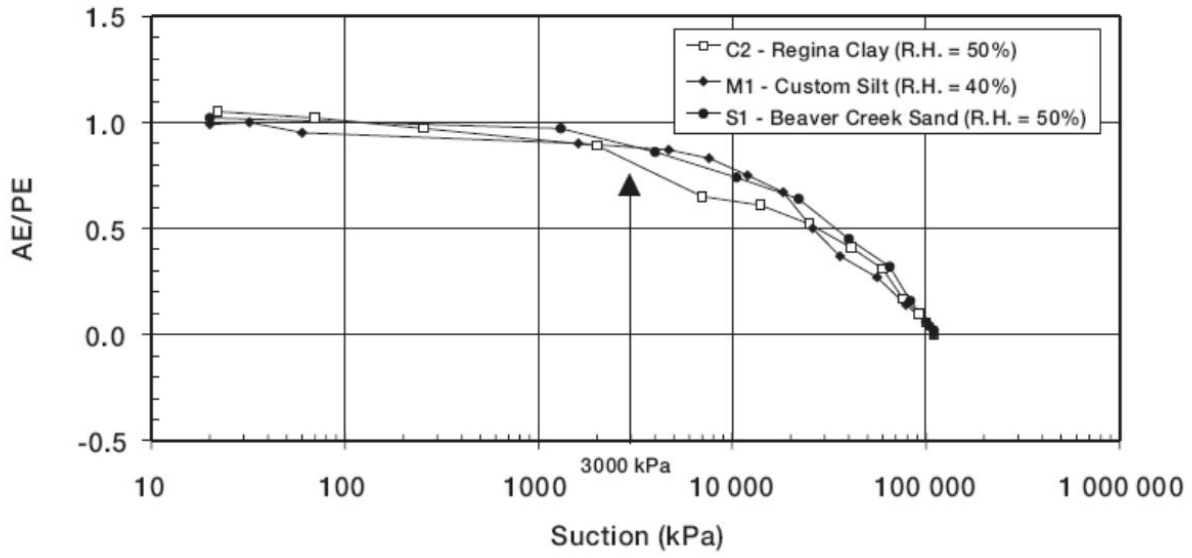

Figure 2.5 Effect of total suction on evaporation (Wilson et al., 1997).

humidity, and wind velocity. A numerical model of the atmosphere-soil boundary layer was developed to simulate heat and moisture exchange between atmosphere and soil (Sasamori, 1970). The atmospheric and soil equations were solved using energy and water mass conservation and the local thermo-dynamic equilibrium of temperature and humidity. The model was applied to the study of energy balance on the soil surface. The specific concern was the wetness of the soil, and the model simulated the clearly distinct characteristics of the energy balance depending on the wetness of the soil. Based on the results of the simulation, if the surface is sufficiently wet, most of the net radiative energy is transformed to latent heat released into the atmosphere. However, for the soil with deficient water the latent heat becomes negligible and most of the net radiation is transformed into sensible heat (Sasamori, 1970).

Wilson (1994) presented a theoretical model for predicting the rate of evaporation from soil surfaces. The model was based on a system of equations for coupled heat and mass transfer in soil, and was used to predict soil evaporation rates for a controlled column evaporation test over a 42-

day period. The values computed by the model agreed well with the values measured for two columns of Beaver Creek sand in their evaporation test.

Katata et al. (2007) developed a 1D soil model to better predict heat and water exchanges in arid and semiarid areas. They incorporated the calculation of evaporation and adsorption in the soil in their model. The good performance of the model was confirmed by comparison of the model results with the measured results in the Negev Desert, Israel. They resulted that evaporation and adsorption processes in the soil have a large impact on the heat and water exchange between the atmosphere and land surface, and are necessary to accurately predict them.

Although numerical simulations provide a valuable tool in developing designs and predicting general barrier performance, they have limitations when it comes to detailed system performance. For example, if numerical simulations are based on inadequate representations of an actual system, or do not recognize the key processes involved, or use parameters with large uncertainties, the potential for large errors exists (Guo & Dixon, 2010).

A finite-element numerical simulation of heat and moisture regimes using the original theory of Philip and de Vries was applied by Novak (2010) to a bare silt-loam soil drying during a 10-day rain-free period. Based on the results, a narrow subsurface evaporation zone developed daily when the surface became dry enough. The subsurface evaporation zone moved down and up most days due to drying and rewetting. Very fine grids near the soil surface were required to simulate this behaviour correctly (Novak, 2010).

Although numerical simulation models for soil water flow and heat transport allow estimation of evaporation rates from unsaturated soils (Saito et al., 2006), determination of soils'

required thermal and hydraulic parameters for the parameterization of the model is laborious (Sakai et al., 2011).

To quantify the specific roles of liquid bridges and of local thermal and capillary gradients on vapor transport at the pore scale, Shahraeeni et al. (2012) considered a mechanistic pore scale model of evaporation and condensation dynamics as a building block for quantifying vapor diffusion through partially saturated media. Simulations of vapor diffusion with isolated liquid phase bridges revealed that enhanced vapor diffusion under isothermal conditions reflects a reduced gaseous diffusion path length. As liquid phase saturation increases, capillary transport becomes significant and pore scale vapor enhancement is limited to low water contents as postulated by Philip and de Vries. According to calculations, with a mild thermal gradient water vapor flux could be doubled relative to diffusion of an inert gas through the same system.

Smits et al. (2012) tested different conceptual and mathematical formulations that are used to estimate evaporation from bare soil. They critically investigated various formulations and surface boundary conditions. To do this, they modified a previously developed theory and developed a numerical model with ability to incorporate these boundary conditions. Their results showed that the approaches based on different boundary conditions varied in their ability to capture different stages of evaporation. They resulted that all approaches have benefits and limitations, and no one approach is most appropriate for every scenario, and there is a need for further research on heat and vapor transfer processes in soil for better modeling accuracy.

Haghighi & Or (2013) proposed a diffusion-turbulence evaporation model to improve the estimation of field-scale evaporative fluxes from drying soil surfaces under natural airflows. The model captures nonlinearities between surface water content and evaporation flux during drying

of porous surfaces. The analysis showed that neglecting diffusion in the longitudinal direction may lead to underestimation of evaporative mass losses from porous surfaces (Haghighi and Or, 2013).

With respect to models of water content redistribution, many numerical approaches are available nowadays by employing different finite difference and finite element methods (Teng et al., 2014). Trautz (2016) used COMSOL Multiphysics software for all numerical simulation with support from MATLAB. COMSOL is a finite element analysis software and has a number of predefined modules that allow the user to easily select the partial differential equations of interest with solvers that are capable of implicitly solving nonlinear problems. He reported that larger evaporation rate was observed in the tightly packed soil region than in the loosely packed soil region. He also observed that stage I evaporation was sustained longer in tightly packed soil region than in the loosely packed soil region.

2.2.11 Computer programs to estimate evaporation

There are few computer programs that used atmospheric coupling in their formulations. SOILCOVER (1994) and its 2D version, VADOSE/W (2002), are soil-atmospheric flux models that link the subsurface saturated/unsaturated groundwater system and the atmospheric system above the soil in an attempt to represent the soil-atmosphere continuum. The above-mentioned programs use the modified Penman equation proposed by Wilson (1990) and estimate potential and actual evaporations. However, they do not couple equilibrium equation with flow equations and cannot calculate stress and strain to estimate displacement in soil surface, which affects evaporation.

2.3 UNSATURATED SOIL

2.3.1 The importance of unsaturated soil

The accelerating pace of development throughout the world places increasing demands on the unsaturated zone. Unsaturated or vadose or aeration zone is the portion of the earth's surface that encompasses the soil and unsaturated sediments that lie above the water table. The unsaturated zone affects the movement of water, nutrients, chemicals, pathogens, and contaminants to (and sometimes from) water table. Of special importance from a vadose-zone perspective are contaminants that have been buried in or released to the unsaturated zone, or contaminants that have been or will be disposed in special vadose zone facilities such as landfills (Fayer, 2000).

Delage (2002) presented experimental systems and procedures of investigating the hydro-mechanical behavior of unsaturated soils. He commented on the water retention properties of unsaturated soils and linked those to various physical parameters and properties of the soils.

A large number of engineering problems are associated with unsaturated soils. One of the most common problems is the collapse of materials such as loess, or loosely compacted fills, which could undergo large settlements after wetting under large stresses. The shear failure of these materials is another major problem. Therefore, a sound understanding of the mechanical behavior of this type of material is required so that the engineer can devise safe and cost-effective solutions to these problems (Jotisankasa, 2005).

A simplified approach with ignoring unsaturated flow above the phreatic surface is no longer acceptable, because it not only ignores an important component of moisture flow in soils, but also greatly limits the types of problems that can be analyzed. It is mandatory to deal with unsaturated flow in actual situations such as transient flow problems (GEO-SLOPE, 2008).

Knowledge of moisture diffusivity properties is required to predict water transport through unsaturated porous media. Obtaining realistic estimates of the moisture diffusion properties of

unsaturated soils is essential for many geotechnical engineering applications. The performance of the structures constructed on unstable and expansive unsaturated soils is significantly affected by vertical deformations of the supporting local subgrade soils. Such deformations are controlled by suction variations in soil. In comparison to saturated soils, water movement in unsaturated (vadose) zone is far more complex due to the fact that hydraulic conductivity and water content versus suction are nonlinear in unsaturated soils (Mabirizi & Bulut, 2009).

Subsurface airflow in unsaturated zones induced by natural forcing can affect evaporation and the unsaturated soil condition. This is important in many environmental and engineering fields, including environmental remediation, water infiltration and groundwater recharge, coastal soil aeration, mine and tunnel ventilation, and gas exchange between soil and atmosphere (Kuang et al., 2013).

2.3.2 Evaporation from unsaturated soil

Feddes et al. (1988) reviewed the principles underlying water dynamics in the unsaturated zone and gave an overview of simulation modeling of soil water flow in the vadose zone. They also presented several practical examples of simulation of flow problems. Soil water flow is highly nonlinear, as both the hydraulic conductivity and the soil water pressure head depend on the soil water content. Exact analytical solutions are only possible for simplified flow under restrictive assumptions. However, numerical solution of the flow equation offers a powerful tool to approximate the real nature of the unsaturated zone for various soil systems.

Water movement through soils goes through a three-component system consisting of soil-atmosphere interface, near surface unsaturated zone, and deeper saturated zone. In the past, groundwater modeling focused primarily on the saturated zone. This focus created a discontinuity

in modeling the natural system because unsaturated zone and soil-atmosphere interface were not represented. Advances in unsaturated soil technology during the past decades led to the routine modeling techniques for saturated/unsaturated soil systems. However, the evaluation of the flux boundary condition imposed by the atmosphere was not that easy (Wilson et al., 1994).

For an infiltration or evaporation problem, a numerical solution using a finite difference method is sensitive to its upper boundary condition and the related soil parameters. |On the other hand, using a traditional finite element method usually yields oscillatory non-physics profiles (Xie et al., 1999). To address this concern, Xie et al. (1999) established a numerical model for the unsaturated flow equation with moisture content as prognostic variable in order to simulate liquid moisture flow in an unsaturated zone with homogeneous soil, and different initial and boundary conditions.

Benson (2007) used four different codes to simulate unsaturated flow with atmospheric interactions. Each code incorporated boundary conditions that reflect atmospheric fluxes. Although the codes were similar conceptually and functioned in a similar manner, they comprised different algorithms, and therefore yield different predictions for the same input. A field validation exercise conducted considering three of the codes demonstrated that the predictions appeared realistic regardless of which code was being used. However, each code provided a different prediction, and none of the predictions were in agreement with the field measurements.

Benson (2007) attributed the differences in predictions, to some extent, to differences in how the atmosphere boundary was implemented. He suggested more research should be conducted to refine how this boundary should be implemented in numerical models. This is particularly complicated by the fact that the space and time evolution of the soil water content in an unsaturated

medium is highly nonlinear due to dependence of both hydraulic conductivity and the soil water potential on the soil water content (Teng et al., 2014).

2.3.3 Isothermal and non-isothermal behavior of unsaturated soil

Ground heat transfer problems in unsaturated soil occur across a range of engineering disciplines. Typically, the phenomenon is important in energy conservation, soil heating, buried electrical cables, ground freezing, soil shrinkage, the design of nuclear waste disposal systems, and geotechnical structures such as soil covers with atmospheric coupling. Ewen and Thomas (1989) stated that, in many cases, the ground would be unsaturated and the coupled influence of moisture migration is important. On the other hand, the deformation of porous media is significant in engineered clay barriers and soil covers. If this deformation is considered as well, the coupling effects among deformation, moisture, and heat should be accounted for.

One of the basic aspects of non-isothermal behavior of unsaturated porous media is the simultaneous movement of heat and moisture. In saturated soil, the coupling is very strong, especially in the presence of large temperature gradients (Moradi et al., 2016). In saturated soil the moisture movement takes place in the liquid phase only. However, in unsaturated soil it occurs in both the liquid and vapor phases. Because of the complex nature of pore spaces and the force field, which acts on the vapor and water, this process is more complex in unsaturated soils.

The modeling of infinitesimal deformation of unsaturated porous media is an important part of establishing a theoretical framework of non-isothermal behavior for such material. Gatmiri and Delage (1995) constructed the basis for development of the non-isothermal theory. The model was developed along similar lines to that of Alonso et al. (1988). The main differences lie in the relationship between strain increments and net stress increments, and the assumption of hyperbolic variations for both bulk modulus (K) and Young modulus (E).

These differences led to a new formulation of the equation of void ratio state surface, which incorporated the two widely used independent variables, i.e., net stress and suction as the state variables. This facilitated the description of water and air pore pressures distributions, and the deformation of porous medium. The coupling effects among suction-stress-deformation were taken into account by introducing the concept of the state surfaces of void ratio and degree of saturation (Gatmiri & Delage, 1995).

Gatmiri (1997) formulated a framework of non-isothermal behavior of unsaturated porous media. His study presented a set of fully coupled thermo-hydro-mechanical equations for saturated and unsaturated porous media. In that formulation, heat and moisture transfer equations in an alternative form based on water and air pore pressures were presented for unsaturated soil. The effects of deformations on the temperature and suction distribution in porous medium, and the inverse effects were also included in this formulation, which was achieved via a new temperature-dependent formulation of state surfaces of void ratio and degree of saturation. He assumed nonlinear (hyperbolic) constitutive law and the mechanical and hydraulic properties of the porous media were considered to be temperature-dependent. The effects of non-homogeneity of soil and phase changes were also introduced.

2.3.4 Stress-strain behavior and deformation of unsaturated soil

In order to simulate the behavior of unsaturated soil, early studies attempted to define a single parameter that describes the behavior of unsaturated soil. These studies intended to combine three variables, i.e., stress (σ), air pore pressure (P_a), and water pore pressure (P_w), into a single effective stress σ'. The first such single parameter approach, is the χ factor proposed by Bishop (1959). However, several researches (Jenning and Burland, 1962; Bishop and Blight, 1963) demonstrated

the major limitations of the approach of Bishop (1959), i.e. not considering the fundamental difference in the behavior of saturated and unsaturated soils. In fact, "total stress" and "suction" contribute to the soil grain stability, and as two independent stress state variables shape the behavior of unsaturated soil.

Coleman (1962), Bishop and Blight (1963) formed the basic frame work of the approach of two-stress state variables. Fredlund and Morgenstern (1976, 1977) showed that any pair of three stress parameters of σ-P_a, σ-P_w, P_a-P_w would be sufficient to describe the mechanical behavior of unsaturated soil. In fact, the set of two-stress state variables is a suitable set of independent stress state variables because no distortion or volume change of an element occur when the individual components of the stress state variables (σ, P_a and P_w) are modified while the stress state variables are kept constant (Fredlund & Morgenstern, 1977). The net total stress σ-P_a, and suction P_a-P_w are the most commonly used variables, because they separate the effects of total stress and suction.

Various constitutive laws have been developed. One of the constitutive laws was the incremental elastic formulation suggested by Coleman (1962), and later by Fredlund (1979). Another constitutive law is based on the state surface concept, which was developed in order to describe the volumetric behavior of soil under the coupled effects of net stress and suction changes (Fredlund and Rahardjo, 1993).

Matyas and Radhakrishna (1968) presented experimental data for state surfaces of void ratio and degree of saturation. Fredlund (1979) suggested explicit mathematical expressions for both state surfaces. Lloret and Alonso (1980) gave alternative expressions for the state surfaces of void ratio and degree of saturation. Gatmiri and Delage (1995) presented explicit expression of void ratio state surface compatible with nonlinear elastic (hyperbolic) constitutive law.

2.3.5 Modeling unsaturated soil

Based on the approach proposed by Alonso et al. (1988), a nonlinear elastic model of unsaturated soil using the new state surface formulations was developed (Nanda, 1989). This model was incorporated in finite element code U-DAM (Gatmiri, 1992), and was used for modeling the coupled flow-deformation of unsaturated soil (Gatmiri & Delage, 1995).

Dye et al. (2011) performed One-dimensional modeling of expansive soil under dry initial conditions (suction of 1,500 kPa) considering both infiltration and evaporation. It was found that small variations in the unsaturated soil hydraulic conductivity function result in significantly different modeling outputs, as expected, while substantial variation in SWCC alone produced almost identical soil response in terms of soil suction when the slope of the SWCC is similar. Therefore, proper characterization of the slope of the SWCC is important to proper suction profile determination (Dye et al., 2011).

2.4 THERMO-HYDRO-MECHANICAL (THM) ANALYSIS

The presence of heat in a geologic medium causes a chain of events. These events are caused by what is called “coupled thermal-hydraulic-mechanical (THM) phenomenon”. The interdependence of each of these three phenomena leads to a coupled behavior that is very complex. However, progress in coupled analyses among pairs of these three phenomena provides a basis for treating all three phenomena in a fully coupled manner.

THM analysis of geo-environmental phenomena and processes acquired increasing importance in research studies and geotechnical engineering applications. The next subsection briefly explains this fact.

2.4.1 The importance of THM analysis

Thermo-hydro-mechanical (THM) coupled processes in porous media are important in many geotechnical engineering problems such as nuclear waste disposal, oil extraction, and geothermal energy and need to be addressed as a THM coupled problem (Schanz 2004; Vardon et al., 2009). Although some commercial analysis tools are already available, there is a need to develop fully coupled and efficient THM codes that can deal with real world problems (Wang et al., 2007).

Transport phenomena, which occur in porous multiphase materials involve interaction of the phases with each other rendering THM coupling even more important. Moreover, in Environmental Geomechanics, it is common to find non-isothermal situations; therefore, attention should be given to the mechanisms involving heat transport. The incorporation of a thermal component leads to numerous additional interactions between phenomena, and inevitably, a high degree of complexity (Gens & Olivella, 2011).

Haxaire et al. (2011) described the governing equations of a fully coupled THM analysis for deformable porous media and highlighted the significant need for practical THM applications, in particular for geo-environmental and geo-energy related problems. The THM phenomenon even starts at the molecular level because temperature is associated with the motion of molecules within a material and this motion is directly related to the kinetic energy of the molecules, including vibrational and rotational motion (Sen, 2015).

2.4.2 Coupled THM phenomenon

Two pioneer studies on moisture movement in soil were carried out at the beginning of the last century. The first study investigated the effect of thermal gradient on the soil moisture movement (Bouyoucos, 1915). He observed that the moisture moved from the warm side to cold

side in a soil sample and concluded that the flow occurs largely in the liquid phase. The second study investigated the moisture movement in both liquid and vapor phases with and without a thermal gradient (Lebedeff, 1927). He reported that surface adsorption and water movement in the vapor phase are the critical components in determining the amount of water retained. He also studied the distribution of water within sand as a function of the height above the water table. He noted that below a certain value of water content, an increase in suction had little effect on the soil water content. The details of his works were reported by Rollins et al. (1954).

Following these pioneering studies, significant research was focused on understanding the physics and nature of the coupled thermal-hydraulic-mechanical phenomenon in porous media. Smith (1943) conducted laboratory tests in order to investigate the moisture movement in soil, focusing on the relative importance of the vapor versus liquid flows in moisture transfer. After observing negligible vapor diffusion, he suggested that the capillary liquid movement induced by vapor condensation should be considered as the mechanism of movement based on liquid flow.

On the other hand, Croney and Coleman (1948) used the Kelvin equation (Tadros, 2013) to relate the vapor pressure to temperature and concluded that the moisture movement normally takes place in the vapor phase. They reported that for each soil, there is an optimum initial water content, at which the maximum water transfer takes place. Similarly, Gouda and Winterkorn (1949) and Winterkorn (1959) stated that the initial moisture content plays a significant role on the moisture movement.

Several investigators assumed that all moisture movement takes place in the vapor phase. This assumption led to using modified Fick's law (1855) for porous media. The comparison between the theoretical results and laboratory tests' results indicated that this assumption

underestimates the quantity of net water vapor transport by a factor of 3 to 10 (Gurr et al., 1952; Rollins et al.1954; and Abdel-hadi and Mitchell, 1981).

Philip and de Vries (1957) and de Vries (1958) presented a basic framework and a comprehensive and representative theory of moisture and heat movement in an unsaturated and incompressible porous medium. In this theory, the moisture and heat transfer equations are formulated in terms of temperature (T) and volumetric moisture content (θ). Their theory assumes that the moisture transfer in unsaturated soil occurs in both vapor and liquid phases under combined influence of gravity and the gradients of temperature and moisture content. This theory differentiates between changes of moisture content in liquid and vapor phases.

Owing to several agreements observed in various studies (Cassel et al., 1969; Dirksen, 1964 among others), the theory of Philip and de Vries (1957) has been generally accepted in soil sciences and geotechnical engineering studies. However, it has some limitations that should be addressed. One of these limitations is the assumption of incompressibility of porous medium. This assumption is not realistic, especially in modeling the behavior of engineered clay barriers that are soft and significantly deformable. Meanwhile, the θ-based formulation is valid for homogeneous soil and cannot consider the hysteresis effects.

In order to overcome these limitations, Sophocleous (1979) and Milly (1982) converted the θ-based formulation to a matrix head-based formulation in order to allow consideration of heterogeneity of soil and hysteresis effects in desiccation and re-saturation conditions.

Dempsey (1978) presented a simplified version of de Vries' (1958) general formulation while Dakshanamurthy and Fredlund (1981b) presented formulations other than Philip and de Vries

(1957). Thomas (1987) presented numerical solution techniques, and Milly (1982) solved saturated/unsaturated soil example problems.

Geraminegad and Saxena (1986) developed a THM model in which the soil deformation was considered. However, their model did not include soil deformations resulting from external loading. Instead, soil deformation was limited to volumetric deformation due to pore air pressure and suction changes.

Devillers et al. (1996) reported test results for thermal consolidation of an unsaturated silty soil in a thermal triaxial apparatus. They observed that void ratio decreased when temperature increased independent of the stress state of samples and reported that thermal compression indices depend on stress state of sample. In addition, Villar et al. (1993) conducted laboratory heating tests to establish the steady state and transient variations of moisture content, temperature and volumetric deformations.

The abovementioned researches advanced our knowledge of coupled thermo-hydro-mechanical greatly, nonetheless the first step in developing a fully coupled THM model for unsaturated soil is choosing adequate independent variables. These variables should represent all significant interaction effects among the different components involved in the coupled process of a deformable unsaturated porous medium with three phases of porous medium, water and air under heating (Gatmiri, 1997).

The phase changes between liquid and gas, evaporation, condensation, and induced moisture transfer under thermal and pore pressure gradients are important aspects in non-deformable unsaturated porous media. Also, the effects of moisture distribution on heat flow are important (Gatmiri, 1997).

Recent developments including successful implementation of the THM model in the finite element code CODE_BRIGHT (Olivella et al. 1996) and the in-situ experiments to validate the model and the work on the design of nuclear waste repositories allowed THM analysis to become a whole part of geomechanics (Haxaire et al., 2011). For example, Eslami et al. (2016) simulated heat dissipation over 180 days in the surrounding soil of buried electrical cables at unsteady state conditions to evaluate the coupled heat and moisture flow around the cables. They reported that the moisture flow was mainly caused by the vapor transport under temperature gradients and emphasized the significant effect of the hydrothermal characteristics of surrounding soil.

2.4.3 THM analysis of unsaturated soil

Wu et al. (2004) presented a THM constitutive model for unsaturated soils and investigated the thermal effect on the soil hydraulic properties. Particularly, they confirmed the thermal softening phenomenon, i.e. decreases in value of the pre-consolidation pressure and in critical value of the suction of the SI (suction increasing) curve with heating process. Likewise, Dumont et al. (2010) developed a simple THM constitutive model for unsaturated soils by extending the effective stress concept to unsaturated soils. They used a minimal number of material parameters based on existing models. The model was verified by evaluating the THM process qualitatively and quantitatively and comparing its predictions with experimental data and previous work.

An unsaturated soil is a three-phase (solid, liquid, and gas) porous medium and contains multiple components. It is subject to the high temperature in some engineering applications, and there are complex interactions between thermal processes (T), fluid flow processes (H), and mechanical processes (M).

Gens & Olivella (2011) developed a mechanistic theoretical formulation encompassing the most relevant THM phenomena and their couplings. The formulation constituted four balance equations corresponding to water mass balance, air mass balance, internal energy balance and momentum balance. Mass balance equations were established in terms of species rather than phases. Advection term was neglected and Henry's law was used to express equilibrium of dissolved air. This formulation can be incorporated into a suitable numerical scheme to analyze THM engineering problems involving unsaturated porous media.

Qin et al. (2012) confirmed the necessity of coupled THM in many applications. Additionally, Cai et al. (2014) derived a coupled formulation based on hybrid mixture theory to model the THM coupling behavior of unsaturated soils.

2.4.4 Modeling THM behavior

The finite element method is the most employed numerical method to treat THM coupled problems. Rutqvist et al. (2001) presented governing equations for coupled THM processes in geological media and compared the formulations of four finite element programs. They concluded that the most apparent difference was the treatment of the gas phase. The investigated FE programs assumed constant and small gas pressure, implying that the gas phase is static and hence no vapor or heat is advected with the bulk gas flow. Thus, the dominant mode of vapor transport in the gas phase is by molecular diffusion caused by the vapor density gradient, which strongly depends on thermal gradient.

Cola et al. (2008) used a fully coupled THM finite element approach to model the groundwater and saturation response of a typical salt marsh of the Venice lagoon in Italy subjected to tide fluctuation and flooding. The study showed the great importance of THM couplings to

explain the groundwater pressure evolution induced by lagoon tide cycles. Jeanne et al. (2014) performed a series of 3D simulations to study the influence of THM processes on the development of an enhanced geothermal system affected by a network of short fault zones. The developed model was calibrated by comparing the numerical results to field observations, including ground surface deformations. The results showed that the main mechanisms of induced seismicity are related to pressure increase caused by injection and cooling.

On the other hand, Guo & Dixon (2010) highlighted the current limitations of using numerical simulations to predict detailed bulkhead performance. The models can use entirely appropriate physical, mechanical, and thermal formulations and relationships but they are often unable to capture the field construction's "reality".

Lu et al. (2010) performed THM analyses on granite and clay barriers using a finite difference model to study the effects of high heat generated by high-level radioactive waste during their half-life period on deformation, stresses and pore pressure variation. They concluded that finite difference modeling is difficult due to the complicated geometry and physical condition and suggested to use a combination of different numerical methods like finite element, finite volume and their combinations.

Similarly, Wang et al. (2011) compared the performance of two alternative flow models for the simulation of thermal-hydraulic coupled processes in low permeable porous media: non-isothermal Richard's and two-phase flow concepts. They found that both models can be used to reproduce the vaporization process provided that the intrinsic permeability is relative high. However, when the intrinsic permeability is low, only the two-phase flow approach provides reasonable results.

2.5 THE APPLICATION OF THM ANALYSIS OF EVAPORATION ON SOIL COVERS

Predicting the flow of water between soil surface and atmosphere is a critical issue in the design of soil covers used for mine tailings, acid generating waste rocks, and other land based disposal systems (Yanful, 1991). Maintaining a water saturated zone above tailings is necessary for soil covers to act as gas diffusion barriers for uranium and sulphide tailings (Yanful and St-Arnaud, 1991). To accomplish this objective, evaporation from the cover surface should be predicted and minimized.

The importance of evaporation for the water balance in soil covers is well documented, especially for covers located in arid or semi-arid areas. For example, Nyhan et al. (1997) found that 86% or more of the precipitation loss observed on soil covers was due to evaporation with only 2-3% due to runoff (Weeks & Wilson, 2003).

The coupled heat and moisture transfer in a deformable, partly saturated porous medium deals with the interrelated effects of various phenomena, which usually lead to a highly non-linear problem with a great number of degrees of freedom at each node (Thomas et al., 1998). This is further complicated when hydro-mechanical coupled effects are extended towards temperature and chemistry effects where the volume change is less documented, which deserves further investigation (Delage, 2002).

In fact, the study of soil covers for waste disposal sites has largely become the study of how soils interact with the atmosphere. Therefore, climate conditions in the area of the cover has been a definitive factor. Earth-atmosphere interactions determine the fate of water added to the cover by precipitation, in terms of how much water evaporates back into the atmosphere, how much runs

off the cover, how much goes into storage within the soil pore space, and how much makes it through the cover into the waste material below (Weeks & Wilson, 2003).

Yanful & Mousavi (2003) underscored the importance of evaporation as it controls the moisture regime and the moisture availability to vegetation. In engineering soil caps and covers used for environmental protection, evaporation and evapotranspiration rates can exert significant influence on suction, unsaturated hydraulic conductivity, and the overall water flux (Yang and Yanful, 2002).

The design of such covers requires a prediction of the balance of precipitation, storage, runoff, evaporation or evapotranspiration. Evaporation is the most difficult part of this balance to obtain. In addition, the design of soil cover requires the computation of soil-atmosphere water fluxes through the cover as a function of soil properties and atmospheric forcing conditions (Gitirana et al., 2006).

To investigate soil cover design options, it is necessary to analyze the anticipated cover long term performance. The challenge is maintaining a high degree of saturation in the cover over a long period. Both downward drainage of water from the cover towards the waste and upward evaporation from the cover towards the atmosphere should be prevented or at least minimized, especially during dry periods (Yanful et al., 2006).

Another aspect that should be considered for compacted clay liners is the compaction of this barrier as it causes many problems. Additionally, the cover must keep its sealing function during the lifetime of the landfill and the waste monitoring period. It is very important to consider the potential differential settlements, because this phenomenon can induce bending strains in the clay layer and create damage (Camp et al., 2007).

Strain localization in a partially saturated soil with inhomogeneous degree of saturation is another concern worthy of consideration. Song et al. (2012) investigated this concern and demonstrated that a non-uniform degree of saturation could serve as an imperfection to trigger strain localization. They concluded that a fully coupled hydro-mechanical model is required to capture the relevant multiphase processes.

2.6 SUMMARY AND CONCLUSIONS

The literature review covered evaluation of evaporation, especially as applied to unsaturated soil in addition to the response of unsaturated soil to the gradients of moisture and temperature in the presence of stress and strain. The modeling of the unsaturated soil ended the section. The importance of THM analysis of unsaturated soil was emphasized, and modeling THM behavior was briefly explained along with the application of THM analysis of evaporation to soil covers.

It is concluded that there is a pressing need for continuous research on evaporation in relation to unsaturated soil and THM analysis. Despite the significant amount of research conducted up to date, some important issues remain unresolved, and further research and analysis are needed. For example, the computer programs widely used in industry for calculating the evaporation of soil covers do not account for the coupling of stress-strain state within the soil (i.e. equilibrium equation) with the water flow, vapor flow, air flow and heat flow equations. The stress-strain behavior of the soil affects its settlement, which changes void ratio and porosity on one hand, and permeability of the soil on the other hand. This can alter the evaporation characteristics significantly and should be accounted for in any reliable evaluation of the actual evaporation and the performance of soil covers.

Therefore, analyzing evaporation from unsaturated soil considering stress and strain in soil surface accompanied by a quantitative comparison of the effect of environmental parameters on potential and actual evaporation, analysis of sensitivity of the evaporation to the environmental parameters, and a parametric study are the three issues focused in this study.

CHAPTER 3

THEORY AND NUMERICAL MODELING

3.1 INTORDUCTION

There are two approaches regarding the combined flow of moisture and heat in unsaturated porous media. One approach considers a combined soil atmosphere model by coupling atmosphere with soil. In this approach, the combined flow of moisture and heat in soil is coupled with atmosphere in soil surface as the boundary. Therefore, not only soil parameters but also atmospheric (environmental) parameters are involved in the analysis. This approach uses thermo-hydro (TH) analysis and is not in deal with mechanical behavior of soil, and cannot estimate strain, stress and soil settlement, because it does not couple equilibrium equation with moisture and heat flow equations. This approach usually is used to deal with water balance in soil surface boundary considering water balance components including precipitation, infiltration and especially evaporation, which is very important in environmental geotechnique and related engineering structures such as soil covers, and could be estimated using this approach.

The other approach regarding the combined flow of moisture and heat in unsaturated porous media uses a thermo-hydro-mechanical (THM) analysis. In this approach equilibrium equation is coupled with moisture and heat flow equations; therefore, strain and stress in soil could be estimated too. However, atmosphere is not coupled and atmospheric (environmental) parameters are not used in the analysis. As a result, evaporation cannot be estimated. In fact, in this approach analysis is performed only inside the soil. The analyses using this approach are performed for some engineering issues in environmental geotechnique field, such as nuclear waste storage.

To bring together the two abovementioned approaches, to be benefited from the advantages of both approaches, in this study equilibrium equation is coupled with moisture and heat flow equations, and at the same time the atmosphere is coupled through a soil-atmosphere model. Therefore, accompanied with soil parameters, atmospheric (environmental) parameters are used too, and not only quantities related to moisture, heat, strain and stress but also potential and actual evaporations could be estimated using program EVAP1, which is developed during this study. The numerical analysis is performed considering plane strain conditions using constitutional models formulated in two-dimensional (2D) finite element program.

The THM formulation for unsaturated porous media is presented first. The developed program incorporates a nonlinear elastic model based on Duncan (1970) in which compatibility with the concept of the state surface of void ratio is ensured to describe the volumetric behavior (Gatmiri, 1997). The water transfer equation in the case of an unsaturated soil is established by considering both the liquid phase and the vapor phase (Gatmiri, 1997). This is based on the approach of Philip and de Vries (1957), which takes into account the transfer of water vapor and the liquid phase under the effect of temperature gradients from a realistic geotechnical viewpoint. The equations for the air movement are then introduced. The effect of the presence of heat in unsaturated porous media is taken into account as well.

A soil-atmosphere model, which is based on energy exchange of soil-atmosphere system is then introduced. This model was used to describe and predict the evaporation rate. The soil-atmosphere model facilitates the determination of the hydraulic and thermal conditions of water on the surface of the soil. The boundary conditions on the surface depend on atmospheric (environmental) parameters (air temperature, net radiation, relative humidity, and wind speed) on one hand, and soil conditions (temperature and suction) on the other hand.

Finally, the adopted method of numerical analysis is presented.

3.2 Numerical studies for THM analysis

Numerical studies in thermo-hydro-mechanical (THM) geo-materials at Centre deskinment et de Recherché en Mécanique des Sols (CERMES) in Paris were initiated to address the problem of nuclear waste storage at great depth, regarding the engineered and geological barriers. This research led to the development of the finite element code, θ-STOCK, incorporating THM coupling in storage barriers (Gatmiri, 1997). The code allows modeling of THM behavior of saturated and unsaturated porous media.

Based on the results of experimental investigations of the non-isothermal behavior of unsaturated soils, Gatmiri (1997) proposed accounting for the transfer of liquid, vapor and gas phases under the effect of the moisture and temperature gradients in a deformable unsaturated soil.

The proposed approach deliberately ignored the microscopic level, assuming that the concepts and principles of continuum mechanics are applicable with measurable macroscopic quantities. The thermal, hydraulic and mechanical loads are considered. Therefore, the studied fields are the displacement of the porous medium, the pressure of the fluid and gas (including water vapor and dry air), and the porous medium temperature. The three aspects, thermal, hydraulic and mechanical phenomena, interact strongly and are treated as fully coupled phenomena. Thus, a strict thermo-hydro-mechanical connection is fully established for geo-environmental applications.

The porous medium is constituted of three continuous phases: a deformable porous medium with connected pores, and two fluids which are present in various forms (liquid, vapor, and dry air). Thermal, hydraulic and mechanical parameters are needed to define the medium. The independent variables used in this approach are: net stress, $\sigma_{ij} - \delta_{ij}\, p_g$; suction, $p_g - p_{w;}$ and

temperature, T. Therefore, the describing fields of the porous medium consist of six unknowns: three displacements, u_x ($\underline{x}$, t), u_y ($\underline{x}$, t), u_z ($\underline{x}$, t); two pressures, p_1 ($\underline{x}$, t), p_2 ($\underline{x}$, t), i.e., pore water pressure, p_w ($\underline{x}$, t) and gas pressure including water vapor and dry air, p_g ($\underline{x}$, t); and Temperature, T ($\underline{x}$, t).

The main points of the approach developed by Gatmiri et al. (1993) are briefly presented first. This relates to heat transfer, moisture transfer, and a deformation in unsaturated porous medium. The thermal state surfaces of void ratio and degree of saturation, used to describe the coupled effects of temperature, moisture and the deformation of porous medium are briefly explained. The full form of the field equations and spatial and temporal discretizations, as well as the general algorithms of θ-STOCK and EVAP1 codes are presented.

In the developed formulation, two theories were modified and combined to describe the coupled behavior of unsaturated porous media under heating. On one hand, the nonlinear theory is extended to non-isothermal conditions (Gatmiri, 1997) to describe the non-isothermal behavior of unsaturated soils under the coupled effects of net stress and suction. In this extension, statements for state surfaces of void ratio and degree of saturation proposed by Gatmiri (1995) are used. On the other hand, the Philip and de Vries (1957) theory of heat and moisture transfer is modified to take into account the deformation of the porous medium. This fully coupled approach is presented in a new suction based formulation, which is more suitable for combination with the theory of deformation of unsaturated soils.

3.2.1 Constituent water

Moisture is composed of two phases: liquid water and water vapor. As indicated by Philip and de Vries (1957), the term "liquid transfer" is used for water transfer exclusively in liquid phase. The transfer of water vapor is called "Vapor transfer".

3.2.1.1 Moisture transfer (liquid water + water vapor)

The transfer of water vapor into an unsaturated soil was described based on the approach of Philip and de Vries (1957). The equations related to the transfer of liquid water and water vapor are combined as below (Gatmiri, 1997):

$$\frac{q}{\rho_w} = \frac{q_v}{\rho_w} + \frac{q_{liq}}{\rho_w} = V + U = -(D_T \nabla T - D_\theta \nabla \theta - D_w \nabla Z) \quad \text{Eq. 3.1}$$

where

D_T: thermal diffusivity of moisture, which is equal to the sum of heat diffusivities of liquid water and water vapor

D_θ: isothermal moisture diffusivity, which is equal to the sum of the isothermal diffusivities of liquid water and water vapor

$D_w \nabla Z$: gravitational part of the equation

Liquid phase transfer was described by Darcy's law, and

$$K_w = K_{wzo}\left[\frac{S_r - S_{ru}}{1 - S_{ru}}\right]^b \left(\frac{\mu_r}{\mu_T}\right) \quad \text{Eq. 3.2}$$

where

K_w: hydraulic conductivity

$K_{wzo} = a \cdot 10^{\alpha e} =$ initial hydraulic conductivity in Z direction

S_r: saturation degree of the soil

S_{ru}: residual saturation degree of the soil

μ_r: dynamic viscosity of water at any arbitrary reference temperature

μ_T: dynamic viscosity of water at any temperature

a, b & α: constants

A hydraulic conductivity variation pattern versus temperature and degree of saturation is shown in Figure 3.1.

3.2.1.2 Conservation of the mass of moisture (liquid water + water vapor)

The equation of moisture mass conservation is written in a similar way to the moisture transfer:

$$\frac{\partial(\theta\rho_w+(n-\theta)\rho_v)}{\partial t} = \frac{\partial(nS_r\rho_w+n(1-S_r)\rho_v)}{\partial t} = -div(\rho_w(U+V)) \qquad \text{Eq. 3.3}$$

where

V: velocity of the water vapor

U: velocity of the liquid water

θ: volumetric water content

n: porosity

S_r: degree of water saturation

ρ_w and ρ_v: densities of water and vapor, respectively.

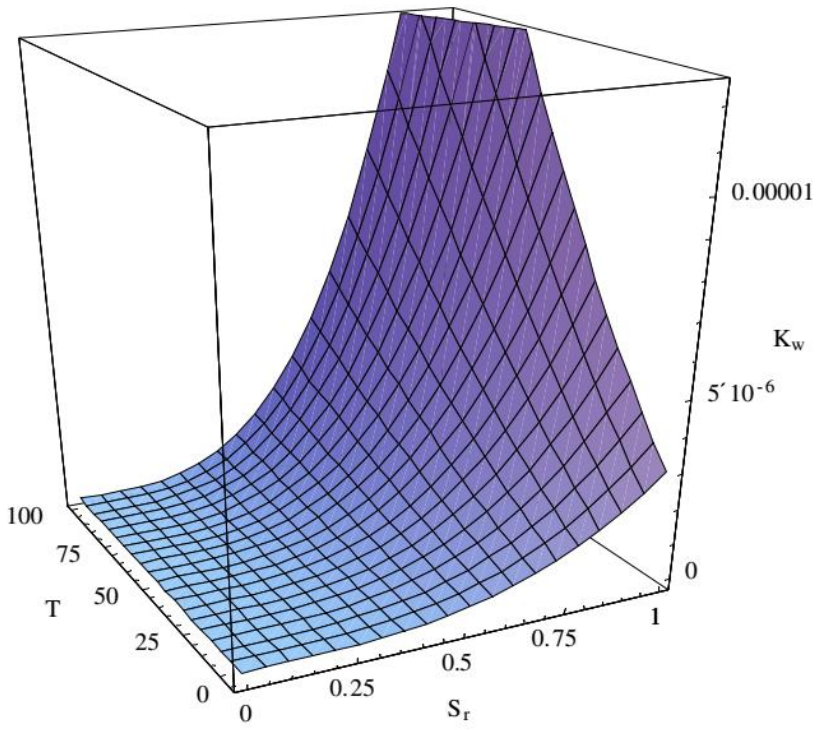

Figure 3.1 Water permeability (m/s) variation with temperature and degree of saturation (Gatmiri and Arson, 2008).

The introduction of the thermal state surfaces of degree of saturation and void ratio, is an important aspect of the approach developed by Gatmiri and Delage (1995). These surfaces are described in the following sections. The thermal state surface of saturation degree connects the variation of the degree of saturation to the states of the suction, temperature and net stress.

The concept of the water retention curve, i.e. soil water characteristic curve (SWCC), which considers the effect of suction on the change of water content, is extended to consider the variations of temperature and net stress in the soil.

By combining Equations (3.1) and (3.3), the final form of the differential equation for moisture transport in unsaturated soil is obtained as:

$$nS_r\left(\frac{\partial \rho_w}{\partial T}|_{P_w=cte}\right)\frac{\partial T}{\partial t} + nS_r\left(\frac{\partial \rho_w}{\partial P_w}|_{T=cte}\right)\frac{\partial P_w}{\partial t} + (\rho_w - \rho_{v)}n\frac{\partial S_r}{\partial t} + \left(S_r\rho_w + \rho_v(1-S_r)\right)\frac{\partial n}{\partial t}$$

$$+ n(1-S_r)\frac{\partial \rho_v}{\partial t} = div(\rho_w D_w \nabla Z) + div(\rho_w D_T \nabla T) + div(\rho_w D_p \nabla(P_g - P_w))$$

Eq. 3.4

3.2.2 Constituent air

3.2.2.1 Air transfer

Considering the effects of the gradients of pressure and temperature on air flow in a THM analysis, the velocity of gas (including water vapor and dry air) in unsaturated soil is described by following equation:

$$V_g = -K_g\beta_{pg}\nabla T - K_g\left(\nabla\left(\frac{P_g}{\gamma_g}\right) + \nabla Z\right) \qquad \text{Eq. 3.5}$$

where

$V_g = \frac{q_g}{\rho_g}$: velocity vector

q_g: gas flux vector

ρ_g: gas density

K_g: gas permeability

P_g: gas pressure

and

γ_g: specific weight of gas

In these equations, it is assumed that the gas pressure depends on the temperature. The gas permeability of the medium, K_g, depends on particle size, pore distribution, soil type, and degree of saturation (Lloret and Alonso 1980; Gatmiri 1992, 1997; Thomas and He 1995; Thomas et al., 1998) as:

$$K_g = c\frac{\gamma_g}{\mu_g}\left[e\left(1-S_r\right)\right]^d \qquad \text{Eq. 3.6}$$

where

μ_g: gas viscosity

e: void ratio

c and d: constants

A diagram of the variation of the gas permeability as a function of the void ratio, e, and the degree of saturation, S_r, is shown in Figure 3.2.

3.2.2.2 Air mass Conservation

The differential equation of the air mass conservation is written as (Gatmiri, 1997):

$$\frac{\partial}{\partial t}\left[n\rho_g\left(1-S_r+HS_r\right)\right] = -\mathrm{div}\left(\rho_g V_g\right) - \mathrm{div}\left(\rho_g HU\right) + \rho_w \mathrm{div}V \qquad \text{Eq. 3.7}$$

where

H: Henry's constant, which corresponds to the dissolution of air in water.

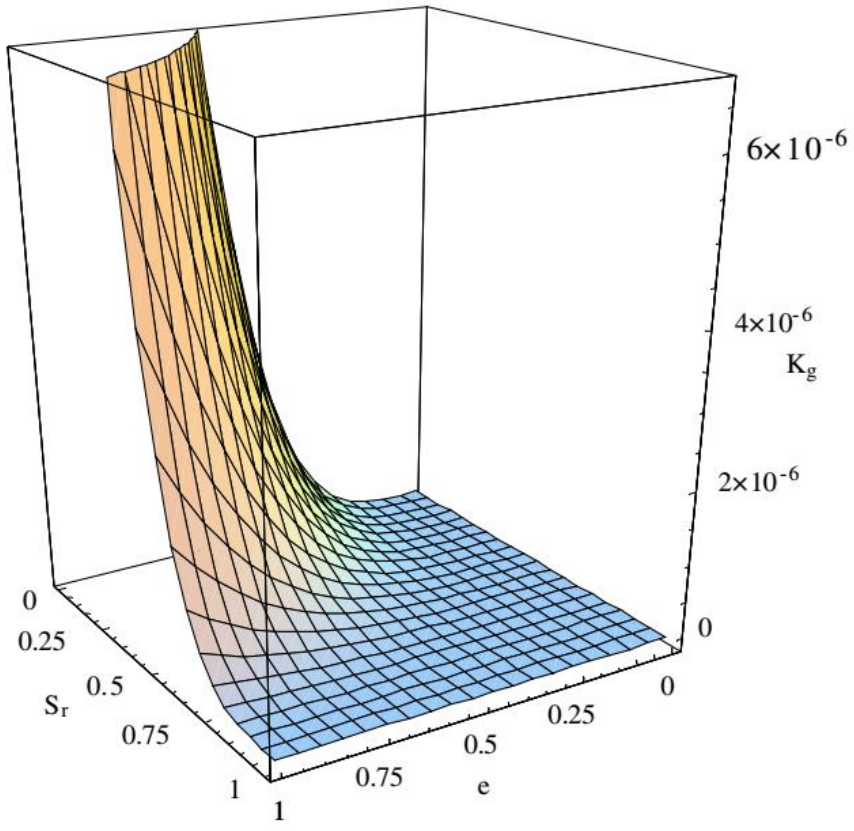

Figure 3.2 Gas permeability (m/s) variation with temperature and degree of saturation (Gatmiri and Arson, 2008).

The other terms were defined before.

The first term on the right hand side of Eq. 3.7 is related to the flow of gas due to the gradient of gas pressure, and the second term describes the movement of the air, which was dissolved in water. The vapor loss due to gas condensation is represented by the third term. Thus, the general partial differential equation of gas transfer in unsaturated soil can be deduced as:

$$\rho_g\left(1-S_r(1-H)\right)\frac{\partial n}{\partial t}+n\left(1-S_r(1-H)\right)\frac{\partial \rho_g}{\partial t}-(1-H)n\rho_g\frac{\partial S_r}{\partial t}=$$

$$\mathrm{div}\left[\left(K_g\rho_g\beta_{Pg}+H\rho_g D_{Tw}-\rho_w D_{TV}\right)\nabla T\right]+\mathrm{div}\left[\left(K_g\rho_g/\gamma_g-H\rho_g D_{Pw}+\rho_w D_{PV}\right)\nabla P_g\right]$$

$$+\mathrm{div}\left[\left(H\rho_g D_{Pw}-\rho_w D_{Pv}\right)\nabla P_w\right]+\mathrm{div}\left[\left(K_g\rho_g+H\rho_g D_w\right)\nabla Z\right] \qquad \text{Eq. 3.8}$$

3.2.3 Behavior of porous medium

Considering the two state variables of suction and net stress, equilibrium equation, and constitutive law of a non-linear and non-isothermal medium are based on the equations as are presented in the following.

3.2.3.1 Equilibrium equation

$$(\sigma_{ij}-\delta_{ij}p_g)_{,j}+p_{g,j}+b_i=0 \qquad \text{Eq. 3.9}$$

where

σ_{ij}: total stress

δ_{ij}: Kronecker delta

b_i: body force

3.2.3.2 Incremental behavior law

For small deformations, the law of behavior of an unsaturated porous medium, under the effect of heat and suction is given by the following equation:

$$d(\sigma_{ij}-\delta_{ij}p_g)=D\,d\varepsilon-F\,d(p_g-p_w)-C\,dT \qquad \text{Eq. 3.10}$$

where

$$F = DD_s^{-1} \quad \text{with} \quad D_s^{-1} = \beta_s m \quad \text{in which} \quad \beta_s = \frac{1}{1+e}\frac{\partial e}{\partial (p_g - p_w)}$$

$$\text{and } m = \begin{bmatrix} 1 & 1 & 0 \end{bmatrix}$$

$$C = DD_t^{-1} \quad \text{with} \quad D_t^{-1} = \beta_t m \quad \text{in which} \quad \beta_t = \frac{1}{1+e}\frac{\partial e}{\partial T}$$

D is a non-linear stress-strain matrix, dependent on temperature and stress.

3.2.3.3 State surface of void ratio

To calculate the volumetric deformation modulus, volumetric strain can be taken into account by means of a state surface of void ratio, which depends on the stress, suction and temperature. Using the same approach as Gatmiri (1995), the formulation of the state surface of void ratio is proposed as (Gatmiri, 1997):

$$e = \frac{1+e_0}{\exp\left[\dfrac{\left[a\left(\dfrac{\sigma - p_g}{p_{atm}}\right) + b\left(1 - \dfrac{\sigma - p_g}{\sigma_c}\right)\left(\dfrac{p_g - p_w}{p_{atm}}\right)\right]^{1-m}}{K_b(1-m)}\right]\exp[c_e(T - T_0)]} - 1 \qquad \text{Eq. 3.11}$$

With this equation, the compatibility with the non-linear behavior of the soil is also provided. Figure 3.3 shows an example of this state surface.

3.2.3.4 State surface of degree of saturation

Although the stress-strain behavior is already coupled to the temperature, the description of the coupling of the volumetric water content to temperature is also necessary for modeling unsaturated soil subjected to the stress and suction.

Based on the experimental data, the state surface of degree of saturation, which is shown in Figure 3.4, is proposed as the following equation.

$$sr = 1 - [a_s + b_s(\sigma - p_g)][1 - \exp(c_s(p_g - p_w))]\exp(d_s(T - T_0)) \quad \text{Eq. 3.12}$$

a_s, b_s, c_s and d_s are constants.

T_0 is reference temperature and the other terms were already defined.

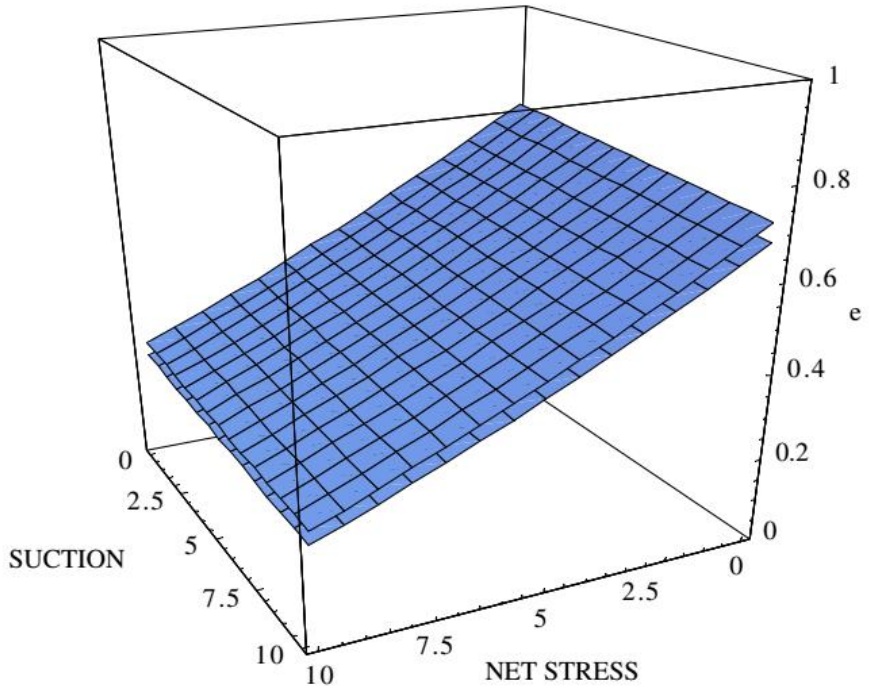

Figure 3.3 State surface of void ratio as a function of suction and net stress (Gatmiri and Arson, 2008).

3.2.4 Heat Equations

Transferring sensible and latent heat in an unsaturated porous medium is described as:

$$Q = -\lambda grad T + \rho_w h_{fg} V_v + \rho_v V_g h_{fg} \left[C_{Pw} \rho_w V_w + C_{pv} \rho_w V_v + C_{pg} \rho_g V_g \right] (T - T_0)$$

Eq. 3.13

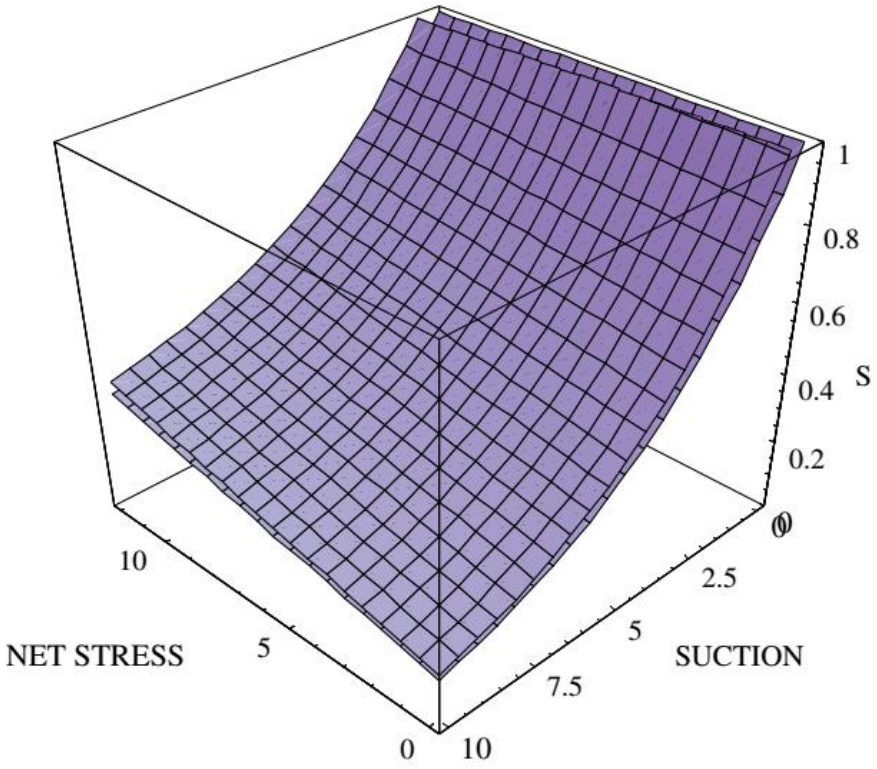

Figure 3.4 State Surface of degree of saturation as a function of suction and net stress (Gatmiri and Arson, 2008).

where

C_{pw}, C_{pv} and C_{pg}: the specific capacities of water, water vapor and gas, respectively

T_0: a reference temperature

h_{fg}: the latent heat of vaporization

λ: the coefficient of Fourier heat diffusion which varies according to the following equation:

$$\lambda = (1-n)\lambda_s + \theta\lambda_w + (n-\theta)\lambda_v \qquad \text{Eq. 3.14}$$

where λ_s, λ_w, and λ_v are the heat diffusion coefficients of the soil, water and water vapor, respectively.

In Eq. 3.13, the first term is related to heat flow by conduction, both of the following terms represent the phenomenon of evaporation, and the latter describes the heat flux convection of liquid, vapor, and gas phases. The equation of energy conservation in a porous medium may be expressed as:

$$\frac{\partial \varphi}{\partial t} + \mathrm{div}Q = 0 \qquad \text{Eq. 3.15}$$

where Q is heat flow and φ is the volumetric bulk heat content of medium, which can be defined as:

$$\varphi = C_T\left(T - T_0\right) + (n-\theta)\rho_v h_{fg} \qquad \text{Eq. 3.16}$$

The specific heat of mixture, C_T, is determined by the specific heat of each phase, based on volume fraction of each phase (de Vries, 1958; Fredlund & Rahardjo, 1993; among others):

$$C_T = (1-n)\rho_s C_{PS} + \theta\rho_w C_{Pw} + (n-\theta)\rho_v C_{PV} + (n-\theta)\rho_g C_{Pg} \qquad \text{Eq. 3.17}$$

The general differential equation for heat transfer in an unsaturated porous medium is obtained by combining equations (3-14) to (3-17):

$$C_T \frac{\partial T}{\partial t} + \left(T - T_0\right)\frac{\partial C_T}{\partial t} + \left(1 - S_r\right)\rho_v h_{fg}\frac{\partial n}{\partial t} - n\rho_v h_{fg}\frac{\partial S_r}{\partial t} + n\left(1 - S_r\right)h_{fg}\frac{\partial \rho_v}{\partial t}$$

$$-\mathrm{div}[\lambda(\theta)\nabla T] + C_{Pw}\rho_w \mathrm{div}\left[\left(-D_{Tv}\nabla T - D_{Pv}\nabla\left(P_w - P_g\right)\right)\left(T - T_0\right)\right] +$$

$$C_{Pv}\rho_w \mathrm{div}\left[\left(-D_{Tv}\nabla T - D_{Pv}\nabla\left(P_w - P_g\right)\right)\left(T - T_0\right)\right] + \qquad \text{Eq. 3.18}$$

$$C_{Pg}\mathrm{div}\left[\left(-\rho_g K_g \beta_{Pg}\nabla T - \rho_g K_g\left(\nabla\rho_g / \gamma_g + \nabla Z\right)\right)\left(T - T_0\right)\right] +$$

$$\rho_w h_{fg}\mathrm{div}\left[-D_{Tv}\nabla T - D_{Pv}\nabla\left(P_w - P_g\right)\right] +$$

$$h_{fg}\mathrm{div}\left[-\rho_v K_g \beta_{Pg}\nabla T - \rho_v K_g\left(\nabla P_g / \gamma_g + \nabla Z\right)\right] = 0$$

3.2.5 Initial Conditions

The initial conditions of the problem are determined from the observation data. The initial vertical stress is calculated from the weight of soil, and/or additional vertical loads. The initial conditions of the considered problem are as follows:

$$t = 0\begin{cases} T(x,y,t) = T_0(x,y) \\ S_r(x,y,t) = S_{r0}(x,y) \\ F(x,y,t) = F_0(x,y) \end{cases} \qquad \text{Eq. 3.19}$$

3.2.6 Boundary conditions

There are four boundary conditions of thermal, hydraulic, mechanical, and air for a thermo-hydro-mechanical problem. For each component of the medium, two types of boundary conditions exist: Dirichlet on boundaries with unknown heads, and Neumann on boundaries with unknown flows.

3.2.6.1 Mechanical boundary conditions

The displacement boundary conditions of the solid are considered on the part Γ_u of Γ part of the domain Ω; and the force boundary conditions are considered on the Part Γ_σ of Γ part of the domain Ω. The following relation links these two parts of the boundary Γ together:

$$\Gamma = \Gamma_\sigma \cup \Gamma_u \quad and \quad \Gamma_\sigma \cap \Gamma_u = \emptyset$$

The part Γ_u of the boundary is devoted to the boundary conditions corresponding to the displacement of the solid. This takes the following form:

$$u(x,t) = U^*(x,t) \qquad \forall x \in \Gamma_u$$

We can assume that this displacement is equal to zero. Otherwise, it would be necessary that the equilibrium condition between the created stress field and the initial stress field be verified. In general, these displacement boundary conditions correspond to conditions at the interface with the external domain of the problem.

• Stress boundary conditions

It is possible to impose distributed surface forces such as T* on the Γ_σ part of the border. We define the stress vector field as follows:

$$\mathrm{T} - \sigma.\mathrm{n} = 0$$

n is normal outward to the boundary. The boundary condition is then:

$$\mathrm{T}(\mathrm{x},\mathrm{t}) = \mathrm{T}^*(\mathrm{x},\mathrm{t}) \qquad \forall \mathrm{x} \in \Gamma_\sigma$$

3.2.6.2 Water boundary Conditions

There are two types of water boundary conditions: Γ_h, which corresponds to the water head, and Γ_{Qh} which corresponds to the imposed water flow. They are represented by:

$$\Gamma = \Gamma_h \cup \Gamma_{Qh} \qquad \text{and} \qquad \Gamma_h \cap \Gamma_{Qh} = \emptyset$$

Pressure boundary condition

Water pressures are boundary conditions that are imposed on the part Γ_w of the boundary Γ. They are expressed by P_w^*:

$$P_w(x,t) = P_w^*(x,t) \qquad \forall x \in \Gamma_w$$

Flux boundary condition

The imposed flow is represented as a function of the recharge:

$$\rho_w(U+V)n - \left(\bar{q}_{(w+v)}\right) = 0 \qquad \forall x \in \Gamma_{Q(w+v)}$$

where $\bar{q}_{(w+v)}$ is the moisture flux (water + vapor).

3.2.6.3 Air boundary conditions

These conditions are for imposed air pressures or flows. By considering a third part of the boundary in two parts of Γ_g and Γ_{Qg}, these conditions are written as:

$$\Gamma = \Gamma_g \cup \Gamma_{Qg} \qquad \text{and} \qquad \Gamma_g \cap \Gamma_{Qg} = \emptyset$$

Gas pressure boundary condition

Generally this occurs on free surfaces where the pressure is equal to the atmospheric pressure as below.

$$P_g(x,t) = P_g^*(x,t) \quad \forall x \in \Gamma_g$$

Gas flux boundary condition

On the part Q_g of the boundary Γ, flows imposed depending on the speed of the air are as follows:

$$\rho_a(V_g + H_c U)n - (\bar{q}_g) = 0 \qquad \forall x \in \Gamma_{Qg}$$

where $\bar{q}_g$ is the gas flow.

3.2.6.4 Thermal boundary conditions

The fourth part of the boundary Γ is divided by two: Γ_T for temperature, and Γ_{QT} for heat flow, with relation as below:

$$\Gamma = \Gamma_T \cup \Gamma_{QT} \qquad \text{and} \qquad \Gamma_T \cap \Gamma_{QT} = \emptyset$$

Q_T is the heat flow.

Temperature boundary condition

On the part Γ_T of the boundary, boundary condition is as below:

$$F(x,t) = F^*(x,t) \qquad \forall x \in \Gamma_T$$

Heat flow boundary condition

The heat flow can be imposed and may be zero. On the part Γ_{QT}, the boundary condition is written as:

$$(Q)n - (\bar{q}_h) = 0 \qquad \forall x \in \Gamma_{QT}$$

3.3 ATMOSPHERIC COUPLING AND ESTIMATING EVAPORATION

Penman (1948) proposed a method of calculating potential evaporation as follows:

$$E = \frac{\Gamma Q + \nu E_a}{\Gamma + \nu} \qquad \text{Eq. 3.20}$$

where

E: potential evaporation per unit time (mm/day)

E_a: $f(u)(e_{sa}-e_a)$

e_{sa}: saturation vapor pressure at the mean air temperature, usually mm.Hg.

e_a: vapor pressure of the air above the evaporating surface, usually mm.Hg.

f(u): $0.35\ (1+0.15U_a)$

U_a: wind speed, usually km/day

Q: heat budget or all net radiation (mm/day)

Γ: slope of the saturation vapor pressure versus temperature curve at the mean temperature of the air

ν: psychrometric constant

Wilson (1990) proposed a modified Penman (1948) approach for atmospheric coupling and estimating actual evaporation. He combined vapor transfer equation with heat transfer equation to determine actual evaporation from soil surface. This method needs atmospheric data like air temperature, net radiation, humidity and wind speed. He presented the "modified Penman equation" as below.

$$E = \frac{\Gamma Q + \nu E_a}{\Gamma + A\nu}$$ Eq. 3-21

where:

E: vertical evaporative flux (mm/day)

Γ: the slope of the saturation vapor pressure versus temperature curve at the mean temperature of the air

Q: net radiant energy available at the surface (mm/day)

ν: psychrometric constant

$E_a = f(u)P_a(B-A)$

$f(u)=0.35(1+0.15\ U_a)$: function dependent on wind speed, surface roughness, and eddy diffusion

U_a: wind speed (km/hr)

P_a: vapor pressure in the air above the evaporating surface

B: inverse of the relative humidity of the air

A: inverse of the relative humidity at the soil surface = $1/h_r$

In fact, Wilson (1990) added parameter "A" to consider unsaturated soil. In the equation presented by Wilson (1990), E is actual evaporation and parameter "A" is equal to the inverse of the relative humidity of the soil. When the soil is saturated, relative humidity is 1, which makes A=1, and the Wilson equation changes to the original Penman equation. Using Wilson equation, both potential evaporation and actual evaporation could be calculated and compared to daily based

experimental results. Usually, during the first few days, both potential and actual evaporations are the same, and evaporation is in stage I of evaporation curve, which was explained in section 2.2.3 in Chapter 2. Later on, actual evaporation decreases because either water supply or hydraulic condition decreases, and stages II and III of the evaporation curve start.

The modified Penman (1948) equation proposed by Wilson (1990) was used in soil-atmosphere model presented in this study.

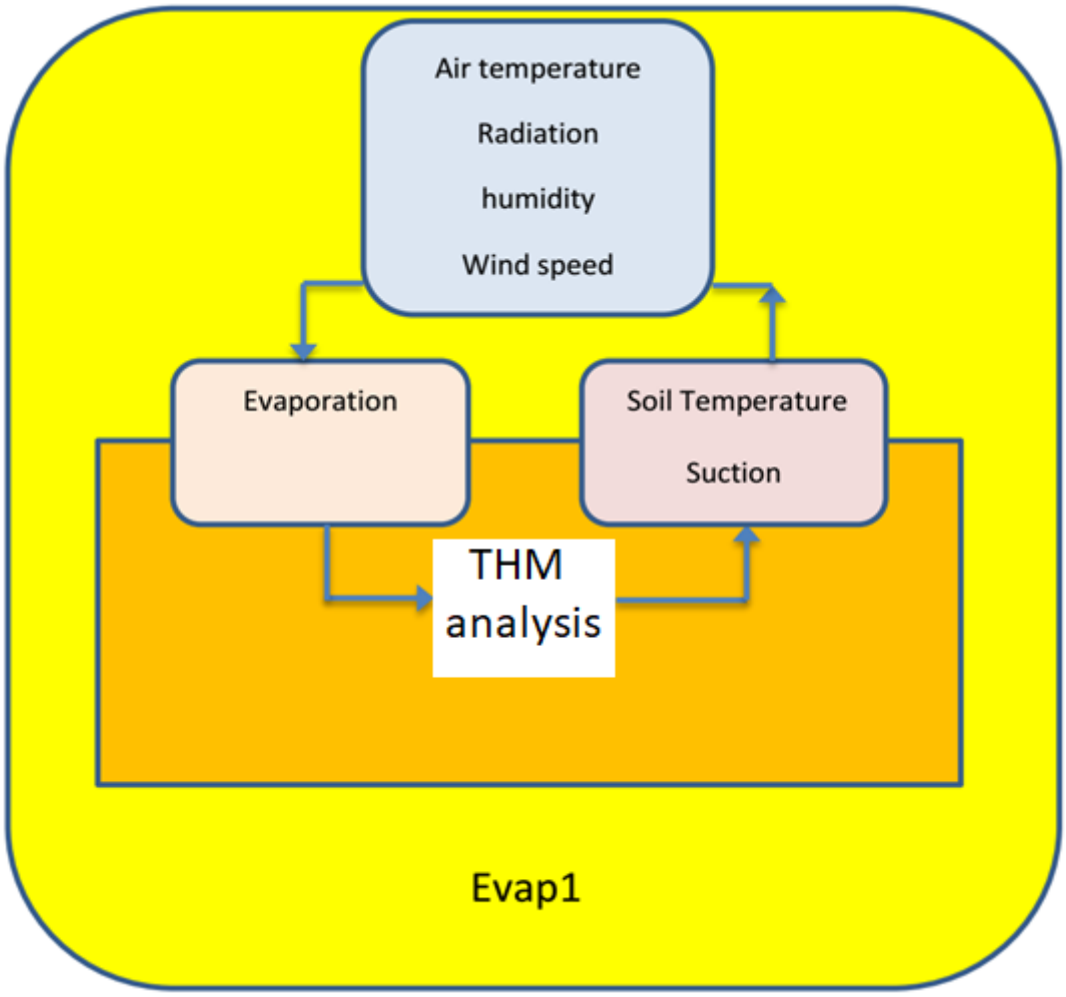

Figure 3.5 Schematic Soil-Atmosphere modeling.

3.3.1 Soil-atmosphere model

This section presents the soil-atmosphere model used in the code EVAP1 to facilitate estimating evaporation from unsaturated soil. The inputs of the model are

A) Atmospheric data including air temperature, net radiation, humidity, and wind speed

B) Temperature and suction in soil surface resulted from THM analysis.

A schematic of this modeling is shown in Figure 3.5.

3.3.2 Thermal boundary conditions in the case of Soil-Atmosphere interaction

The thermal boundary conditions at the soil-atmosphere interface are determined from meteorological data.

3.3.3 Water boundary conditions in the case of Soil-Atmosphere interaction

Soil vapor pressure can be calculated as the product of the saturation vapor pressure at soil surface temperature and the relative humidity at the soil surface. Saturated vapor pressure can be calculated by:

$$e_{vs} = 610,8 \exp\left(\frac{17,27T}{T+237,3}\right) \quad \text{Eq. 3.22}$$

The relative humidity of the surface can be calculated using the soil suction:

$$h_r = \exp(\frac{\psi g}{RT}) \quad \text{Eq. 3.23 where}$$

ψ: total suction at the soil surface, N/m^2

g: gravity acceleration, 9.81 m/s^2

R: gas constant = 8.314 J/mol.Kelvin

T: temperature, Kelvin

The water vapor pressure at the surface is therefore calculated as:

$$e_s = h_r e_{vs} \qquad \text{Eq. 3.24}$$

Soil temperature is used in Eq. 3.23 to estimate relative humidity, which is used in Eq. 3.21 to estimate actual evaporation.

Figure 3.6 shows the boundary conditions of the model.

3.4 DISCRETIZATION OF THE SYSTEM

Given the complexity of partial differential equations governing the proposed model, the development of analytical solutions is difficult, even for simple situations. The Galerkin method widely used in finite element analysis was used to solve the system of the established equations, considering the previously mentioned general boundary conditions.

3.4.1 Spatial discretization

The method of weighted residuals is applied and the Galerkin type of weighting functions are used to discretize the spatial domain Ω. The overall shape of the matrix equations, represented in terms of the unknowns on the nodes, is as follows:

$$\begin{bmatrix} 0 & 0 & 0 & 0 \\ 0 & -[K_{TT}] & -[K_{Tw}] & -[K_{Ta}] \\ 0 & -[K_{wT}] & -[K_{ww}] & 0 \\ 0 & -[K_{aT}] & -[K_{aw}] & -[K_{aa}] \end{bmatrix} \begin{Bmatrix} U \\ T \\ P_w \\ P_a \end{Bmatrix} + \begin{bmatrix} [R] & [R_{uT}] & [R_{uw}] & [R_{ua}] \\ [C_{TU}] & [C_{TT}] & [C_{Tw}] & [C_{Ta}] \\ +[C_{wu}] & +[C_{wT}] & +[C_{ww}] & +[C_{wa}] \\ [C_{au}] & [C_{aT}] & [C_{aw}] & [C_{aa}] \end{bmatrix} \begin{Bmatrix} \dot{U} \\ \dot{T} \\ \dot{P}_w \\ \dot{P}_a \end{Bmatrix} = \begin{Bmatrix} \dot{F}_\sigma \\ F_T \\ F_w \\ F_a \end{Bmatrix}$$

Eq. 3.25

The terms of this matrix are presented in Appendix A.

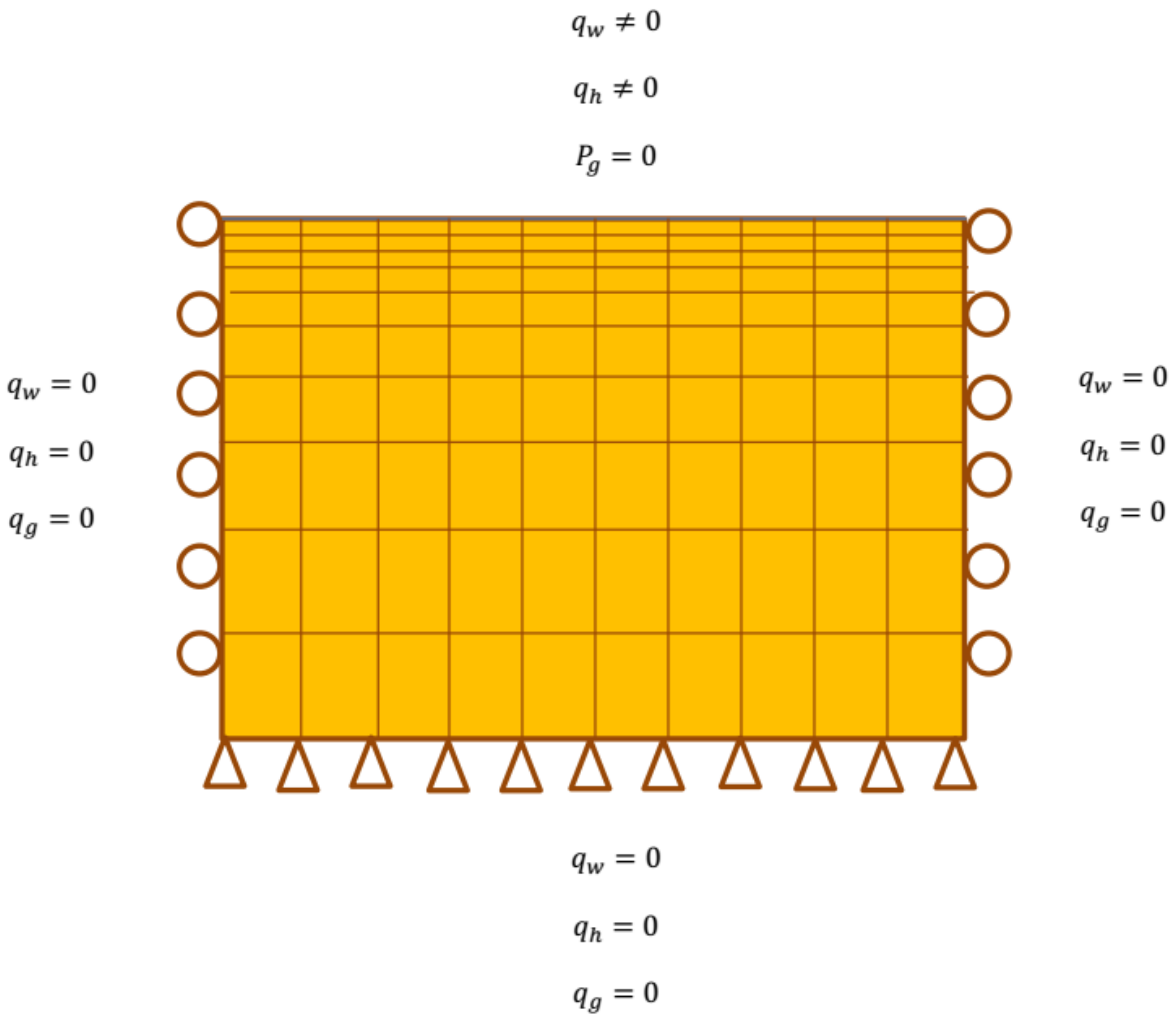

Figure 3.6 Boundary conditions of soil-atmosphere model,

q_w = water flux, q_h = heat flux, q_g = gas flux, and P_g = gas pressure

3.4.2 Temporal Discretization

The time discretization is described by the following equations:

$$\int_{t0}^{t_1} u(t)dt = \left[(1-\theta)u_o + \theta u_1\right]\Delta t = \left[u_0 + \theta \Delta u\right]\Delta t \qquad \text{Eq. 3.26}$$

$$\int_{t_0}^{t_1} \dot{u}(t)dt = \Delta u \qquad \text{Eq. 3.27}$$

where u_0 and u_1 are the values of the variable u at times t_0 and t_1, respectively. The time step is $\Delta t = t_1 - t_0$ and θ indicates the type of interpolation; θ = 0 corresponds to the explicit (forward) method. This method does not give satisfactory results for poorly conditioned differential equations. Taking θ = 1, the resolution becomes implicit (backward) method, and by taking θ = 1/2, Crank-Nicholson algorithm is obtained. Thus the choice of θ affects the stability and the accuracy of the algorithm. For θ ≥1/2 the solution is unconditionally stable regardless of the initial conditions.

The vector of external loads $(\{rr\}_{k+1})_i$ imposed during the current increment (between t_k and t_{k+1}) is calculated in the subroutine bargo, which uses the subroutines loadnode, flotnode, flownode, floanode, flowevapnode and flotevapnode.

Calculations of nodal loads due to imposed surface physical load, and surface loads due to temperature, water, and air flows are performed in subroutines "loadnode", "flotnode", "flownode", and "floanode" respectively. In "loadnode" the calculation is immediate, since it directly imposes stress increments to the concerned nodes. In subroutines "flotnode", "flownode", and "floanode" force vector is not stored. The calculation is performed from flow imposed on the current load increment (load step) and the increment of previous load.

The nodal loads due to imposed surface water and temperature flows due to evaporation (for water and heat transfer respectively) are calculated in new subroutines of “flowevapload” and “flotevapnode”.

3.4.3 Stability and Accuracy

The stability and accuracy conditions of the solution algorithm of the equations for completely coupled unsaturated soil were described in detail by Gatmiri and Magnin (1994) and Gatmiri et al. (1998). For isoparametric quadrilateral elements, which are used in the program, the accuracy criteria are set as follows:

The criteria for the lower limit for water transfer:

Δt should be the biggest of three amounts as below.

$$\Delta t \geq \frac{\alpha_3 n^2 (\Delta h)^2}{6\theta C_w (n^2+1)}, \Delta t \geq \frac{\alpha_3 n^2 (\Delta h)^2}{3\theta C_w (2n^2-1)}, \Delta t \geq \frac{\alpha_3 n^2 (\Delta h)^2}{3\theta C_w (2-n^2)} \qquad \text{Eq. 3.28}$$

The criteria for the lower limit for air transfer:

Δt should be the biggest of three amounts as below.

$$\Delta t \geqslant \frac{\beta_2 n^2 (\Delta h)^2}{6\theta C_a (n^2+1)}, \Delta t \geqslant \frac{\beta_2 n^2 (\Delta h)^2}{3\theta C_a (2n^2-1)}, \Delta t \geqslant \frac{\beta_2 n^2 (\Delta h)^2}{3\theta C_a (2-n^2)} \qquad \text{Eq. 3.29}$$

where

$$\alpha_3 = -e g_2 - S_r g_3 \quad \text{and} \quad \beta_2 = (1-S_r)(g_4 - g_3) - e(g_2 - g_1)$$

$$g_1 = \frac{\partial S_r}{\partial(\sigma - u_a)}, g_2 = \frac{\partial S_r}{\partial(u_a - u_w)}, g_3 = \frac{\partial e}{\partial(\sigma - u_a)}, g_4 = \frac{\partial e}{\partial(u_a - u_w)} \qquad \text{Eq. 3.30}$$

Δh: the element size

θ: indicator of the interpolation type

It is important that a value should be selected for the lower limit to avoid spatial oscillations. These criteria depend on two state surfaces of void ratio and degree of saturation as well as their derivatives.

3.4.4 Time stepping

An adaptive time stepping scheme is used by the model to automatically calculate the size of the time step. The first time step is specified by the user. The time step is controlled by controlling magnitudes of minimum and maximum time steps, which are defined by the user in input file.

3.4.5 Variability of input parameters

Different parameters used in each run are as below. The parameters could vary depending on the investigated case.

No. of time steps

Max and min time step

Integration constant teta

Boundary conditions in x and y directions

Water, air, and temperature boundary conditions

Initial condition data

Unit weight of solid grains

Minimum and max daily relative humidity of the air

Minimum and max daily temperature of the air

Daily wind speed

Daily solar radiation

Number of days to simulate

Degrees latitude of the site

Soil cohesion

Soil internal friction degree

Soil bulk modulus

n coefficient in hyperbolic model

tensile strength of soil

initial temperature

initial saturation degree

horizontal and vertical hydraulic conductivity of soil

air conductivity

latent heat

heat capacities of soil, water and air

heat conductivities of soil, water and air

Residual saturation degree

Viscosity

State surface data

Initial values

Boundary conditions

3.4.6 Assumptions

There are some assumptions with any theory. The assumptions in the theory used in this study are as below.

Infinitesimal deformation of unsaturated porous media;

Elastic nonlinear behavior of porous media

The abovementioned were assumed considering the nature and thickness of used soils in soil covers and settlement in soil surface.

3.5 PROGRAM ALGORITHM

The main part of the program is managed directly by the module "Markaz", which is shown in Figure 3.7, which presents the general flowchart of the program. White subroutines are subroutines from θ-STOCK to do THM analysis. Some of them are modified for atmospheric coupling. Gray color distinguishes subroutines and functions for soil-atmosphere model.

The program is divided into five parts, and each part includes several subroutines with tasks as follow. Points 2, 3 and 5 are established for modeling soil-atmosphere interface.

1. Acquiring input data calculating initial conditions

2. Acquiring meteorological data

3. Calculation of boundary conditions on the soil-atmosphere boundary

4. Generating nodal loads and acquisition of data in the time steps

5. Generating nodal loads from boundary conditions of soil-atmosphere interface

6. Generating the overall stiffness matrix

7. Creating the system of equations of the final solution

8. Other calculations

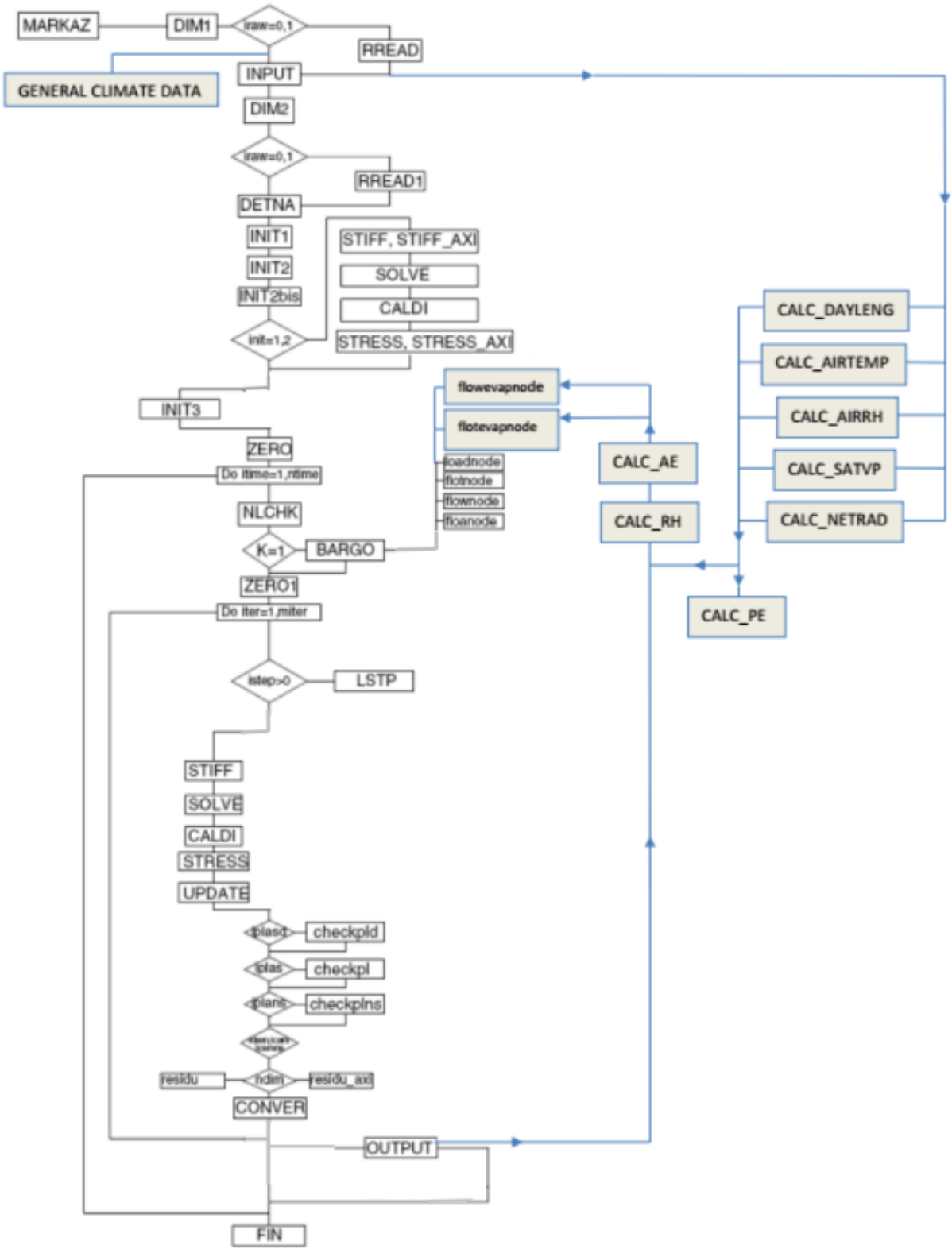

Figure 3.7 Flowchart of the program

It should be noted that the elementary stiffness matrices are calculated with different procedures called Stif4D (for dry elements), Stif4C (for saturated elements), and Stif4U (for unsaturated elements) in a plane strain configuration. Figure 3.8 shows a more detailed description of Stiff block, which is one of the main parts of the program.

3.6 SUBROUTINES AND FUNCTIONS

Appendix B presents a list of subroutines and functions of program EVAP1 and their functionality within the program and the tasks they accomplish. From total 64 subroutines and functions of EVAP1, the 31 Black written subroutines are intact subroutines of program θ-Stock. The 15 subroutines and functions that are written in red are the added ones. The 5 and 13 subroutines written in green and blue are modified and repeated subroutines, respectively.

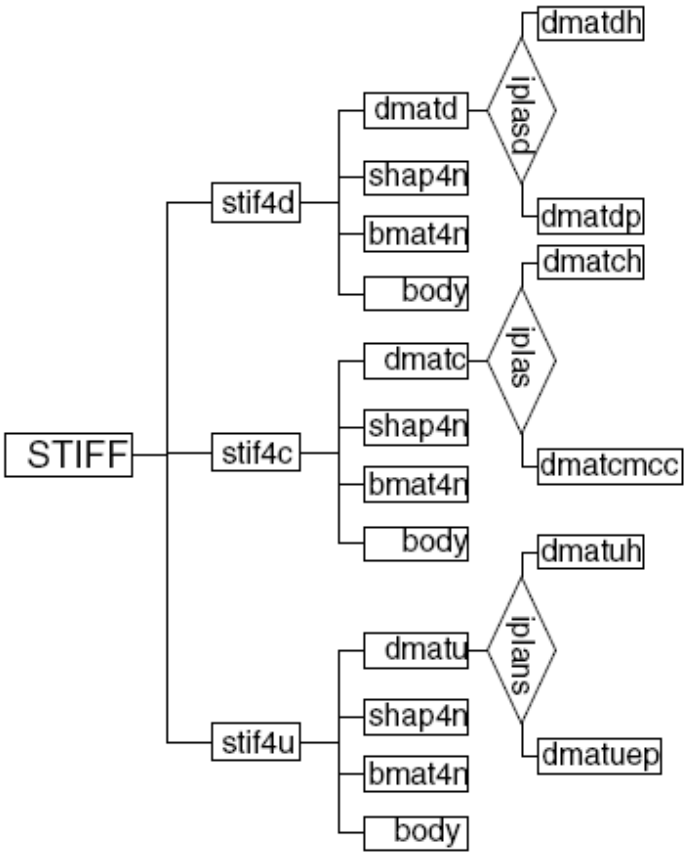

Figure 3.8 Flowchart to calculate the stiffness matrices for the three types of the elements.

3.7 SUMMARY

Based on the literature review of the different soil-atmosphere interaction models presented in Chapter 2, a method based on the energy exchange over ground was adopted for modeling the soil-atmosphere interaction. The soil-atmosphere model was coupled to THM analysis (Gatmiri, 1997) to develop EVAP1, a two-dimensional plane strain finite element program for thermo-hydro-mechanical analysis of evaporation from unsaturated soils.

The program includes four-noded drained, saturated and unsaturated elements. A hyperbolic model is used for drained and saturated elements. The state surface-hyperbolic model is used for unsaturated elements. The program considers hydraulic anisotropic soils and different boundary conditions considering state surfaces of void ratio and degree of saturation. It also considers element pressures (water and air) based on boundary values considering physical loading, air flow, water flow and heat flow conditions and atmospheric coupling. Atmospheric parameters of air temperature, net radiation, humidity, and wind speed are used on a daily basis to calculate potential and actual evaporations.

CHAPTER 4

VALIDATION OF THE PROGRAM AND NUMERICAL ANALYSES

4.1 INTRODUCTION

To verify program EVAP1, the soil column drying test of Wilson (1990), and soil column test of Yang and Yanful (2002) are used. The verified program is then used to conduct a parametric study in order to investigate the effects of variation in environmental parameters (i.e. air temperature, relative humidity, net radiation and wind speed) on evaporation. In each analysis, the magnitude of one parameter is varied while the magnitudes of all other environmental parameters are kept unchanged. Accordingly, the effects of varying the considered parameter on potential and actual evaporations are investigated.

In addition, a sensitivity analysis is performed to identify the environmental parameter that influences evaporation the most. Finally, further analyses are conducted to estimate evaporation with and without considering soil settlement, and the results are compared to investigate the effect of THM analysis considering soil settlement on the magnitude of evaporation from unsaturated soil.

4.2 SET OF DATA USED IN THE MODEL FOR UNSATURATED SOILS

The data set used for unsaturated soils are presented in Tables 4.1 to 4.3. The mechanical and model parameters for unsaturated soils are listed in Table 4.1.

Table 4.1 Mechanical and model parameters for unsaturated clay (Gatmiri, 1997) and sand (Ghasemzadeh, 2006)

Mechanical parameters		sand	clay
ν	Poisson coefficient	0.3	0.35

ρ_s	Solid grains density	2650 kg/m^3	2750 kg/m^3
K_l	Loading modulus number	878	125
K_b	Bulk modulus number	981	25
m	Void ratio state surface parameter	0.35	0.6
P_{atm}	Atmosphere pressure	102 kPa	102 kPa
a_e	Void ratio state surface parameter	67.6	1.5
b_e	Void ratio state surface parameter	6.39	0.15
c_e	Void ratio state surface parameter	-0.3e-3	-0.25e-3
d_e	Void ratio state surface parameter	0.33	0.63
σ_e	Void ratio state surface parameter	8e6	0.8e6
a_s	Degree of saturation state surface parameter	0.8	1
b_s	Degree of saturation state surface parameter	-0.2088e-4	-0.212e-14
c_s	Degree of saturation state surface parameter	-0.108855e-3	0.12e-7
d_s	Degree of saturation state surface parameter	0 .1e-4	0.1e-15

The thermal parameters pertinent to unsaturated soils are presented in Table 4.2.

Table 4.2 Thermal parameters for unsaturated clay (Gatmiri, 1997) and sand (Ghasemzadeh, 2008)

Thermal parameters		sand	clay
h_{fg} (J.kg^{-1})	Latent heat of vaporization	2.4e6	2.4e6
λ_a (J.m^{-1}.s^{-1}.°C^{-1})	Air thermal conductivity	0.0258	0.0258
λ_s (J.m^{-1}.s^{-1}.°C^{-1})	Solid grain thermal conductivity	2	2
λ_w (J.m^{-1}.s^{-1}.°C^{-1})	Water thermal conductivity	0.6	0.6
C_{ps} (J.kg^{-1}.s^{-1}.°C^{-1})	Specific heat capacity of soil	575	800

C_{pw} ($J.kg^{-1}.s^{-1}.°C^{-1}$)	Specific heat capacity of water	4180	4180
C_{pv} ($J.kg^{-1}.s^{-1}.°C^{-1}$)	Specific heat capacity of vapor	1870	1870
C_{pg} ($J.kg^{-1}.s^{-1}.°C^{-1}$)	Specific heat capacity of gas	1000	1000

The hydraulic parameters pertinent to unsaturated soils are presented in Table 4.3.

Table 4.3 Hydraulic parameters for unsaturated clay (Gatmiri, 1997) and sand (Ghasemzadeh, 2008)

Hydraulic parameters		sand	clay
K_{w0}	Saturated permeability (m/s)	1.2e-9	0.132e-9
α	Coefficient	5	5
d	Coefficient	3	3
S_{ru}	Residual degree of saturation	0.05	0.05

4.3 DRYING SOIL COLUMN TEST OF WILSON (1990)

Wilson (1990) performed a series of column tests on a sandy material. Two columns of Beaver Creek sand, initially close to saturation, were allowed to dry over a 42-day period. The columns were placed in an environmental chamber, and the change in mass was monitored daily to determine the actual evaporation from the columns. The columns were 30 cm in height. The air temperature was kept at 38 degrees Celsius and the air relative humidity was measured continually along with temperatures and relative humidity within the soil columns.

Figure 4.1 shows the configuration of the column test of Wilson (1990). Figures 4.2 and 4.3 present the hydraulic and thermal properties of Beaver Creek sand, respectively. Figure 4.4 shows the curves of measured evaporation versus time for the two test columns of Wilson (1990). Figure

4.5 presents experimental results of Wilson (1990) and the modeling results of program EVAP1 for potential and actual evaporations during the test period of 42 days.

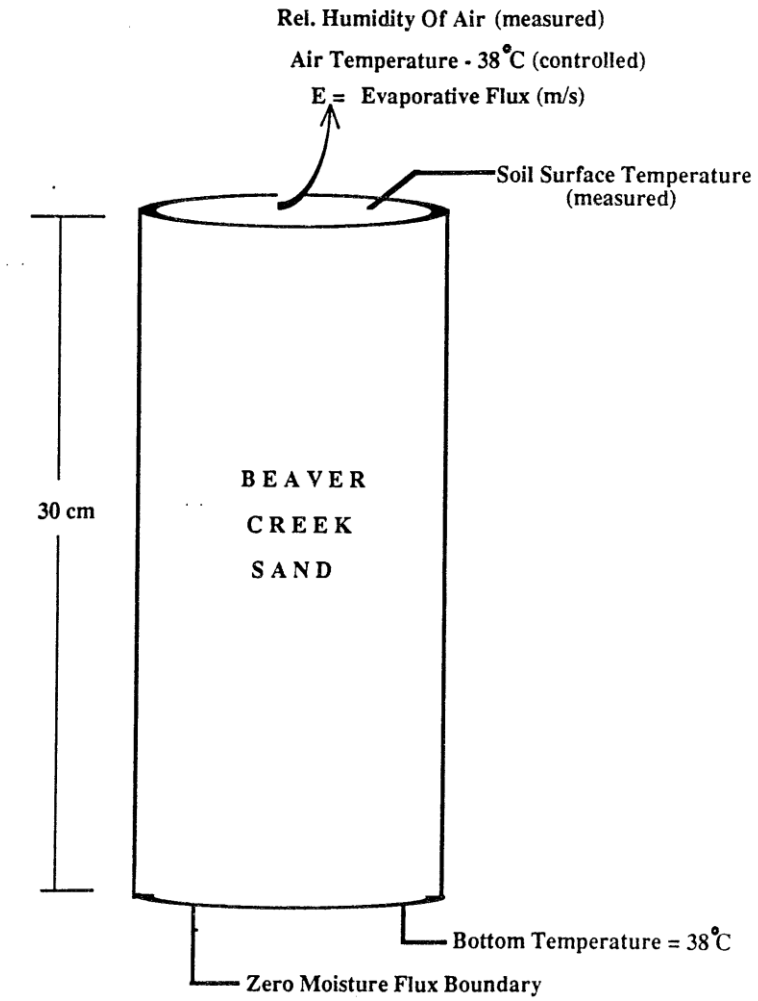

Figure 4.1 Problem configuration for the column test of Wilson (1990).

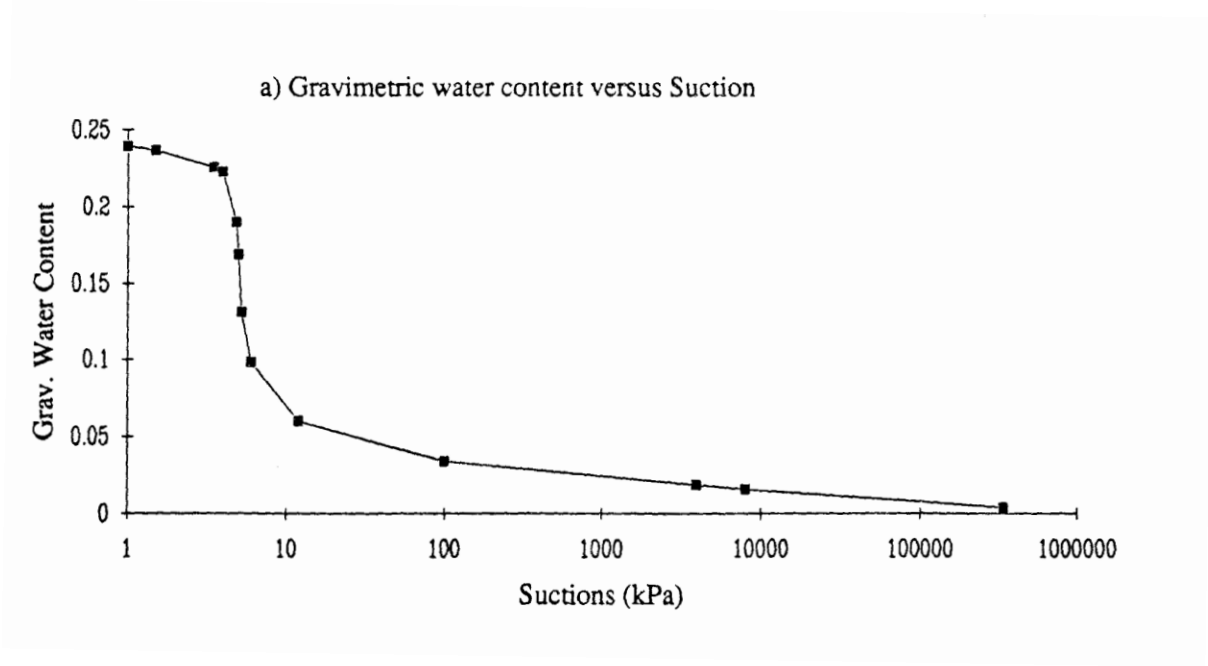

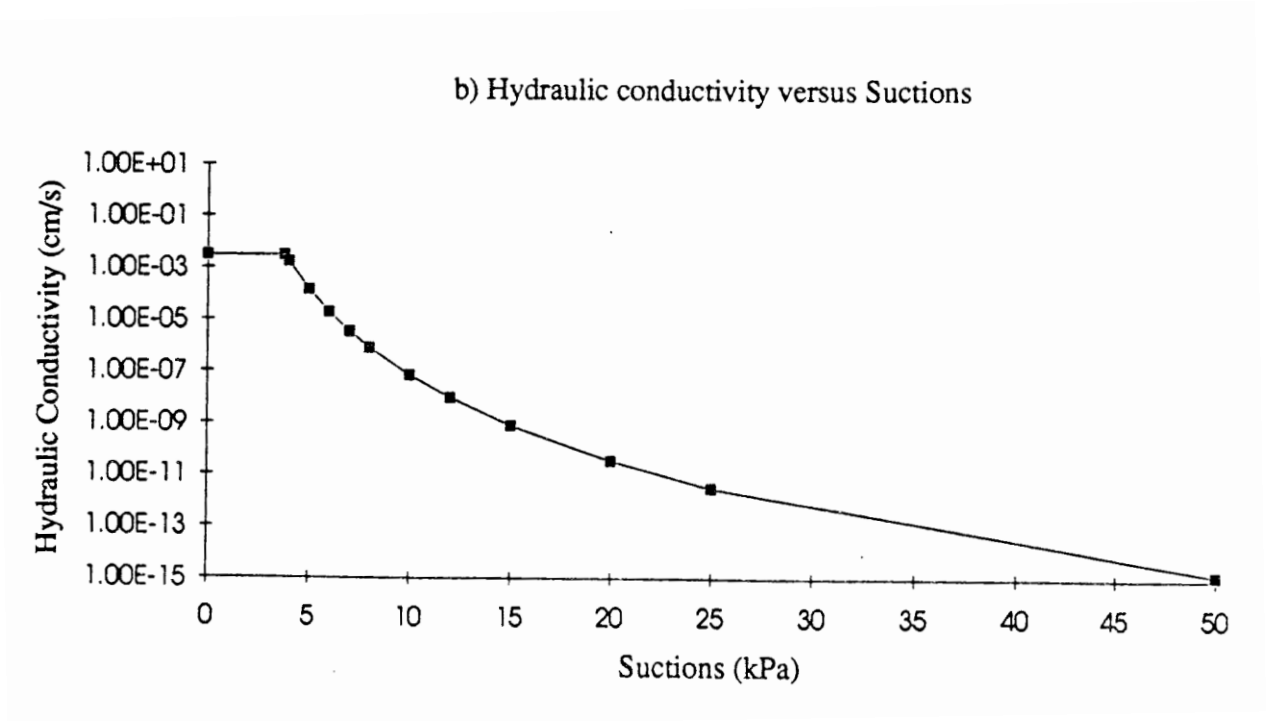

Figure 4.2 Hydraulic properties of Beaver Creek sand.

a) Thermal conductivity versus Gravimetric water content

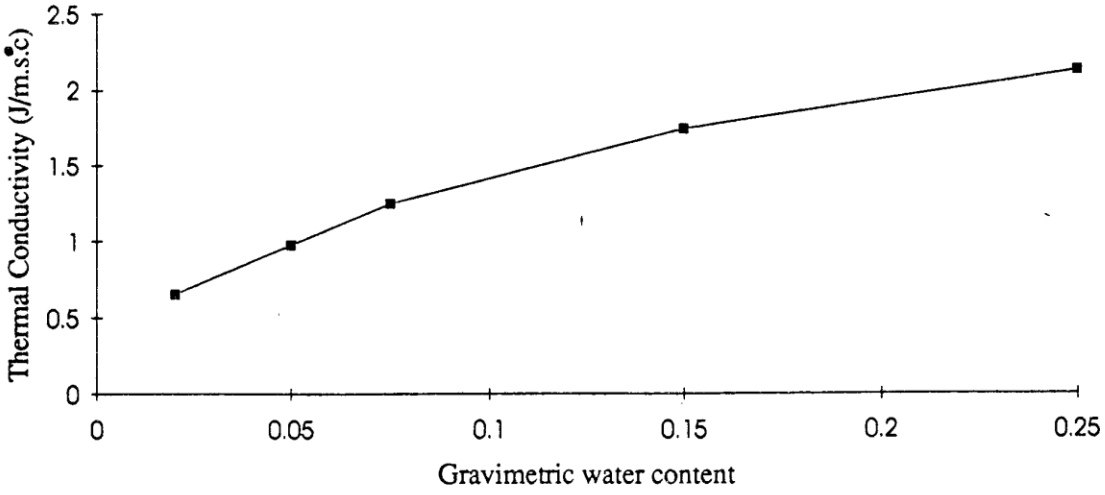

b) Volumetric specific heat versus Gravimetric water content

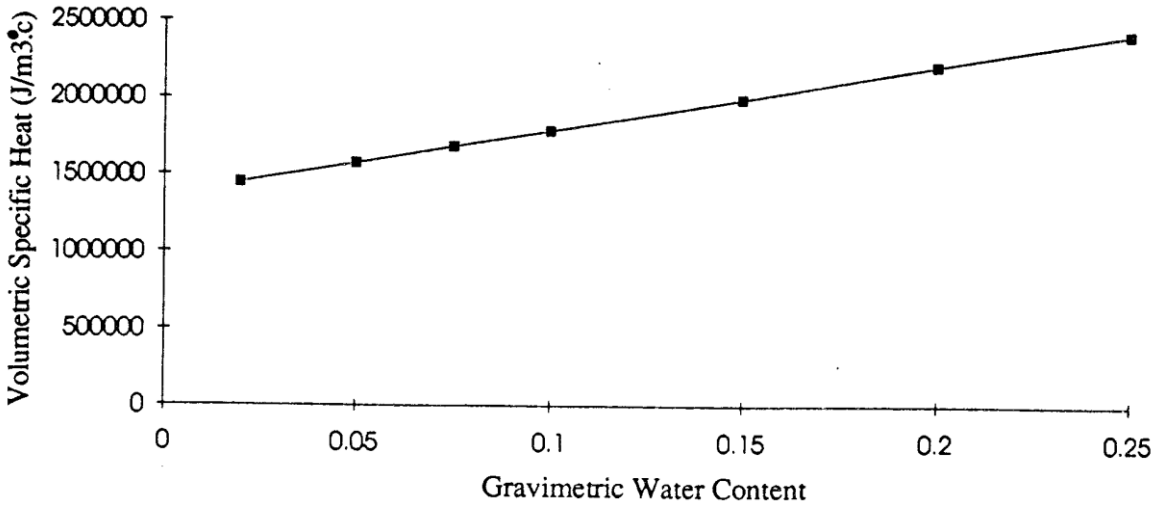

Figure 4.3 Thermal properties of Beaver Creek sand.

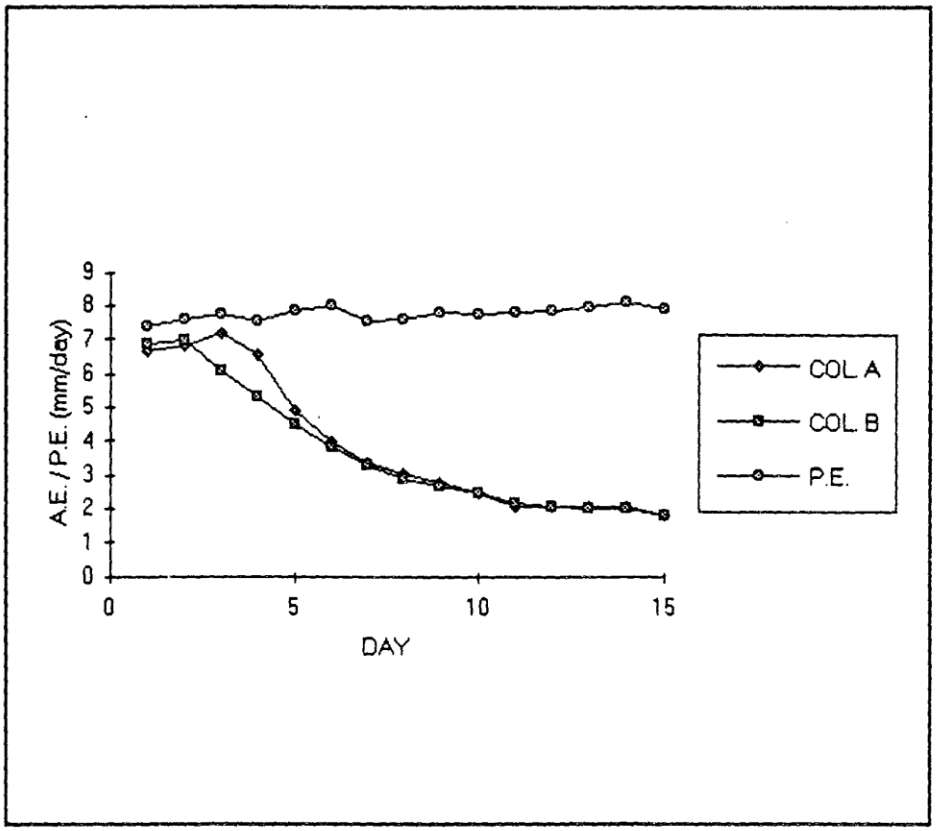

Figure 4.4 Measured evaporation curves versus time for two 30 cm high columns of Beaver Creek sand under controlled environment, Wilson (1990). (A.E.: Actual evaporation; P.E.: Potential evaporation).

As it is shown in Figure 4.4, the potential evaporation is the same for both tests because it is dependent on the environmental data only. However, the actual evaporation differs because the soils in the two columns are somehow different. The sharp decline in actual evaporation from soil columns A and B occurs after about 4 and 2.5 days, respectively from the beginning of the test.

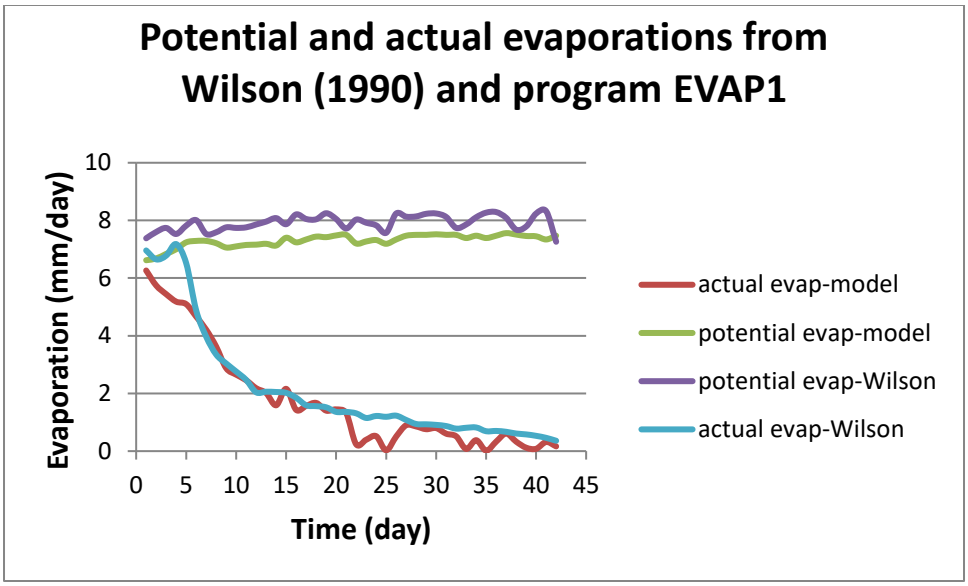

Figure 4.5 Potential and actual evaporations from experimental results of Wilson (1990) and numerical results of program EVAP1.

As Figure 4.5 shows, the trend of actual evaporation and potential evaporation from the model agree with experimental results of Wilson (1990). However, there are minor differences between actual evaporation curves during early days and around days of 25 (about 1 mm/day) and 35 (about 0.5 mm/day). Also, the potential evaporation from the experiment is about 0.5 mm/day more than the model result most of the days.

Figure 4.6 shows the soil suction from drying soil column test of Wilson (1990) and the model. As the figure shows, suction at early days is less from the test than the model. That is why the evaporation from Wilson (1990) test is more than the model during early days in Figure 4.5.

Figure 4.7 compares the relative humidity from the drying column test of Wilson (1990) and the numerical model predictions. As can be noted from Figure 4.7, initially the numerical model predicted lower relative humidity during early days, which is consistent with less suction and more evaporation.

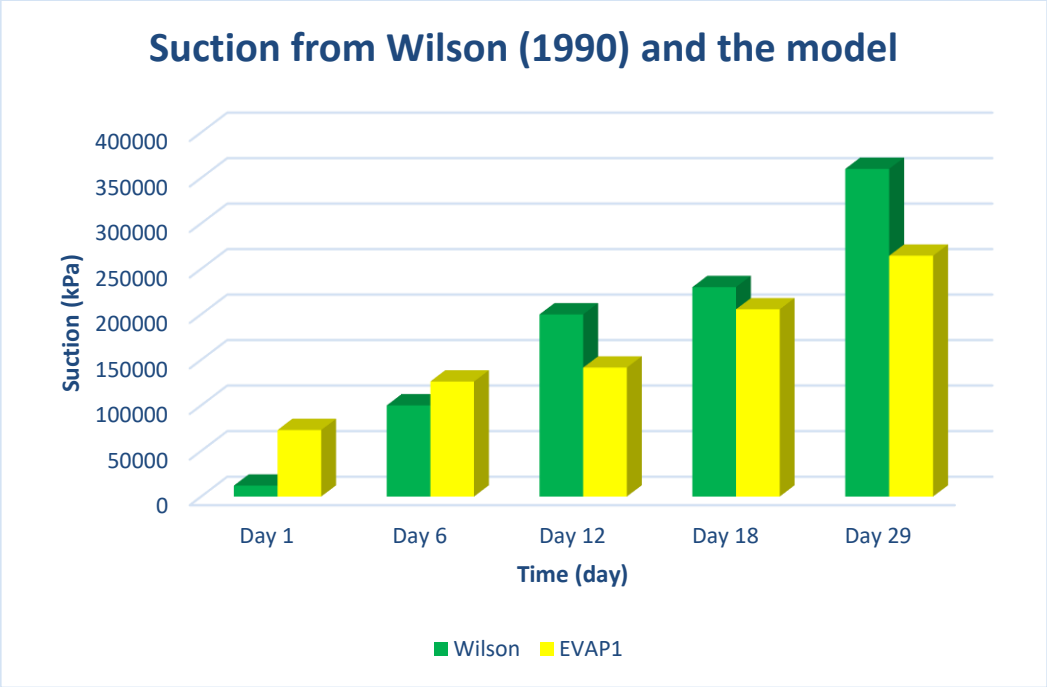

Figure 4.6 Suction magnitudes from the drying column test of Wilson (1990) and the model.

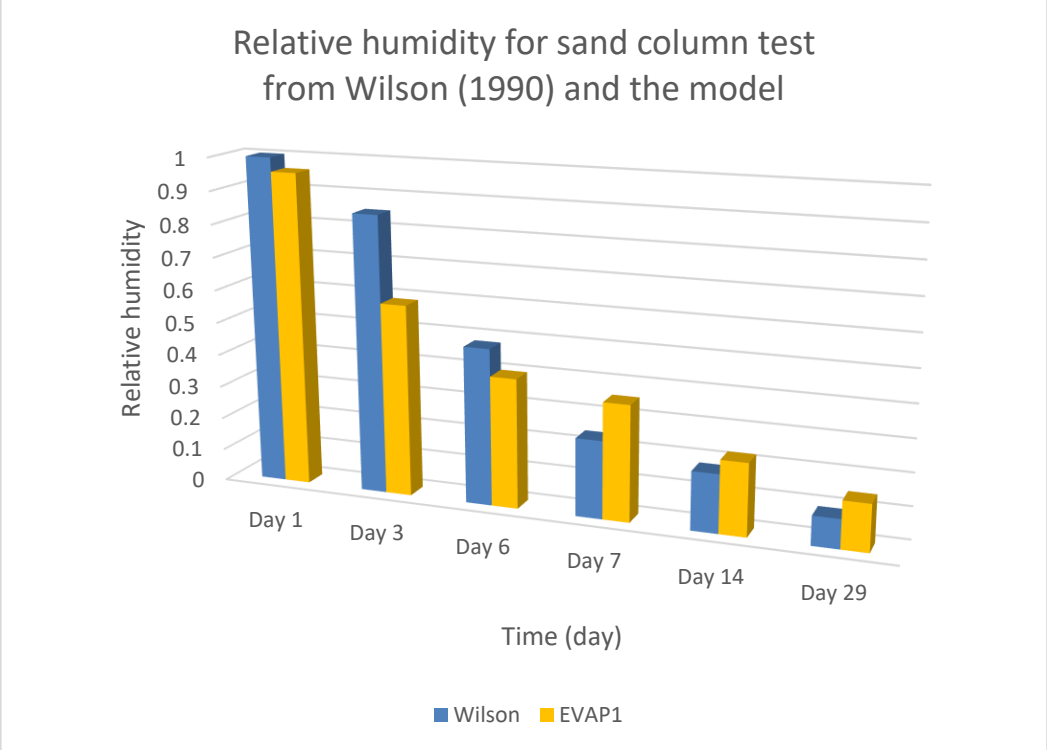

Figure 4.7 Relative humidity of soil from column test of Wilson (1990) and the model.

Figure 4.8 presents the settlement of the soil column used in the drying test of Wilson (1990). THM analysis made it possible to calculate the displacement magnitudes. Logarithmic scale was used for the horizontal axis because of the wide range of the settlement.

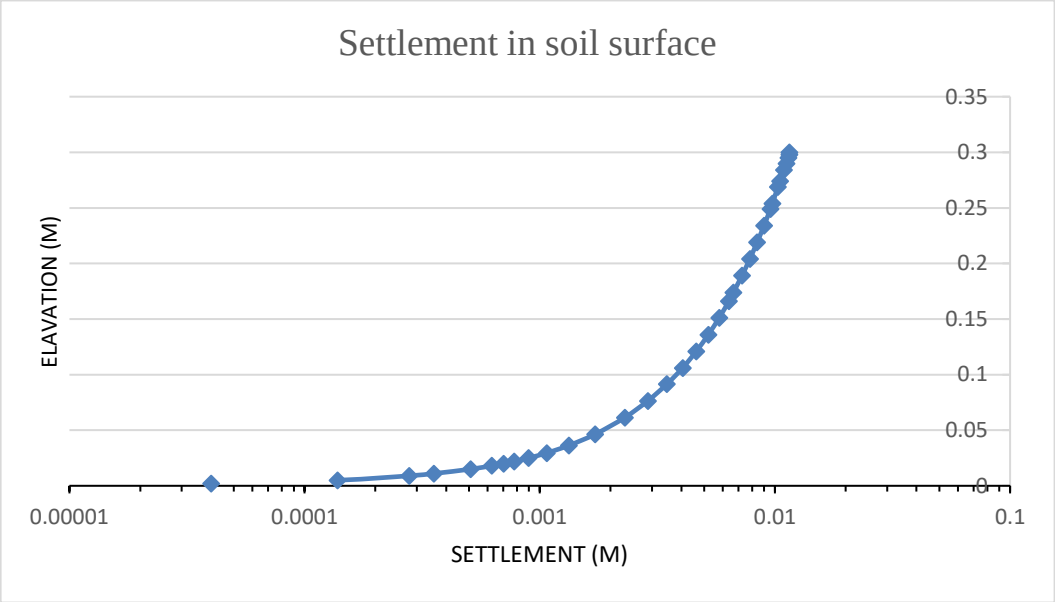

Figure 4.8 Settlement of soil column of Wilson (1990) drying test.

4.4 SOIL COLUMN TEST OF YANG AND YANFUL (2002)

4.4.1 Materials and experimental procedures

The second experiment, which its results are used to validate EVAP1, is an evaporation test with a system consisting of an evaporation column and a water supply drainage system. It was used by Yang and Yanful (2002) to measure evaporation and drainage from the soil samples under specified water table levels. The soil sample was prepared at its optimum water content and then compacted with the same energy as in the standard Proctor test ASTM, 1987 to obtain similar densities and porosities in both compaction and SWCC tests.

A water supply drainage system consisting of a 2.5 m long, 6.35 mm inner diameter plastic tube and a 1-l Mariotte bottle was used to maintain a constant water level. Soil evaporation and drainage were initiated simultaneously, following saturation. During the test, the soil column and the whole test system were weighed daily to obtain the mass of water lost separately by evaporation and drainage.

Water content was measured by TDR and gravimetry oven-dry method. During the evaporation and drainage tests, laboratory temperature and relative humidity were monitored using a digital hygrometer/thermometer. To optimize the evaporation rate from the soil, a desk-fan was used to blow air above the test column and the applied wind speed from the fan was measured using an air velocity meter. Laboratory lighting provided the only radiation to the soil surface.

The evaporation column measured 115 mm in diameter and 255 mm in height. Each column was instrumented with time-domain reflectometry (TDR) probes and thermocouples along its height to measure water content and temperature, respectively.

Figure 4.9 shows a schematic of the test system. The location of the datum and the various water levels used in the tests are presented in Figure 4.10. Figure 4.11 presents hydraulic conductivity-suction functions for test soils.

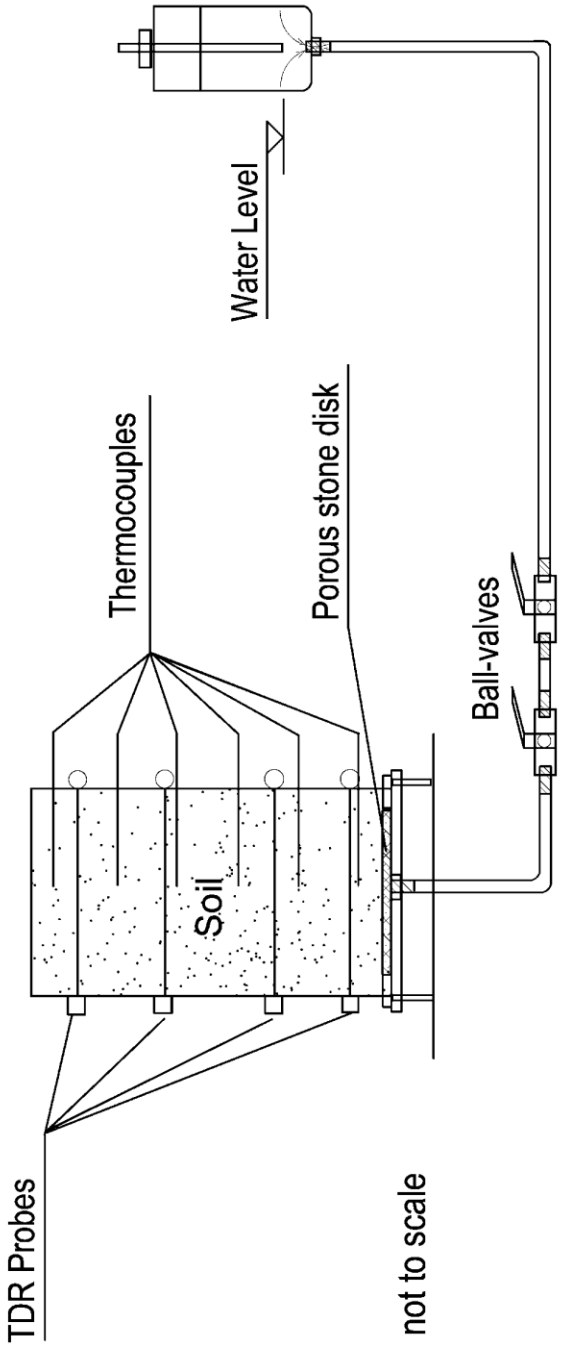

Figure 4.9 Schematic of the test system (Yang and Yanful, 2002).

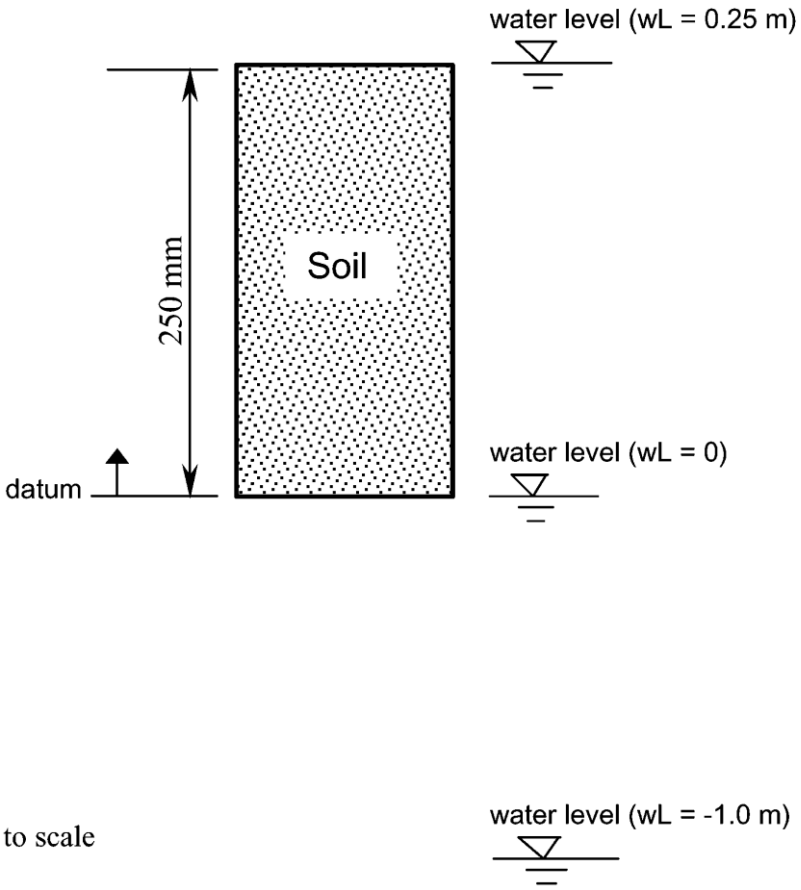

Figure 4.10 Schematic of typical soil column showing datum and locations of water levels used in Yang and Yanful (2002) test.

The measured potential evaporation for the fine sand test started at almost 19 mm/day and increased to about 20 mm/day at the end of the test. The numerical model predicted potential evaporation at 17 mm/day.

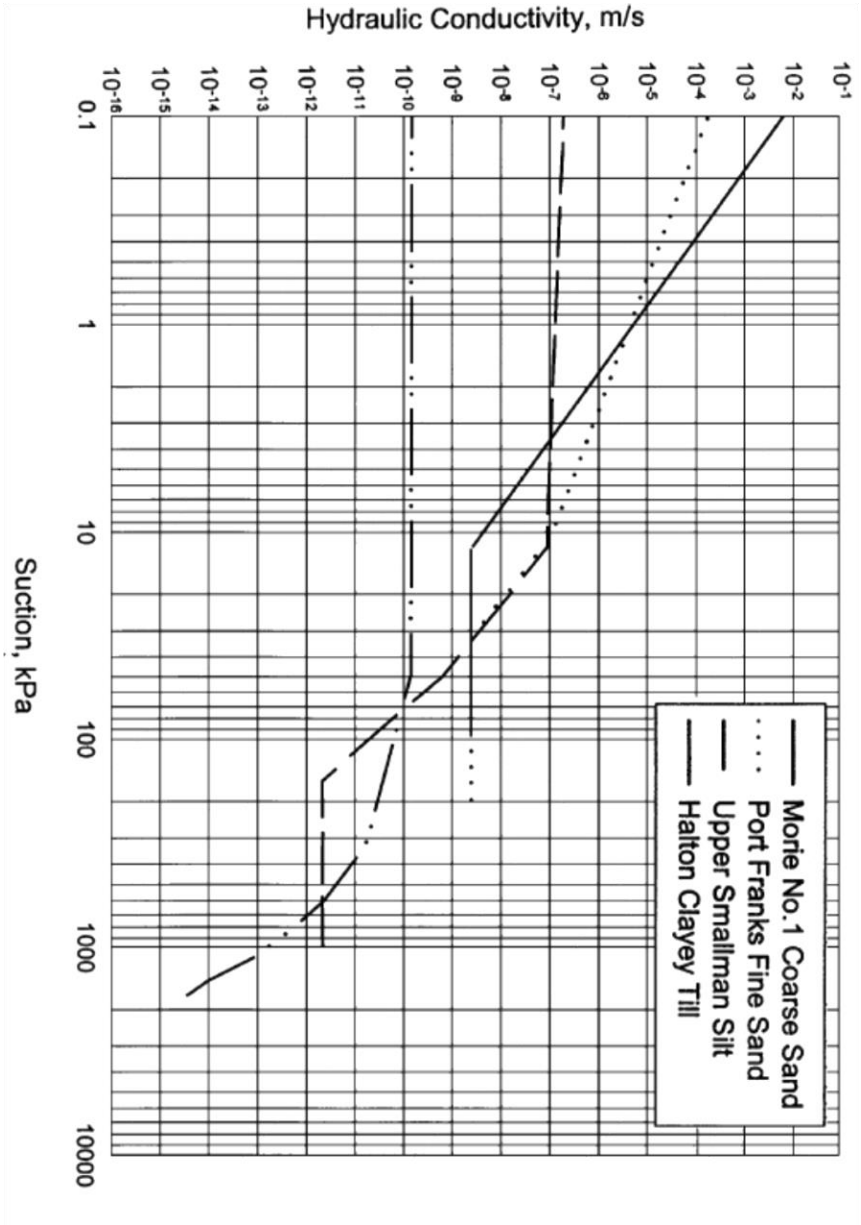

Figure 4.11 Hydraulic conductivity-suction functions for test soils.

It should be mentioned that there are some differences between the results of the test and the numerical model. One reason for the differences could be the measurement, observation and equipment errors with the experiment, and inability of the program to simulate all real facts which govern the test conditions.

4.4.2 Water level at 0.25 m

Figure 4.12 displays potential and actual evaporations for fine sand for water level at 0.25 m. As can be noted from Figure 4.12, potential evaporations from the test and the numerical model are about 19 and 17 mm/day, respectively. Actual evaporation from the test started at 16 mm/day and fluctuated between 14 and 17.5 mm/day. The model predicted actual evaporation of approximately 17 mm/day.

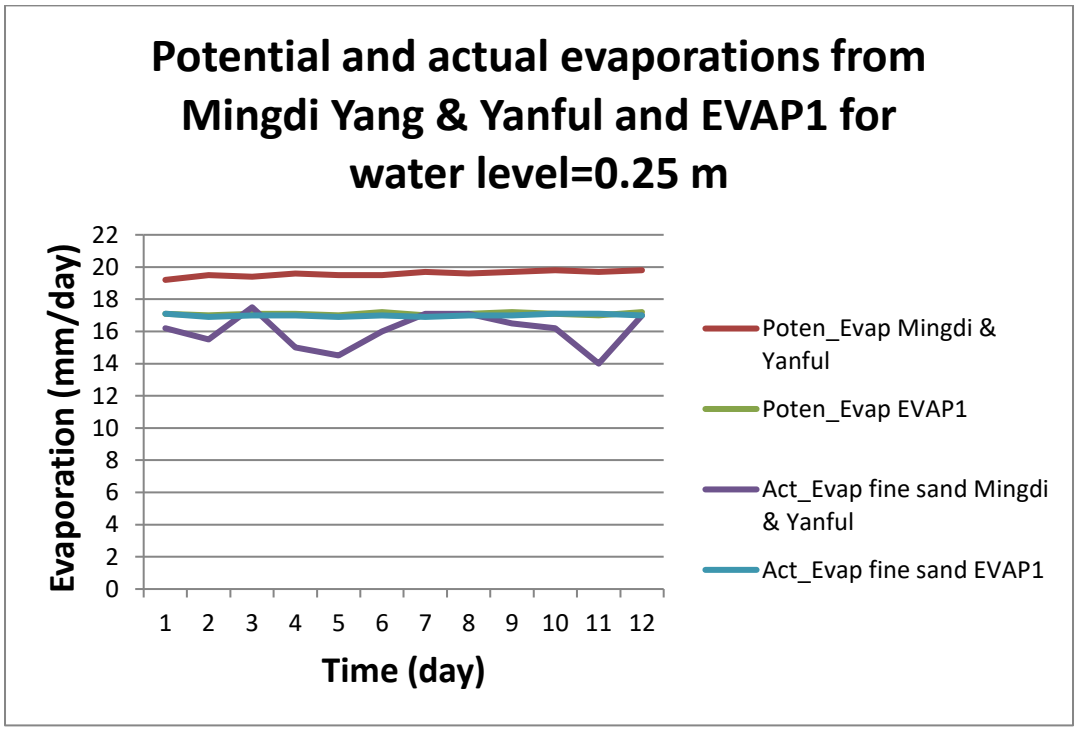

Figure 4.12 Potential and actual evaporations for find sand and silt from Yang and Yanful (2002) test and the model for water level at 0.25 m.

4.4.3 Water level at 0 m

Figure 4.13 presents potential and actual evaporations for fine sand and clayey till with water level at 0 m. The trends of the evaporation rates from the numerical model agree with the test results. Potential evaporations measured from the test and predicted from the numerical model are almost constant at 19.5 and 17.5 mm/day, respectively. For the clayey till, actual evaporation from the test was 4 mm/day at the beginning and decreased to 2 mm/day at the end of the test. Actual evaporation obtained from the numerical model for the clayey till started at about 8 mm/day at the beginning and ended at 4 mm/day.

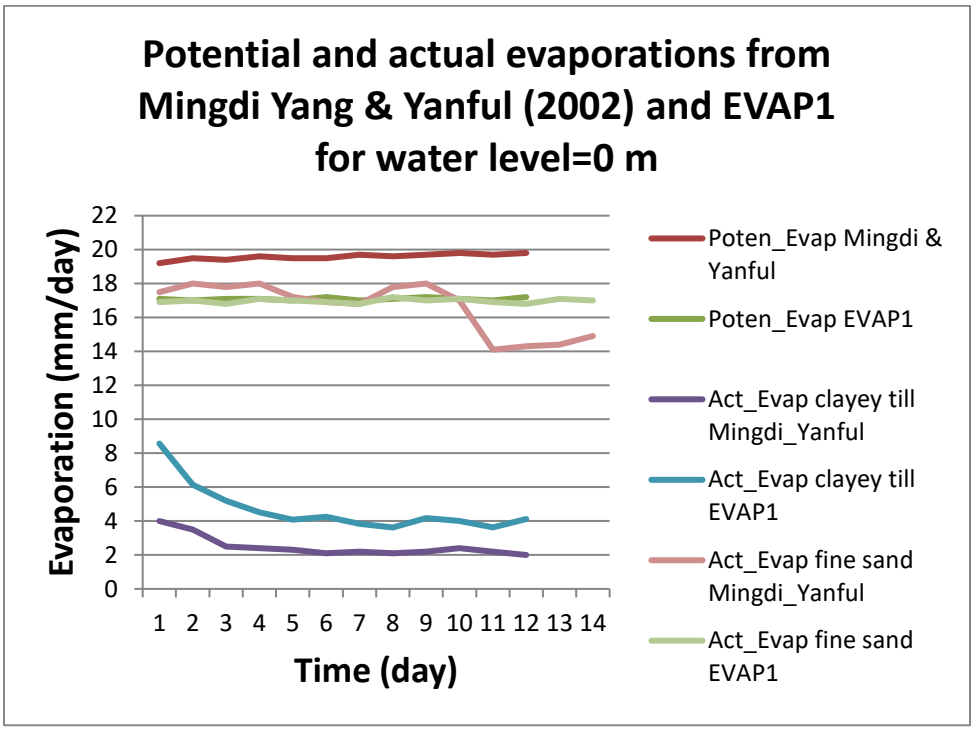

Figure 4.13 Potential and actual evaporations for find sand and clayey till from Yang and Yanful (2002) test and the model for water level at 0 m.

For the fine sand, actual evaporations measured from the test and calculated from the numerical model started with about 17 mm/day and remained very close to each other and almost constant until day 11. After that, the measured actual evaporation decreased to 14 mm/day on day

12 and ended with almost 15 mm/day. The numerical model, however, predicted actual evaporation at 17 mm/day.

4.4.4 Water level at -1 m

As displayed in Figure 4.14, the potential evaporation obtained from the test started with 19 mm/ day, and increased slightly to 19.9 mm/day at the end of the test. The potential evaporation calculated from the numerical model was almost constant at 17 mm/day with minor fluctuations.

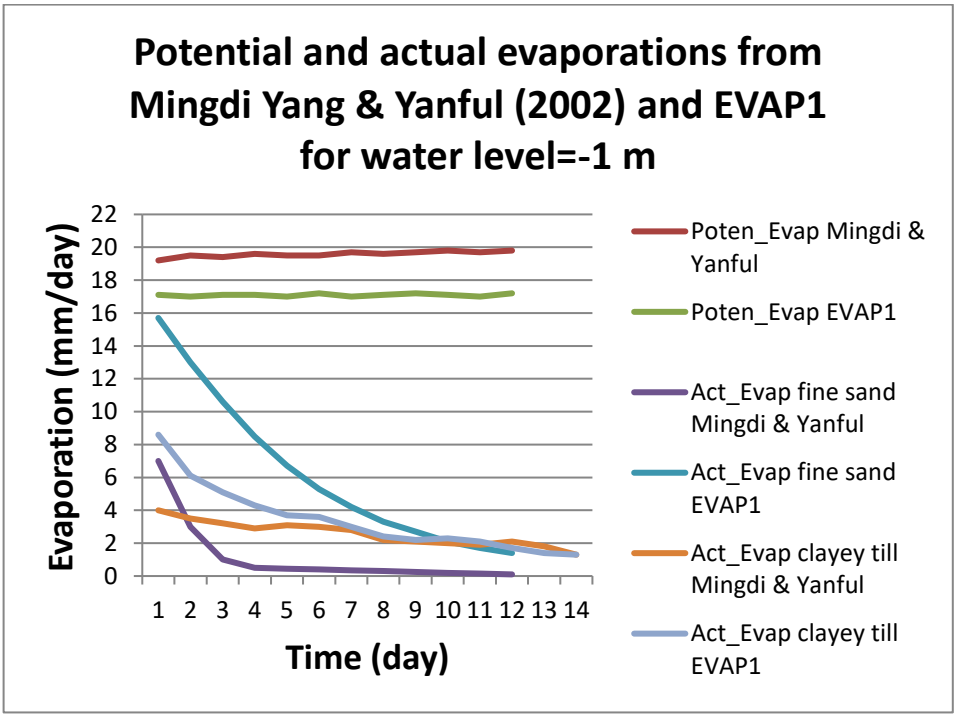

Figure 4.14 Potential and actual evaporations for find sand and clayey till from Yang and Yanful (2002) test and the model for water level at -1 m.

The decreasing trend of actual evaporation with time is confirmed. Also, the trends of the decrease of actual evaporation from the numerical model is consistent with the test results for both find sand and clayey till. For the fine sand, actual evaporations measured from the test and those

calculated from the numerical model started at 7 and 15.8 mm/day, and ended at 0.1 and 1.7 mm/day, respectively.

For clayey till, the actual evaporations measured from the test and that calculated from the numerical model started at 4 and 8.5 mm/day, respectively; but became almost the same after day 6 and remained almost equal at 1.5 mm/day to the end of the test.

4.5 PARAMETRIC STUDY AND SENSITIVITY ANALYSIS

There are four main environmental parameters that directly affect potential and actual evaporations. These parameters are: air temperature, air humidity, net radiation and wind speed. In this section, the effect of these parameters on evaporation is investigated one by one qualitatively and quantitatively. These parameters are changed one at a time, while keeping all other parameters unchanged, and the effect of this change is studied. Air temperature, air humidity, net radiation and wind speed are considered, respectively.

In addition, the sensitivity of evaporation to each of those four environmental parameters is investigated.

4.5.1 The effect of temperature on evaporation

The potential and actual evaporations were estimated with three different maximum temperatures of 21, 16 and 11˚C. The minimum temperature was 1˚C. These temperatures were selected because July is the hottest month in Toronto with an average temperature of 21°C (70°F) and the coldest is January at -3°C (28°F) (Holiday Weather, 2017). Wind speed was kept constant as 11.2 km/hr because according to the annual average wind speed in Canadian cities (Environment Canada, 2017) the amount of wind that London, Ontario averages in a year is 14.1 km/hr (Table 4.4).

Table 4.4 Annual average wind speed in some of Canadian cities (Environment Canada, 2017)

Days	City	Annual average wind MPH	KPH
3	Abbotsford, British Columbia	5.2	8.3
28	Calgary, Alberta	8.8	14.2
3	Edmonton, Alberta	7.4	11.8
18	Halifax, Nova Scotia	9.4	15.1
28	Hamilton, Ontario	10.1	16.2
9	London, Ontario	8.7	14.1

Net radiation was selected as 80 W/m^2 according to Figure 4.15 (NASA, 2017).

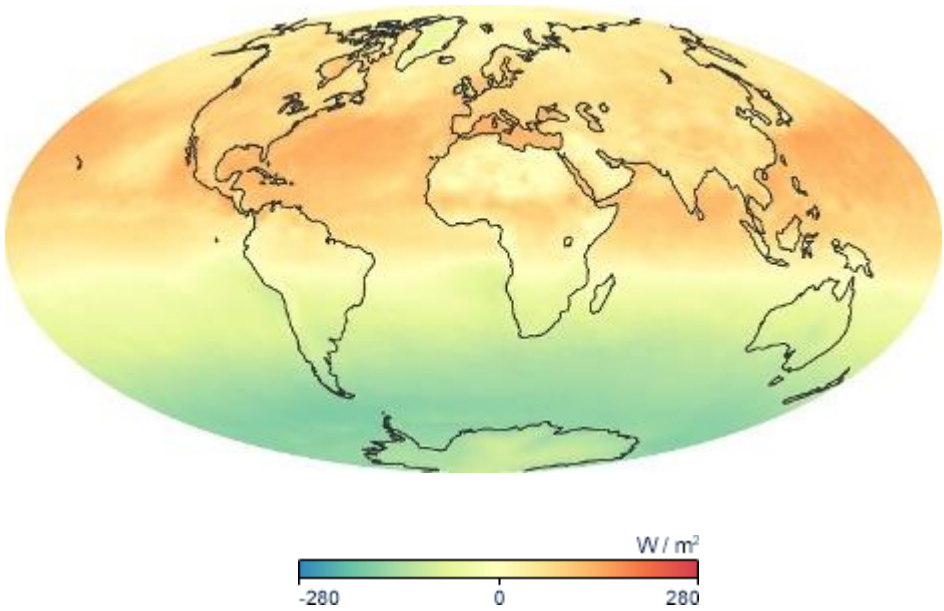

Figure 4.15 Net Radiation map (NASA Earth Observatory, 2017).

Maximum and minimum humidity were selected as 0.8 and 0.4, according to Table 4.5 (Current Results, 2017). The normal humidity levels throughout the year at Canada's largest cities are listed below.

Table 4.5 Average Annual Humidity at some of Canadian Cities (Current Results, 2017)

Annual relative humidity averages

City	Morning	Afternoon
Abbotsford, British Columbia	85	62
Calgary, Alberta	72	48
Edmonton, Alberta	76	54
Halifax, Nova Scotia	87	71
Hamilton, Ontario	86	65
Kelowna, British Columbia	82	52
Kingston, Ontario	81	67
Kitchener - Waterloo, Ontario	88	74
London, Ontario	85	64

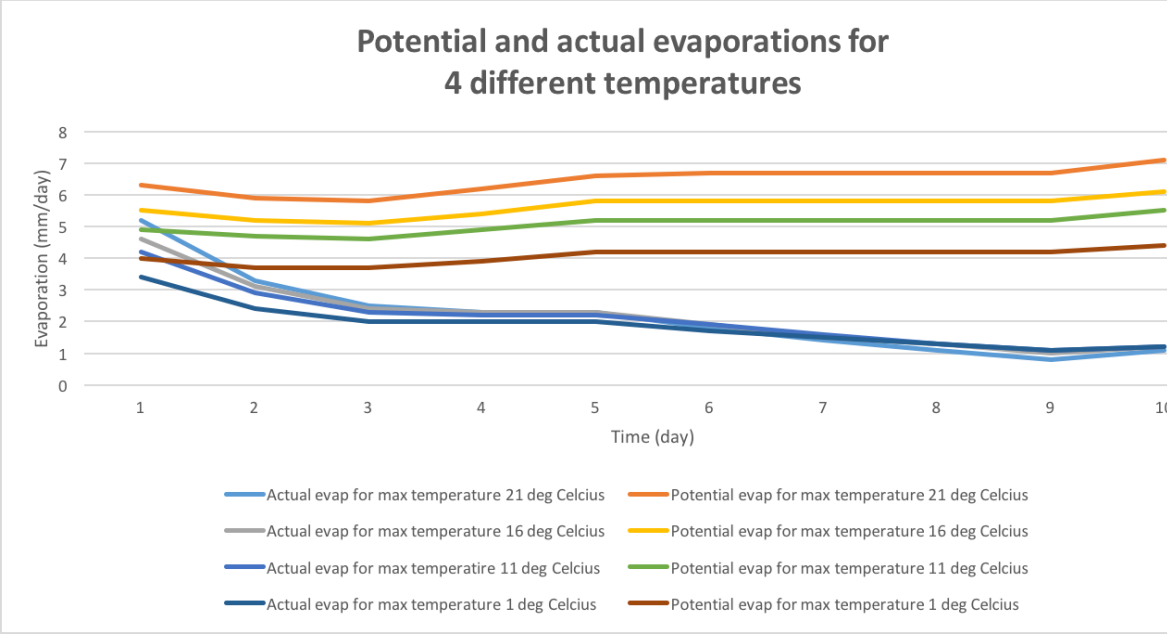

Figure 4.16 Potential and actual evaporations for four different temperature values

The results shown in Figure 4.16, and also the output data, demonstrated that by decreasing the average temperature from 21 to 16, 11˚C and 1 ˚C, the starting potential evaporation decreased from 6.3 to 5.5, 4.9 and 4 mm/day, respectively, and the actual evaporation decreased from 5.2 to 4.6, 4.2 and 3.4 mm/day, respectively. Therefore, even though the decrease of average temperature from 21 to 16 and from 16 to 11˚C is the same (i.e. 5˚C), the decrease of the starting potential evaporation is not the same and instead is 0.8 and 0.4, respectively.

Similarly, the decrease of the starting actual evaporation is not the same; instead it is 0.6 and 0.4, respectively. It means that the relation is nonlinear, and from evaporation estimation viewpoint the effect of temperature change is more important at higher temperatures. In addition, actual evaporations exhibited a decreasing trend with time, which is logical. Actual evaporation reaches the same amount of almost 1 mm/day on day 10 for the four studied temperature values.

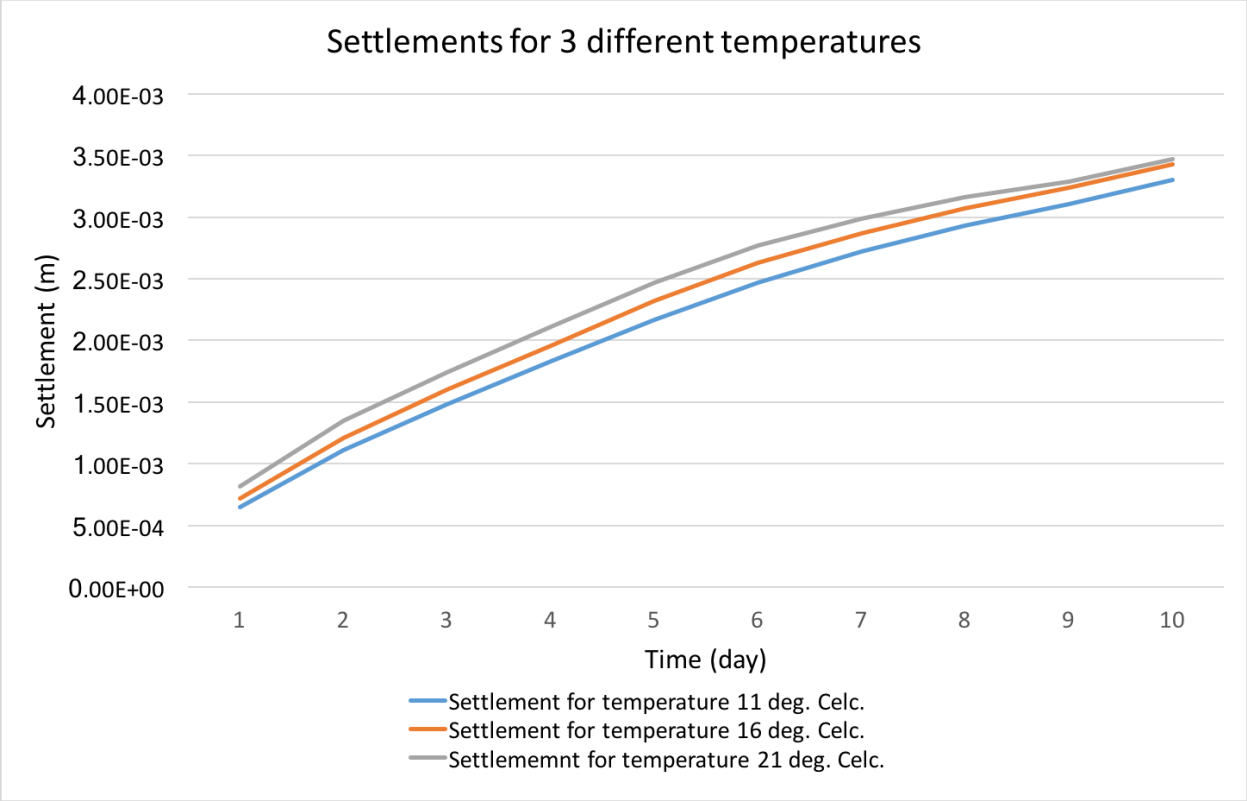

Figure 4.17 Soil settlement for three different temperature values

Figure 4.17 presents soil settlement for the three examined temperature values. In higher degrees, evaporation is more; therefore, effective stress and as a result, settlement is more. At the beginning, evaporation at 3 temperatures almost equals potential evaporation; therefore, the displacements are close to each other. Also at the end the evaporation at the 3 temperatures is minimized regarding the residual water content of the soil. Therefore, soil settlement again is almost the same. However, in the middle, the settlement difference at different temperatures is more because still soil can supply water for different evaporation rates at different temperatures. difference is.

Figure 4.18 presents potential and actual evaporations for three other temperature values.

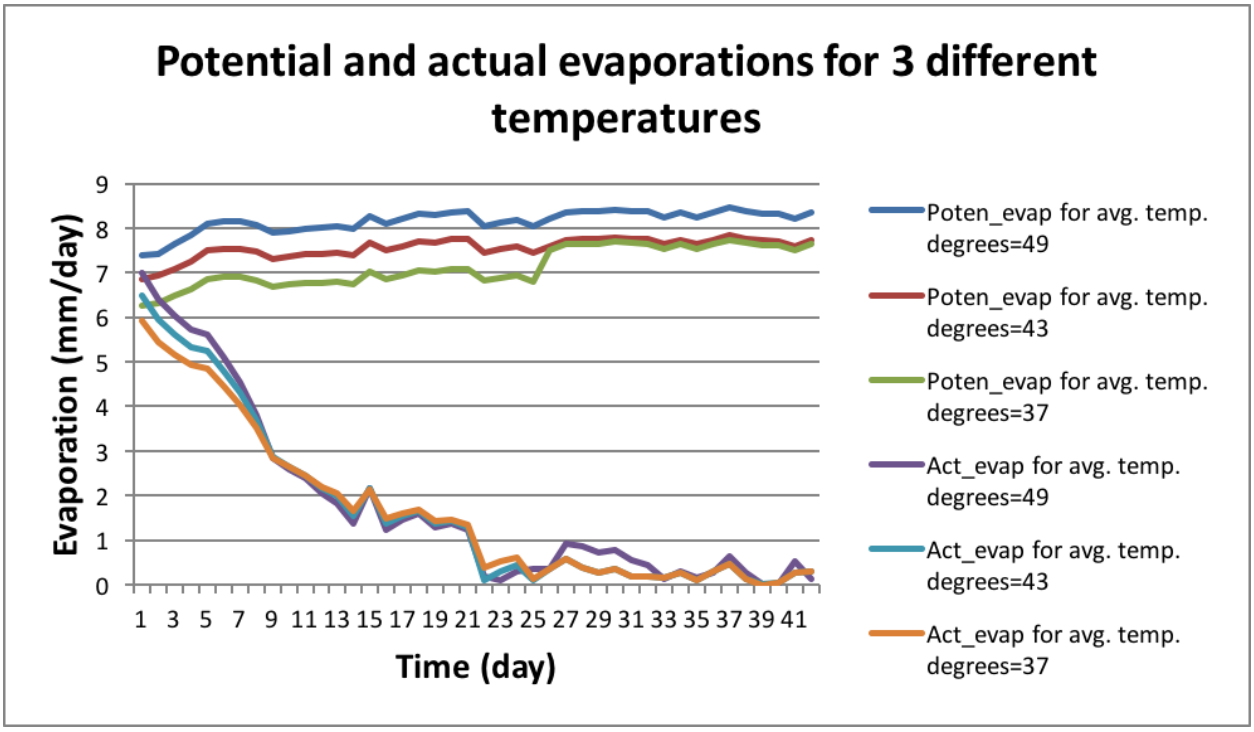

Figure 4.18 Potential and actual evaporations for three other temperature values

4.5.2 The effect of humidity on evaporation

In this section, the maximum humidity varied from 0.7 to 0.8 and 0.9, and the minimum humidity varied from 0.3 to 0.4 and 0.5, considering Table 4.5. The other parameters were kept as before, i.e. maximum and minimum temperatures as 21 and 1˚C, wind speed as 11.2 km/hr, and net radiation as 80 W/m^2.

As Figure 4.19 shows, with the increase of minimum humidity from 0.3 to 0.4 and 0.5 (same increase of 0.1), and with the similar increase of maximum humidity from 0.7 to 0.8 and 0.9 (considering Table 4.5) the starting potential evaporation decreases from 7.2 to 6.3 and 5.4 mm/day, respectively. Similarly, actual evaporation decreases from 6.1 to 5.2 and 4.3 mm/day, respectively. The results are presented in Figure 4.19 and it is observed that the numerical model

correctly predicted that evaporation decreases as the humidity increases. Also, the decreasing trend of actual evaporation with time is confirmed.

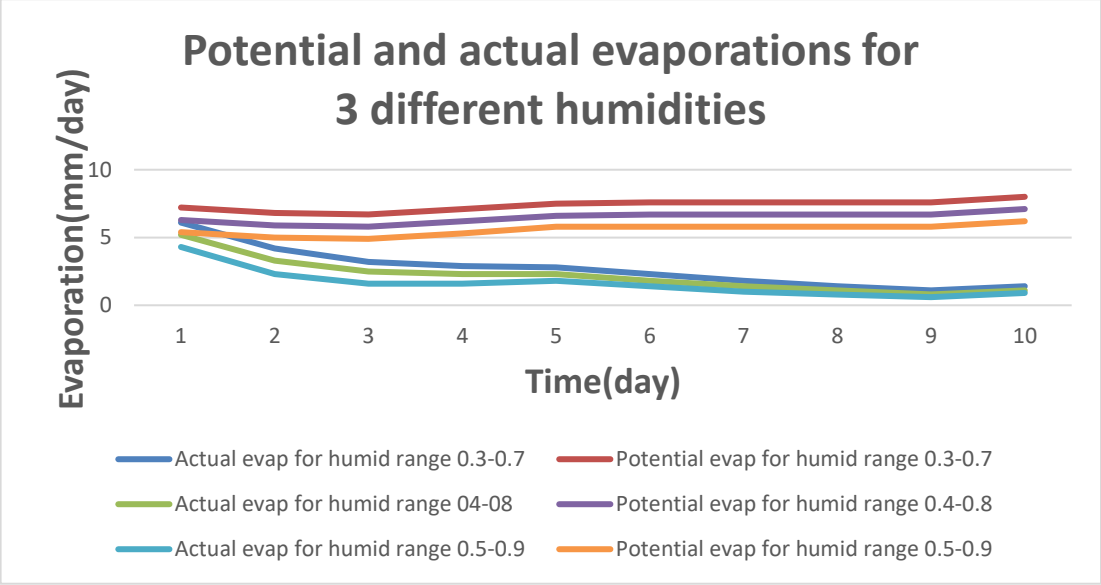

Figure 4.19 Potential and actual evaporations for three different humidity values

Figure 4.20 shows settlement at three abovementioned humidity values. More humidity causes less evaporation and it leads to less effective stress and less settlement.

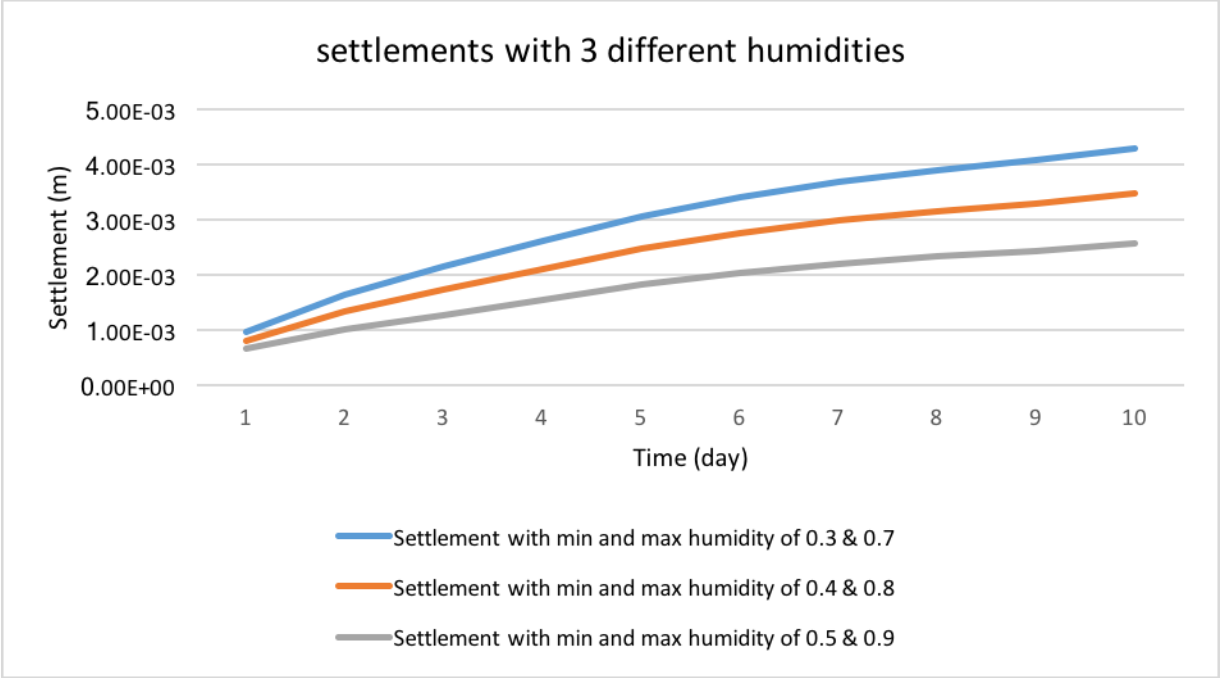

Figure 4.20 Soil settlement for three humidity values

4.5.3 The effect of net radiation on evaporation

In this section, three values of net radiation were considered, i.e. 80, 110 and 140 W/m^2, respectively, considering Figure 4.15. The other parameters were kept constant: maximum and minimum temperatures as 21 and 1˚C, respectively (considering Holiday Weather, 2017); maximum and minimum humidity as 0.8 and 0.4, respectively (considering Table 4.5); and wind speed as 11.2 km/hr (considering Table 4.4). As Figure 4.18 shows, as net radiation increases, the evaporation increases as well, which is a correct trend, but in a nonlinear fashion as is explained below. Also, the actual evaporation has a decreasing trend with time, which is correct.

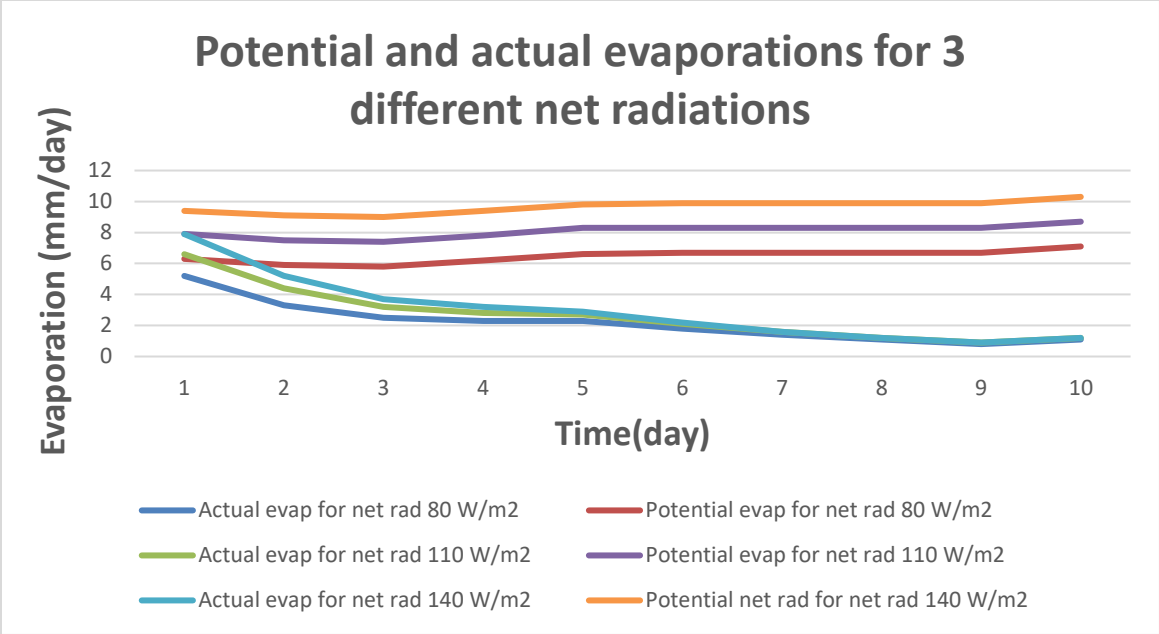

Figure 4.21 Potential and actual evaporations for three different net radiation values

The change of starting potential and actual evaporations due to 30 W/m^2 increase in net radiation from 80 to 110 W/m^2 was 6.3 to 7.9 mm/day, and 5.2 to 6.6mm/day, respectively; i.e. 1.6 mm/day increase in potential evaporation and 1.4 mm/day increase in actual evaporation. However, another increase of 30 W/m^2 in net radiation from 110 to 140 W/m^2 changed potential evaporation from 7.9 to 9.4 mm/day (i.e. 1.5 mm/day increase), and actual evaporation from 6.6 to 7.9 mm/day (i.e. 1.3 mm/day increase).

The two paragraphs above, imply an important reality: when net radiation increases to some extent, evaporation increases to some extent, but another increase of radiation to the same extent does not increase evaporation the same amount. This is a familiar concept in literature too. Usually to keep increasing or decreasing a parameter does not lead to the continuous and similar increase or decrease of the investigated phenomenon. For example, although making the finite element mesh smaller helps the accuracy of the results of a finite element analysis, to keep making the mesh

smaller does not necessarily help with the same amount of increase in accuracy, and even it may hurt the accuracy of the analysis results by affecting vice versa.

Figure 4.22 presents soil settlements for three abovementioned net radiation values. As Figure presents, more radiation causes more evaporation, which in turn causes more effective stress and more settlement.

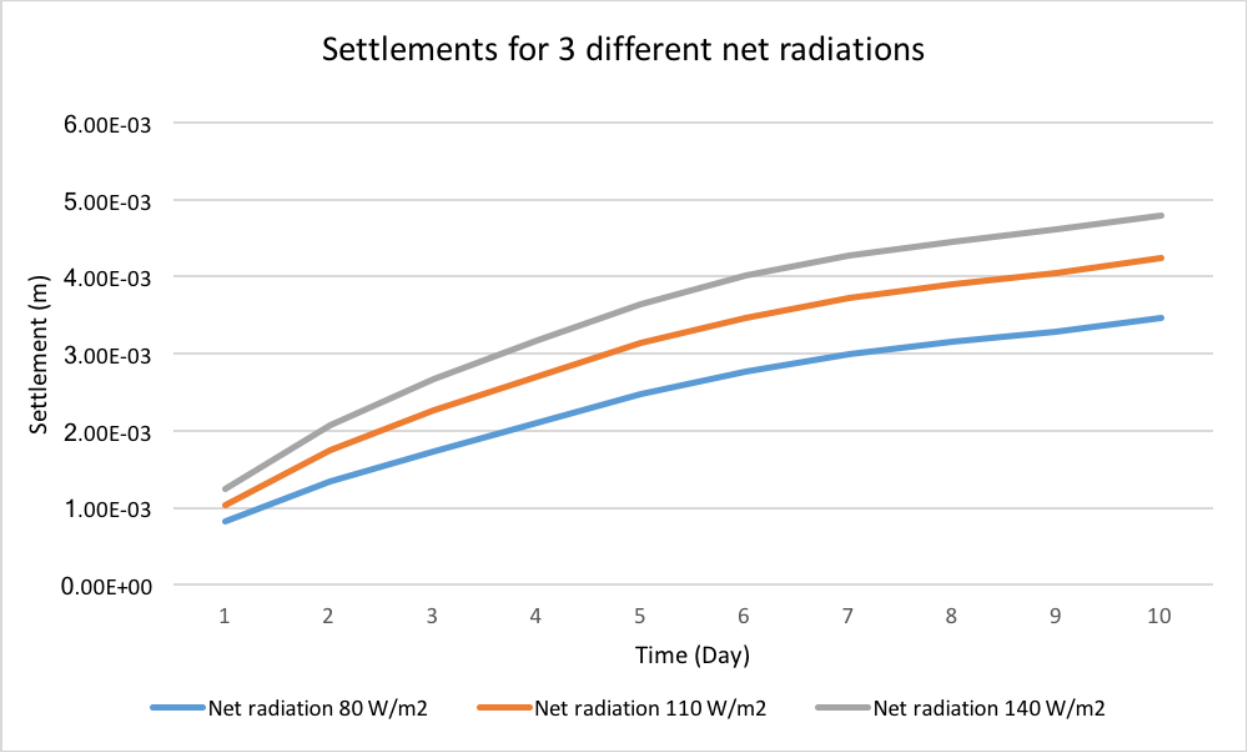

Figure 4.22 Soil settlement for three net radiation values

Figure 4.23 shows potential and actual evaporations for three other net radiation values. Again, increasing radiation increases evaporation in a nonlinear manner.

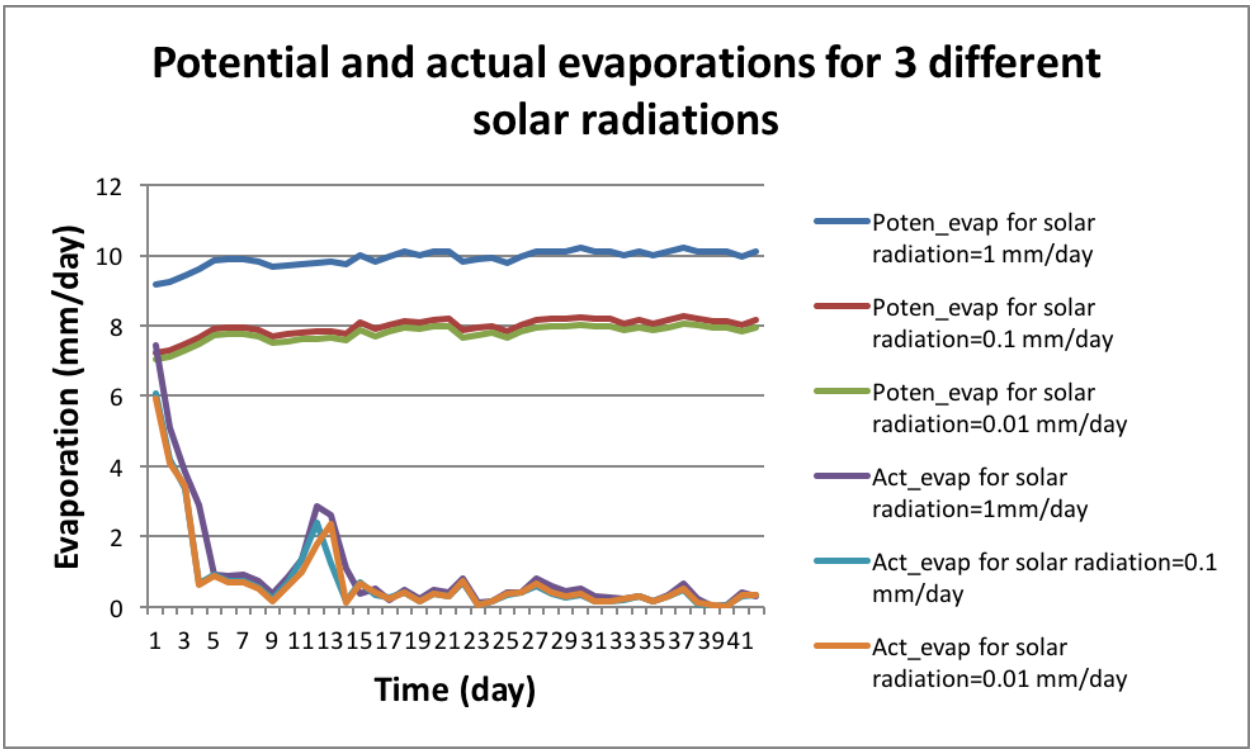

Figure 4.23 Potential and actual evaporations for three other net radiation values

4.5.4 The effect of wind speed on evaporation

Three different wind speeds were considered in the analysis, i.e. 11.2, 14.7 and 18.4 km/hr, considering Table 4.4. The other parameters were kept constant: maximum and minimum temperatures as 21 and 1˚C, respectively (considering Holiday Weather, 2017), maximum and minimum humidity as 0.8 and 0.4, respectively (considering Table 4.5); and the net radiation as 80 W/m^2 (considering Figure 4.15). Figure 4.19 shows the results.

The obtained results presented in Figure 4.19 demonstrate that increasing wind speed increases both potential and actual evaporations. As wind speed increased from 11.2 to 14.7 km/hr, the starting potential evaporation increased from 6.2 to 6.5 mm/day. Also, increasing wind speed from 14.7 km/hr to 18.4 km/hr increased the starting potential evaporation from 6.5 to 6.8 mm/day.

However, increasing wind speed from 11.2 to 14.7 km/hr increases the starting actual evaporation from 5.24 to 5.40 mm/day, while increasing wind speed from 14.7 to 18.4 km/hr increases the starting actual evaporation from 5.40 to only 5.47 mm/day, i.e. nonlinear effect.

It should be noted that starting evaporation was considered in these comparisons, instead of ending evaporation because the latter is not as accurate due to the diminishing evaporation at the end (usually less than 1 mm).

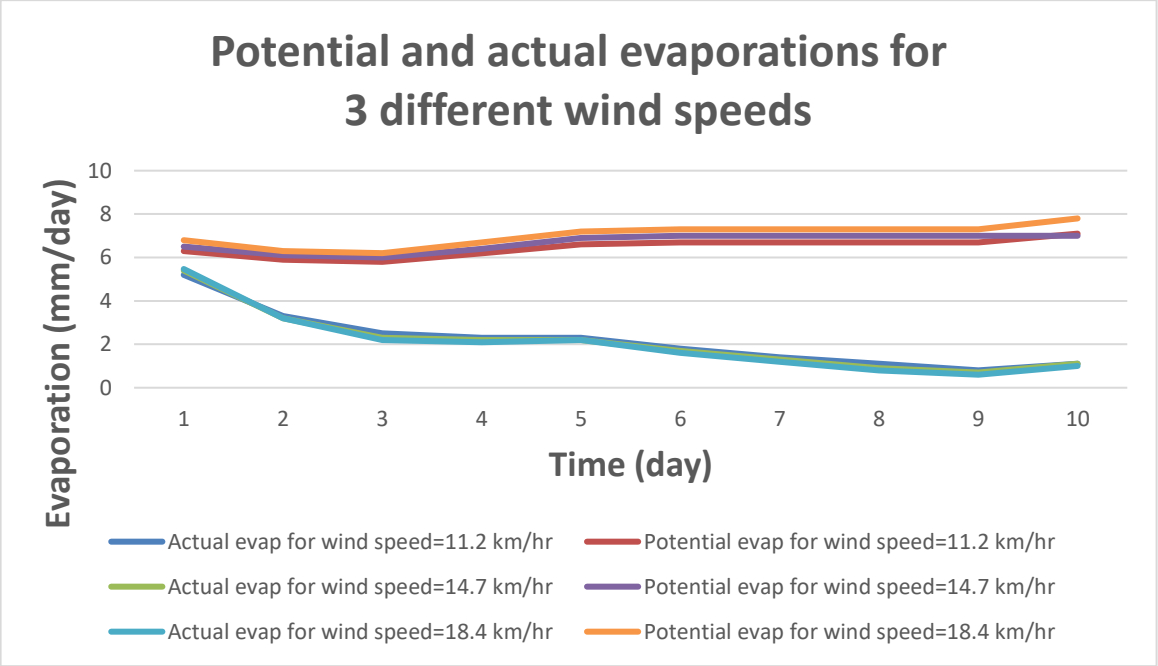

Figure 4.24 Potential and actual evaporations for three different wind speed values

Figure 4.25 presents soil settlement for three wind speed values.

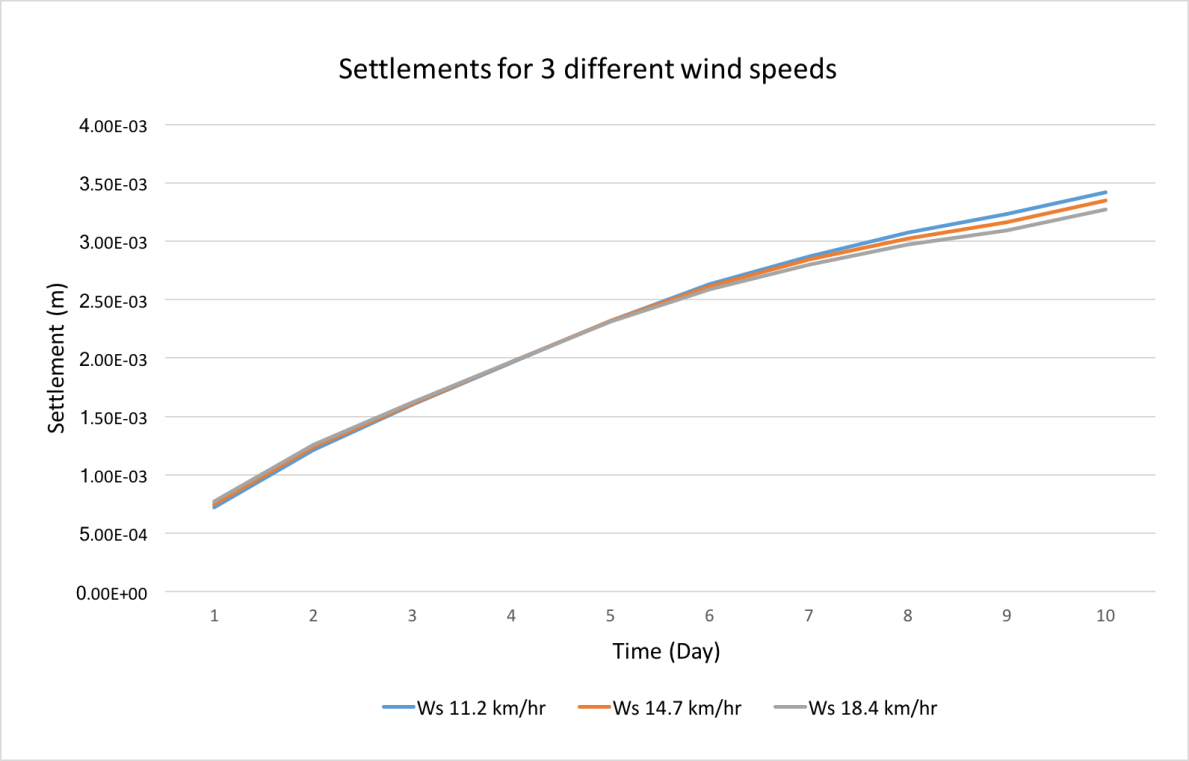

Figure 4.25 Soil settlement for three wind speed values

Figure 4.26 shows potential and actual evaporations for three other wind speed values. Again, increasing wind speed increases evaporation rate in a nonlinear manner.

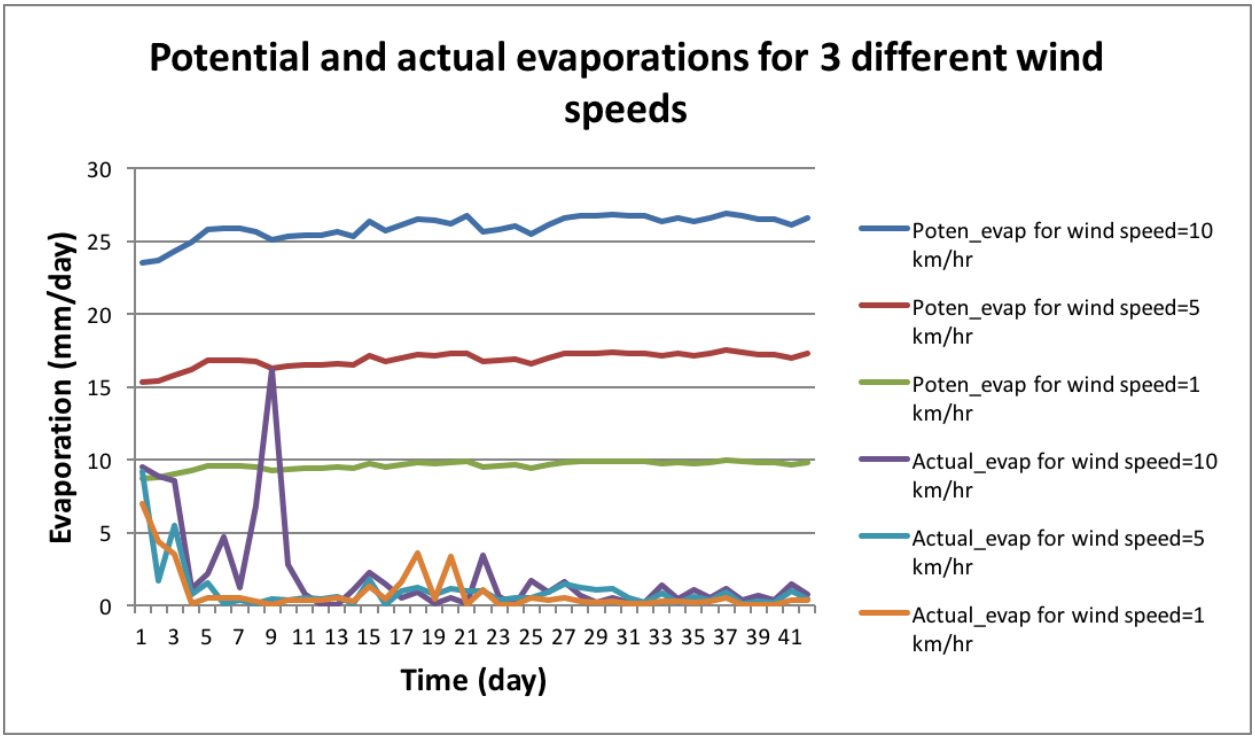

Figure 4.26 Potential and actual evaporations for three other wind speed values

4.5.5 Sensitivity analysis

The objective of this analysis is to identify the environmental parameter that affects evaporation the most. Therefore, in this section the effects of the four main parameters on evaporation are compared.

Using Figure 4.16 and the output data, it was deduced that 0.31% change in temperature caused 12% change in potential evaporation, and 11% change in actual evaporation. On the other hand, considering Figure 4.17 and more accurately the output data, 12% change in humidity led to 14% change in potential evaporation, and 17% change in actual evaporation.

Meanwhile, considering Figure 4.18 and the output data, 27% change in net radiation caused

20% change in both potential and actual evaporations. Finally, according to Figure 4.19 and using the output data 24% change in wind speed led to 5% change in potential evaporation and 3% change in actual evaporation.

Having an overall look at the above-mentioned material, it is clear that evaporation is sensitive the most to humidity. The second, third and fourth parameters that evaporation is sensitive to are net radiation, temperature and wind speed, respectively.

4.6 THE EFFECT OF THM ANALYSIS ON EVAPORATION

In this section, the effect of THM analysis, which enables considering soil settlement, on evaporation from unsaturated soil is investigated.

Due to the soil settlement, void ratio and porosity decrease. Hydraulic conductivity of soil depends on void ratio as below:

$$K_{wz} = K_{wzo}\left[\frac{S_r - S_{ru}}{1 - S_{ru}}\right]^b \left(\frac{\nu_r}{\nu_T}\right) \qquad \text{Eq. 3-2}$$

$$K_{wzo} = a \cdot 10^{\alpha e}$$

where

e: void ratio

(The other terms were defined in Chapter 3).

And gas permeability also depends on void ratio as below:

$$K_g = \frac{b\gamma_g}{\mu_g}\left[e\left(1 - S_r\right)\right]^C \qquad \text{Eq. 3-6}$$

where

e: void ratio

(The other terms were defined in Chapter 3).

The soil settlement, which decreases void ratio decreases conductivities too and it, in turn, decreases evaporation. Therefore, neglecting THM behavior leads to neglecting soil settlement, and consequently neglecting the decrease in void ratio, which for the abovementioned reason overestimates evaporation from unsaturated soil surface, and that is what the model shows in Figure 4.27.

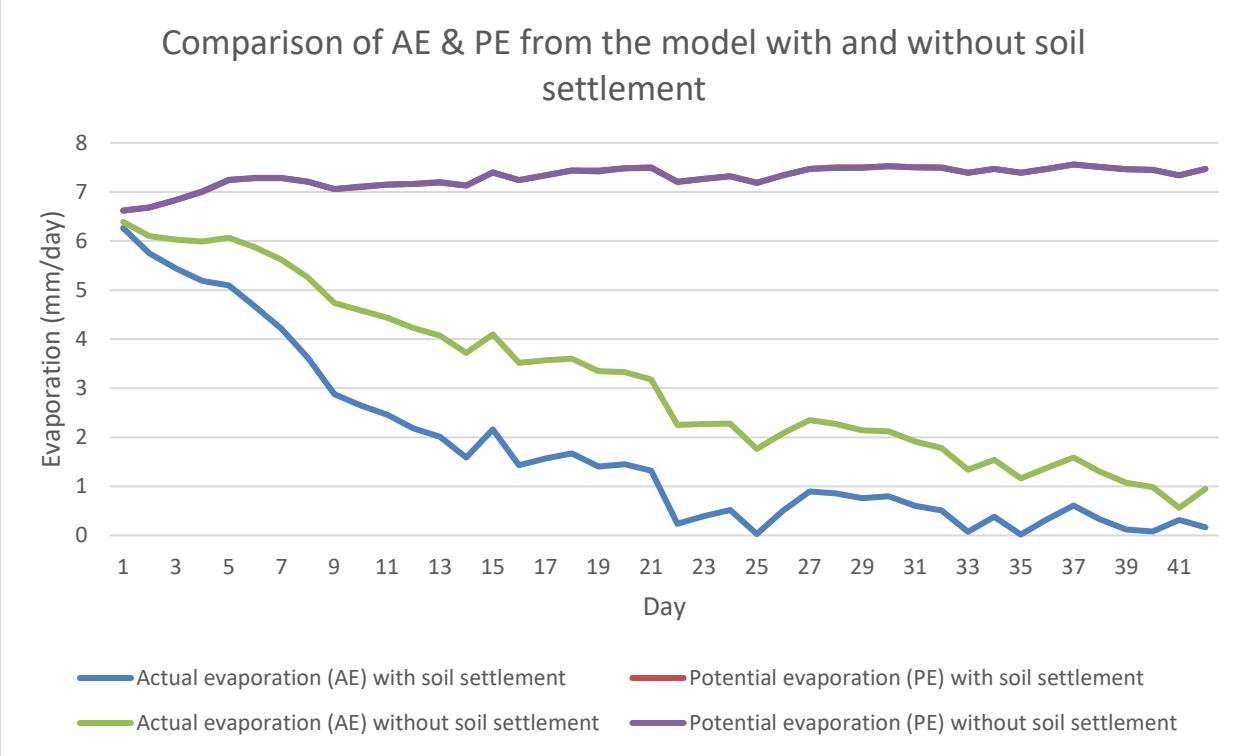

Figure 4.27 A comparison between potential and actual evaporations with and without considering soil settlement

As Figure 4.27 shows, potential evaporation is the same, because it depends only on environmental parameters, which are the same for both analyses. However, actual evaporation is different because it depends on soil properties too, which is different because of different void ratios, as was mentioned before. Meanwhile, the two graphs are close to each other both at the beginning, when still there is not much settlement, and at the end when the water content was decreased to residual water content and the evaporation was minimized.

4.7 SUMMARY AND CONCLUSION

In this chapter, first program EVAP1 was validated using Wilson (1990) drying column test, and column test of Yang and Yanful (2002). The comparison results were acceptable.

Next, a parametric study was performed and the effects of the changes of the main environmental parameters, i.e. air temperature, air humidity, net radiation and wind speed on evaporation were investigated one by one. According to the results, the increase of temperature, net radiation and wind speed increased the potential and actual evaporations. However, the increase of humidity decreased the evaporation. The evaporation changes due to the changes of those parameters were mostly nonlinear.

A sensitivity analysis was performed next to find out to which environmental parameter evaporation is more sensitive. The results showed that evaporation changes the most with the change of air humidity. The net radiation, air temperature and wind speed were the second, third and fourth effective parameters, respectively, which their changes made more changes in evaporation amount.

The chapter was ended with investigating the effect of THM analysis on evaporation estimate.

The result showed that using THM analysis which enables considering soil settlement, evaporation amount was estimated less. In other words, neglecting soil settlement overestimates evaporation.

CHAPTER 5

SUMMARY, CONCLUSIONS, AND SUGGESTIONS FOR FUTURE RESEARCH

5.1 SUMMARY

There are two approaches regarding the combined flow of moisture and heat in unsaturated porous media. One approach considers a combined soil atmosphere model by coupling atmosphere with soil. This approach uses thermo-hydro (TH) analysis and is not in deal with mechanical behavior of soil, and cannot estimate strain, stress and soil settlement. The other approach uses a thermo-hydro-mechanical (THM) analysis. In this approach equilibrium equation is coupled with moisture and heat flow equations; therefore, strain and stress in soil could be estimated too. However, atmosphere is not coupled and atmospheric (environmental) parameters are not used in the analysis. As a result, evaporation cannot be estimated.

In this study, equilibrium equation is coupled with moisture and heat flow equations, and at the same time the atmosphere is coupled through a soil-atmosphere model to be benefited from the advantages of both the abovementioned approaches. Therefore, accompanied with soil parameters, atmospheric (environmental) parameters are used too, and not only quantities related to moisture, heat, strain and stress but also potential and actual evaporations could be estimated using program EVAP1, which is developed during this study. The numerical analysis is performed considering plane strain conditions using constitutional models formulated in two-dimensional (2D) finite element program.

The theoretical formulation was a combination of two extended theories. The first part was an extension of the theory presented by Milly (1982) based on the theory of Philip and de Vries

(1957). The second part was the extension of the isothermal deformation theory of unsaturated soil to thermal effects.

A complete set of equations was presented in which the suction-based equations of moisture, heat and air transport were combined with the equilibrium equation of porous medium and constitutive law relation with the state surfaces of void ratio and degree of saturation (Gatmiri and Delage (1995), Gatmiri (1997)). These state surfaces are temperature-dependent.

Numerical solution of this set of fully coupled equations by the numerical method of finite element for spatial discretization and single step integration in time was used. Atmospheric coupling was performed using modified Penman equation presented by Wilson (1990). Atmospheric parameters of temperature, humidity, wind speed and net radiation were used in calculating evaporation from unsaturated soil surface.

To do validation, the results of the soil column tests of Wilson (1990) in predicting potential and actual evaporations from unsaturated soil were compared with EVAP1 results and a good agreement was achieved. Also, the results of Yang and Yanful (2002) test to estimate evaporation from 4 different soils with 3 different water levels were compared with the model results, which was acceptable.

5.2 CONCLUSIONS

A parametric study was performed to show the effect of the change of each of the four main environmental parameters (temperature, humidity, net radiation and wind speed) on potential and actual evaporation amounts. The results of the study are as below.

5.2.1 The effect of temperature

The potential and actual evaporations were estimated with three different average temperatures. Based on the results, the decrease of temperature decreased the evaporation. However, although the decrease of the maximum temperature from 21 to 16 ˚C and from 16 to 11 ˚C was the same (5˚C), the decrease of the potential was not the same. In fact, the effect of temperature change on evaporation amount was not linear. Regarding actual evaporation, the result was almost the same as potential evaporation. Meanwhile, actual evaporations correctly showed a decreasing trend.

5.2.2 The effect of humidity

In this section, all parameters were kept constant except for humidity, and the potential and actual evaporations due to a 12% change in humidity were estimated and compared with unchanged condition. The results showed correctly that evaporation decreases with the increase in humidity. However, the change in evaporation was nonlinear. In other words, the decrease in potential evaporation due to a 12% increase in humidity was not the same amount as the decrease in potential evaporation with another 12% increase in humidity. In fact, the decrease was less than before.

5.2.3 The effect of net radiation

The only parameter that changed in the analysis was net radiation. According to the results, the trend in the change of potential and actual evaporations was correct; i.e. decreasing net radiation decreased evaporation. Again, the change was not linear. Meanwhile, the change in both potential and actual evaporations were 20% due to a 27% change in net radiation.

5.2.4 The effect of wind speed

As it was expected, the increase in wind speed increased both potential and actual evaporations. However, the change was again nonlinear. Meanwhile, a 24% change in wind speed led to only 5% change in potential evaporation and 3% change in actual evaporation.

Therefore, when any of the four environmental parameters change to some extent, evaporation changes as well, but the same change in an environmental parameter does not change evaporation by the same amount as before.

5.2.5 Sensitivity analysis

Also, a sensitivity analysis was performed to find out the most important parameter from four main environmental parameters. The analysis result showed that humidity, net radiation, temperature and wind speed are the most important parameters in that order.

5.2.6 The effect of THM analysis

THM analysis enables the settlement of soil surface to be considered. Soil settlement decreases void ratio and porosity, which in turn decreases hydraulic conductivity and air conductivity, which in turn decreases evaporation. Therefore, neglecting soil settlement leads to overestimation of evaporation. A better estimation of actual evaporation considering soil settlement will be helpful in many fields including environmental geotechnics, where analysing the long-term performance of engineering structures such as soil covers, directly depends on the evaporation amount during the life-time of the structure.

5.3 RECOMMENDATIONS FOR FUTURE RESEARCH

The following recommendations can be made for further development of the model:

Calibration of parameters and extension of the program by probable modifications, to model the real cases, including cracks, fissures and other features;

Estimating the amount of evaporation change due to ruts that result from soil settlement and retention of water at the soil surface and its influence on the amount of evaporation;

Investigating other kinds of soils to acquire a more general idea about evaporation from different kinds of soils with and without considering soil settlement;

Extending the capability of the program to estimate oxygen diffusion and to consider the effect of vegetation on evaporation;

Instrumentation of a field case and measuring settlement in the soil surface over time, and comparing the measurements with the results from the model to have a better and more documented judgment on the model results, and to understand the limitations of the model;

Performing a parametric study and analysis of the sensitivity of evaporation from other kinds of soils, like silt and coarse sand, which are used in different layers of soil covers, to environmental parameters of air temperature, humidity, net radiation and wind speed, using THM approach.

REFERENCES

Abdel-Hadi O., and Mitchell J. K., 'Coupled heat and water flows around buried cables', J. Geotech. & Geoenviron. Eng., Div. Am. Soc. Civ. Eng., 107, Gt11, 1461-1487 (1981).

Abtew w. and Melesse A., 'Evaporation and evapotranspiration, measurements and estimations', Springer (2013).

Alonso E.E., Battle F., Gens A., and Lloret A., 'Consolidation analysis of partially saturated soils. Application to earth dam construction', Proc. Int. Conf. on Numerical Methods in Geotechnics. Innsbruck, 1303-1308 (1988).

Assouline, S., Tyler, S. W., Selker, J. S., Lunati, I., Higgins, C. W., and Parlange, M. B., 'Evaporation from a shallow water table: Diurnal dynamics of water and heat at the surface of drying sand', Water Resources Research, 49(7), 4022-4034 (2013).

Benson C., 'Modeling unsaturated flow and atmospheric interactions', Theoretical and Numerical Unsaturated Soil Mechanics, 187-201 (2007).

Bishop A. W., 'The principle of effective stress', Tek. Ukeblas., 39, 859-863 (1959).

Bishop A. W., and Blight G. E., 'Some aspects of effective stress in saturated and partly saturated soils', Géotechnique, 13(3), 177-197 (1963).

Blight G. E., 'Interaction between the atmosphere and the earth', Geotechnique, 47(4), 715-767 (1997).

Blight G. E., 'Measuring evaporation from soil surfaces for environmental and geotechnical purposes', Water SA (South African Water Resource Comission), 28(4), (2002).

Bouyoucos G. J., 'Effect of temperature on thermomovement of water vapor and capillary moisture in soils', Journal of Agricultural Research, 5, 141-172 (1915).

Brutsaert W., 'Daily evaporation from drying soil: universal parametrization with similarity',

Water Resources Research, 50, 3206-3215 (2013).

Cai G-Q, Zhao C-G, Sheng D-C, and Zho A-N, 'Formulation of thermo-hydro-mechanical coupling behavior of unsaturated soils based on hybrid mixture theory', Acta Mechanica Sinica, 30(4), 559-568 (2014).

Camp S., Gourc J. P., Ple O., and Villard P., 'Mechanical behavior of a clay layer for landfill cap cover application: experimental investigation and numerical modelling', Theoretical and Numerical Unsaturated Soil Mechanics, 203-209 (2007).

Cassel D. K., Nielsen D. R., and Biggar J. W., 'Soil-Water movement in response to imposed temperature gradients', Soil Science Society of America, Proc., 33, 493-500 (1969).

Ciocca F., Lunati Ivan, and Parlange M. B., 'Effects of the water retention curve on evaporation from arid soils', Geophysical Research Letters, 41, 3110-3116 (2016).

Cola S., Sanavia L., Simonini P., and Schrefler B. A., 'Coupled thermohydromechanical analysis of Venice lagoon salt marshes', Water Resources Research, 44 (2008).

Coleman J. D., 'Stress-strain relations for partly saturated soil, Correspondence', Géotechnique, 12(4), 348-350 (1962).

Croney D., and Coleman J. D., 'Soil thermodynamics applied to movement of moisture in road foundation', 7th International Congress for Applied Mechanics Proceedings, 3**,** 163-177 (1948).

Current Results, https://www.currentresults.com/Weather/Canada/Cities/humidity-annual-average.php (2017).

Dakshanamurthy V., and Fredlund D. G., 'Predicting of moisture flow and related heaving or shrinking in unsaturated soil continua', Proceedings of the Eighth Canadian Conference of Applied Mechanics, Moncton, 2, 281-282, 1981b.

Das B., Hendrickx J., and Borchers B., 'Modeling transient water distributions around landmines in bare soils', Soil Sci., 166(3), 163-173 (2001).

Davarzani H., Smits IK., Tolene R. M., and Illangasekare T., 'Study of the effect of the wind speed on evaporation from soil through integrated modeling of the atmospheric boundary layer and shallow subsurface', Water Resources Research, 50, 661-680 (2014).

Delage P. 'Experimental Unsaturated Soil Mechanics', Proc. 3rd Int. Conf. On Unsaturated Soils, UNSAT 2002, (3), 973-996 (2002).

Dempsey B. J., 'A mathematical model for predicting coupled heat and water movement in unsaturated soil', Int. J. Numer. Anal. Meth. Geomech., 2, 19-34 (1978).

Devillers P., Saix C., and El Youssoufi M. S., 'Loi de comportement thermo-hydromécanique pour les sols non saturés : identification in situ des indices de compression thermique', Can. Geotech. J., 33, 250-259 (1996).

De Vries D. A., `Simultaneous transfer of heat and moisture in porous media', Trans. Am. Geophys. Un., 39(5), 909-916 (1958).

Dirksen C., 'Water movement and frost heaving in unsaturated soil without an external source of water', Ph. D. Thesis, Cornell University (1964).

Djalal K., 'The effect of cracks and geomorphology on evaporation from clay soils', M. Sc. Thesis, Carleton University (2014).

Dumont M., Taibi S., Fleureau J-M, and Abou Bekr, 'Modelling the effect of temperature on unsaturated soil behaviour', C. R. Geoscience, 342, 892-900 (2010).

Duncan J. M. and Chang C. Y., ‘Nonlinear analysis of stress and strain in soils’, Journal of the Soil Mechanics and Foundations Division, ASCE, 96, SM5, Proc. Paper 7513, 1629-1653 (1970).

Douville H., Ribes A., Decharme B., Alkama R., and Sheffield J., ‘Anthropogenic influence on multidecadal changes in reconstructed global evapotranspiration’, Nat. Clim. Change, 3, 59–62 (2013).

Dye H. B., Houston S. L., and Welfert B. D., ‘Influence of Unsaturated Properties Uncertainty on Moisture Flow Modeling’, Geotech. Geol. Eng., 29(161), (2011).

Environment Canada, Meteorological Service of Canada, Canadian Climate Normals, ‘1981-2010 Climate Normals & Averages’ (2017).

Eslami H., Cuisinier O., and Masrouri F., ‘Modeling of coupled heat and moisture flows around a buried electrical cable’, E3S Web of Conferences 9, E-UNSAT (2016).

Ewen J. and Thomas H. R., 'Heating unsaturated medium sand', Géotechnique, 39(3), 455-470 (1989).

FAO website: http://www.fao.org/docrep/X0490E/x0490e07.htm#air%20humidity (2017).

Fayer M. J., ‘UNSAT-H Version 3.0: Unsaturated Soil Water and Heat Flow Model’, the US Department of Energy, Pacific Northwest National Laboratory (2000).

Feddes R. A., Kabat P., Van Bakel P. J. T., Bronswijk J. J. B., and Halbertsma J., ‘Modelling soil water dynamics in the unsaturated zone-State of the art’, Journal of Hydrology, 100, 69-111 (1988).

Fick A., ‘On liquid diffusion’, Philosophical Magazine, 10(63), 30–39 (1855).

Fredlund D. G., and Morgenstern N. R., 'Stress state variables for unsaturated soils', J. Geotech. Eng. Am. Soc. Civ. Eng., 103(5), 447-466 (1977).

Fredlund D. G., and Morgenstern N. R., 'Constitutive relations for volume change in unsaturated soil', Can. Geotech. J., 13(3), 261-276 (1976).

Fredlund D. G., 'Appropriate concepts and technology for unsaturated soils', Can. Geotech. J., 16, 121-139 (1979).

Fredlund D. G., and Rahardjo H., 'Soil mechanics for unsaturated soils', John Wiley and Sons Incorporation, Hoboken, US (1993).

Fredlund D. G., Stone J., Stianson J., and Sedgwick A. 'Determination of water storage and permeability functions for oil sands tailings', Proceedings tailings and mine waste, Vancouver BC (2011).

Gardner W. R., 'Some steady state solutions of the unsaturated moisture flow equation with application to evaporation from water table', Soil Science, 85(4), 228-232 (1958).

Gardner W. R., and Hillel D., 'The relation of external evaporation condition to the drying of soils', J. Geophys. Res., 67, 4319-4325 (1962).

Gardner H. R., and Hanks R. J., 'Evaluation of the evaporation zone in soil by measurement of heat flux', Soil Sci. Soc. Am. Proc. 30, 425-428 (1966).

Gatmiri B, and Magnin P., 'Minimum time step criterion in FE analysis of unsaturated consolidation: Model UDAM', In Proc 3rd Eur Spec Conf on Num Meth in Geo Eng, Manchester, UK (1994).

Gatmiri B., and Delage P., 'Nouvelle formulation de la surface d'état en indice des vides pour un modèle non linéaire élastique des sols non saturés', Proc. 1st Int. Con. Unsaturated Soils, 2, 1049-1056 (1995).

Gatmiri B., ‘Evolution du code U-DAM; Description détaillée et mode d'emploi’, Rapport du CERMES, ENPC. (1992).

Gatmiri B., ‘Fully coupled thermal-hydraulic-mechanical behavior of saturated porous media (soils and fractured rocks), new formulation and numerical approach’, Final Report CERMES-EDF (1995).

Gatmiri B. and Delage P., ‘A formulation of fully coupled thermal-hydraulic-mechanical behavior of unsaturated porous media - numerical approach’, Int. j. Numer. Anal. Methods Geomech., 21(3), 199-225 (1997).

Gatmiri B., ‘Final report’, CERMES, ENPC. (1997).

Gatmiri B., Jenab-Vossoughi B., and Delage P., ‘Validation of θ-Stock, a finite element software for the analysis of thermo-hydro-mechanical behavior of engineering clay barriers’, proceedings of NAFEEMS World Congress, Rhode Island, USA (1999).

Gatmiri B., and Arson C., ‘θ-STOCK, a powerful tool of thermohydromechanical behaviour and damage modelling of unsaturated porous media’, Computers and Geotechnics, 35, 890-915 (2008).

Gens A., and Olivella S., ‘THM phenomena in saturated and unsaturated porous media: Fundamentals and formulation’, Journal Revue Francaise de Genie Civil, 693-717 (2011).

GEO-SLOPE International Ltd., Vadose Zone Modeling with VADOSE/W 2007, Third Edition (2008).

Geraminegad M., and Saxena S. K., 'A coupled thermoelastic model for saturated-unsaturated porous media', Géotechnique, 36(4), 539-550 (1986).

Ghasemzadeh H., ‘Heat and contaminant transport in unsaturated soil’, International Journal of Civil Engineering, 6 (2), (2008).

Ghembaza M. S., Taibi S., and Fleureau J-M, 'Some aspects of the effect of the temperature on the behavior of unsaturated sandy clay', Experimental Unsaturated Soil Mechanics, 243-250 (2007).

Gitirana Jr. G., Fredlund M. D., and Fredlund D. G., 'Numerical modeling of soil-atmosphere interaction for unsaturated surfaces', Unsaturated Soils, 658-669 (2006).

Gouda K. R. S. and Winterkorn H. F., 'Theoretical and experimental exploration of the practical possibilities of electro-osmosis', Final Report on Beach Sand Stabilization Research, Part V (1949).

Granger R. J. 'An examination of the concept of potential evaporation', Journal of Hydrology (1989a).

Gouda K. R. S. and Winterkorn H. F., 'Theoretical and experimental exploration of the practical possibilities of electro-osmosis', Final Report on Beach Sand Stabilization Research, Part V (1949).

Gupta A., and Cosmato D., 'How relative humidity affects evaporation', http://www.brighthub.co/environment/science-environmental/articles/104601.aspx (2011).

Gurr C. G., Marshall T. J., and Hutton J. T., 'Movement of water in soil due to a temperature gradient', Soil Sci., 74, 335-345 (1952).

Haghighi E., and Or D., 'Evaporation from porous surfaces into turbulent airflows: coupling eddy characteristics with pore scale vapor diffusion', Water Resources Research, 49, 8432-8442 (2013).

Haxaire A., Galavi V., and Brinkgreve R. B. J., 'Fully coupled thermo-hydro-mechanical analysis for unsaturated soils in Plaxis', Delft University of Technology (2011).

Holiday Weather, www.holiday-weather.com/toronto/averages/ (2017)

International Glossary of Hydrology WMO, UNESCO World Meteorological Organization, 3rd edition (1974).

Ito M., Azam S., and Hu Y., 'A two-stage model for moisture-induced deformations in expansive soils', Environmental Systems Research, 3(19), (2014)

Jeanne P., Rutqvist J., Dobson P. F., Walters M., Hartline C., and Garcia J., 'The impacts of mechanical stress transfers caused by hydromechanical and thermal processes on fault stability during hydraulic stimulation in a deep geothermal reservoir', International of Rock Mechanics and Mining Sciences, 72, 149-163 (2014).

Jenning J. E. B. and Burland J. B. 'Limitations to the use of effective stresses in partly saturated soil', Géotechnique, 12, 125-144 (1962).

Jensen M. E., Burman R. D., and Allen R. G. E., 'Eds. Evaporation and Irrigation Water Requirements', ASCE Manuals and Reports on Engineering Practices, 70, pp. 360 (1990).

Jotisankasa A., 'Collapse behavior of a compacted silty clay', Ph. D. thesis, Imperial College London (2005).

Katata G., Nagai H., Ueda H., Agam N., and Berliner P. R., 'Development of a land surface model including evaporation and adsorption processes in the soil for the land-air exchange in arid regions', American Meteorological Society (2007).

Kebede S., Travia Y., Alemayehub T., and Marca V., 'Water balance of Lake Tana and its sensitivity to fluctuations in rainfall', Blue Nile basin, Ethiopia. J. Hydrol., 316, 233-247 (2006).

Kobayashi T., 'The effect of the temperature gradient on the evaporation from bare soils with dry surfaces', Proceedings of the Yokohama Symposium, IAHS publication no. 212 (1993).

Kuang X., Jiao J. J., and Li H., 'Review on air flow in unsaturated zones induced by natural forcing', Water Resources Research, 49, 6137-6165 (2013).

Lagerloef G., Schmitt R., Schanze J., and Kao H.-Y., 'The ocean and the global water cycle', Oceanography, 23(4), 82-93 (2010).

Lebedeff A. F., 'The movement of ground and soil waters', 1st International Congress of Soil Science, Proceedings, 1, 459-494 (1927).

Lehmann P., Assouline S., and Or D., 'Characteristic lengths affecting evaporative drying of porous media, Phys. Rev. E, 77(5), (2008).

Liu B., Xu M., Henderson M., and Gong w., 'A spatial analysis of pan evaporation trends in China 1955–2000', J. Geophys. Res., 109 (2004).

Linacre E. T., 'Evaporation trends', Theor. Appl. Climatol., 79, 11-21 (2004).

Liu X. C.; Xu W. j., Zhan L. T., and Chen Y. M., 'Laboratory and numerical study on enhanced evaporation process in a loess soil column subjected to heating', Journal of Zhejiang University-SCIENCE (Applied Physics & Engineering), 17(7), (2016).

Lloret A., and Alonso E. E., 'Consolidation of unsaturated soils including swelling and collapse behavior', Géotechnique, 30(4), 449-477 (1980).

Lloret A., Villar M. V., Sanchez M., Gens A., Pintado X., and Alonso E., 'Mechanical behaviour of heavily compacted bentonite under high suction changes', Geotechnique, 53(1), 27-40 (2003).

Lu Y., Wu X., and Cui Y., 'On the thermo-mechanical properties of unsaturated soils', Journal of Rock Mechanics and Geotechnical Engineering, 2(2), 143-148 (2010).

Mabirizi D., and Bulut R., 'Unsaturated soil moisture drying and wetting diffusion coefficient measurements in laboratory', Project No: OTCREOS7.1-11, Oklahoma State University (2009).

Machibroda R. T., 'Evaluation of evaporative fluxes from mine tailings using the modified Penman formulation', Ph. D. thesis, Saskatoon, University of Saskatchewan, Canada (1994).

Matyas E. L., and Radhakrishna H. S., 'Volume change characteristics of partially saturated soils', Géotechnique, 18, 432-448 (1968).

MEND, 'Report 1.25.1 SOILCOVER users' manual version 2.0', 1996.

Milly P. C. D., 'Moisture and heat transport in hysteretic, inhomogeneous porous media: A matric heat-based formulation and a numerical model', Water Resources Research, 18(3), 489-498 (1982).

Moradi A., Smits K. M., Lu N., and McCartney J. S., 'Heat Transfer in Unsaturated Soil with Application to Borehole Thermal Energy Storage', Vadose Zone Journal, Soil Science Society of America, 6(3), (2016).

Nanda N., 'Analysis of consolidation of embankment dams during construction', Rapport du CERMES-ENPC (1989).

NASA, NASA Earth Observations (NEO), global maps, 'Net radiation map' (2017).

Neriah A. B., Assouline S., Shavit U., and Weisbrod N., 'Impact of ambient conditions on evaporation from porous media', Water Resources Research, 50(8), 6696-6712 (2014).

Novak M. D., 'Dynamics of the near-surface evaporation zone and corresponding effects on the surface energy balance of a drying bare soil', Agricultural and Forest Meteorology, 150(10), 1358-1365 (2010).

Nyhan J. W., Schofield T. J., and Starmer R. H., 'A water balance study of four landfill cover designs varying in slope for semiarid regions', J. Environ. Qual., 26, 1385-1392 (1997).

Olivella S., and Gens A. 'Vapor transport in low permeability unsaturated soils with capillary effects', Transport in Porous Media, 40, 219-241 (2000).

Peel M. C., and McMahon T. A., 'Estimating evaporation based on standard meteorological data-progress since 2007', Progress in Physical Geography, 38(2), 241-250 (2014).

Penman H. L., 'Gas and vapor movement in soil', J. Agric. Sci., 30, 437-462 (1940).

Penman H. L., 'Natural evapotranspiration from open water, bare soil and grass', Proc. R. Soc. London Ser. A., 193, 120-145 (1948).

Philip J.R. and De Vries D. A., 'Moisture movement in porous materials under temperature gradients', Trans. Am. Geophys. Un., 38, 222-232 (1957).

Pontius F. 'An updated global energy balance', The drinking water advisor, retrieved from http:/drinkingwateradvisor.com (2012).

Prat M., 'Recent advances in pore-scale models for drying of porous media', Chem. Eng. J., 86, 153-164 (2002).

Qin B., Chen Z. H., Fang Z. D., Sun S. G., Fang X. W. and Wang J., 'Analysis of coupled thermo-hydro-mechanical behavior of unsaturated soils based on theory of mixtures I', Appl. Math. Mech., Engl. Ed. 31(12), 1561-1576 (2010).

Rianna G., Pagano L., and Urciuoli G., 'A physical model to investigate the influence of atmospheric variables on soil suction in Pyroclastic soils', Unsaturated soils: Research and applications, 221-227 (2012).

Rollins R. L., Spangler M. G., and Kirkham D., 'Movement of soil moisture under a thermal gradient', Highway Research Board proceedings, 33**,** 492-508 (1954).

Rosenberg N. J., Blad B. L., and Berma S. B., 'Microclimate, the biological environment', John Wiley and Sons Inc., 209-287 (1983).

Rutqvist J., Borgesson L., Chijimatsu M., Kobayashi A., Jing L., Nguyen T. S., Noorishad J., and Tsang C. F., 'Thermohydromechanics of partially saturated geological media: governing equations and formulation of four finite element models', International Journal of Rock Mechanics & Mining Sciences, 38, 105-127 (2001).

Saito H., Simunek J., and Mohanty B. P.' 'Numerical analysis of coupled water, vapor, and heat transport in the vadose zone', Vadose Zone J., 5, 784-800 (2006).

Sakai M., Jones S. B., and Tuller M., 'Numerical evaluation of subsurface soil water evaporation derived from sensible heat balance', Water Resources Research, 47 (2011).

Sasamori T., 'A numerical study of atmospheric and soil boundary layers', Journal of the Atmospheric Sciences (1970).

Schanz M., and Pryl D., 'Dynamic fundamental solutions for compressible and incompressible modeled poroelastic continua', Int. J. Solid Struct., 41, 4047-4073 (2004).

Seager R., Ting M., Held I., Kushnir Y., Lu J., Vecchi G., Huang H., Harnik N., Leetmaa A., Lau N., Li C., Velez J., and Naik N., 'Model projections of an imminent transition to a more arid climate in southwestern North America', Science, 316(5828), 1181-1184 (2007).

Sen M., 'Analytical heat transfer', University of Notre Dame (2015).

Shahraeeni E., Lehmann P., and Or D., 'Coupling of evaporative fluxes from drying porous surfaces with air boundary layer: characteristics of evaporation from discrete pores', Water Resources Research, 48 (2012).

Shokri N., Lehmann P., and Or D., 'Characteristics of evaporation from partially wettable porous media', Water Resources Research, 45 (2009).

Shokri N., Lehmann P., and Or D., 'Evaporation from layered porous media', Journal of Geophysical Research, 115 (2010).

Shokri N., and Or D., 'What determines drying rates at the onset of diffusion controlled stage-2 evaporation from porous media?', Water Resources Research, 47(9), (2011).

Smits K. M., Ngo V. V., Cihan A., Sakaki T., and Illangasekare T. H., 'An evaluation of models of bare soil evaporation formulated with different land surface boundary conditions and assumptions', Water Resources Research, 48 (2012).

Smits, K., Eagen, V., and Trautz, A., 'Exploring the effects of atmospheric forcing on evaporation: experimental integration of the atmospheric boundary layer and shallow subsurface, J. Vis. Exp., 100 (2015).

Smith W. O., 'Thermal transfer of moisture in soils', American Geophysical Union, Transaction, 24**,** 511-523 (1943).

Song X., Idinger G., Borja R. I., and Wu W., 'Finite element simulation of strain localization in unsaturated soils', Unsaturated soils: Research and applications, 189-195 (2012).

SOILCOVER, Mine Environment Neutral Drainage (MEND) (1994).

Sophocleous M., 'Analysis of water and heat flow in unsaturated-saturated porous media, Water Resources Research, 15(5), 1195-1206 (1979).

Stocker T. F., Qin D. H., Plattner G. K., Tignor M. M. B., Allen S. K., Boschung J., Nauels A., Xia Y., Bex V., and Midgley P. M., 'Climate Change 2013: The Physical Science Basis', Cambridge Univ. Press, New York, pp.7 (2013).

Su T., Feng T., and Feng G., 'Evaporation variability under climate warming in five reanalyses and its association with pan evaporation over China', Journal of Geophysical Research: Atmospheres, 120, 8080-8098 (2015).

Tadros T., 'Kelvin Equation', Encyclopedia of colloid and interface science, Springer Berlin Heidelberg, 679-680 (2013).

Teng J., Yasufuku N., Ishikura R., and Jiang Z., 'Modeling soil water redistribution in unsaturated zone during evaporation process', Unsaturated soils: Research and applications, Khalili Russell & Khoshghalb (Eds) Taylor & Francis Group, 537-543 (2014).

Thomas H. R., 'Nonlinear analysis of heat and moisture transfer in unsaturated soil', Journal of Engineering Mechanics ASCE, 13(8), 1163-1180 (1987).

Thomas H. R., and He Y., 'Analysis of coupled heat, moisture and air transfer in a deformable unsaturated soil', Géotechnique, 45, 677-689 (1995).

Thomas H. R., Yang H. T., He Y., and Jefferson A. D., 'Solving coupled thermo-hydro-mechanical problems in unsaturated soil using a substructuring-frontal technique', Communications in numerical methods in engineering, 14, 783-792 (1998).

Thornthwaite C. W., ‘An approach toward a rational classification of climate’, Geographical review, 38, 55-94 (1948).

Thornthwaite C. W. and Mather j. R., ‘The water balance, second printing’, Publications in climatology, Drexel Institute of Technology, Centerton, New jersey, 8(1), (1955).

Trautz A. C., ‘Heat and mass transfer in porous media under the influence of near-surface boundary layer atmospheric flow’, Ph. D. thesis, Dep. of Civil and Envir. Eng., Colorado University (2016).

VADOSE/W, Geo-Slope International Ltd. (2002).

Valiantzas J. D., ‘Simplified versions for the Penman evaporation equation using routine weather data’, Journal of Hydrology, 331, 690-702 (2006).

Van Heerwaarden C. C., de Arellano J. V., and Teuling A. J., ‘Land atmosphere coupling explains the link between pan evaporation and actual evapotranspiration trends in a changing climate’, Geophysical Research Letters, 37 (2010).

Vardon, P. J., Banicescu, I., Cleall, P. J., Thomas, H. R., and Philp, R. N., ‘Coupled thermo-hydro-mechanical modelling: A new parallel approach’, Proc., PDSEC-09 Workshop of the IEEE IPDPS 2009 Conf., Rome (2009).

Villar M. V., Cuevas J., Fernandez A. M. and Martin P. L., ‘Effects of the interaction of heat and water flow in compacted bentonite’, Proceedings of International workshop thermomechanics of clays and clay barriers, Bergamo : ISMES (1993).

Wang X., ‘Vapor flow resistance of dry soil layer to soil water evaporation in arid environment: an overview’, Water, 7, 4552-4574 (2015).

Wang W., Adamidis P., Hess M., Kemmler D., and Kolditz O., 'Parallel finite element analysis of THM coupled processes in unsaturated porous media', Theoretical and Numerical Unsaturated Soil Mechanics, 165-175 (2007).

Wang, K. C., and Liang S., 'An improved method for estimating global evapotranspiration based on satellite estimation of surface net radiation, vegetation index, temperature, and soil moisture', J. Hydrometeorol., 9, 712-727 (2008).

Wang, K. C., Dickinson R. E., Wild M., and Liang S., 'Evidence for decadal variation in global terrestrial evapotranspiration between 1982 and 2002: 1. Model development', J. Geophys. Res., 115 (2010a).

Wang, K. C., Dickinson R. E., Wild M., and Liang S., 'Evidence for decadal variation in global terrestrial evapotranspiration between 1982 and 2002: 2. Results', J. Geophys. Res., 115 (2010b).

Wang W., Rutqvist J., Gorke U-J, Birkholser J. T., and Kolditz O., 'Non-isothermal flow in low permeable porous media: a comparison of Richards' and two-phase flow approaches', Environ. Earth Sci., 62, 1197-1207 (2011).

Wang H., Rezaee R., and Saeedi A., 'Evaporation process and pore size distribution in tight sandstones: a study using NMR and MICP', Procedia Earth and planetary science, 15, 767-773 (2015).

Wang X., 'Vapor flow resistance of dry soil layer to soil water evaporation in arid environment: An overview', Water, 7(8), 4552-4574 (2015).

Weaver J., and Tillman F., 'Uncertainty and the Johnson-Ettinger model for vapor intrusion calculations', U.S. Environ. Prot. Agency Publ. EPA/600/R-05/110, 43 pp., Office of Research and Development, EPA, Washington, D. C. (2005).

Weeks B., and Wilson G. W., 'Net radiation and the prediction of evaporation from sloped soil surfaces', Geotechnical news (2003).

Wilson G. W., 'Soil evaporative fluxes for geotechnical engineering problems', Ph. D. thesis, University of Saskatchewan, Saskatoon, Canada (1990).

Wilson G. W., Fredlund D. G., and Barbour S. L., 'Coupled soil-atmosphere modeling for soil evaporation', Can. Geotech. *J*., 31, 151-161 (1994).

Wilson G. W., Fredlund D. G., and Barbour S. L., 'The effect of soil suction on evaporative fluxes from soil surfaces', Can. Geotech. J., 34, 145-155 (1997).

Winterkorn H. F., 'Mass transport phenomenon in moist porous systems as reviewed from the thermo-dynamics of irreversible processes, Highw. Res. Bd Bull., 40 (1959).

Wu W., Li X., Charlier R., and Collin F., 'A thermo-hydro-mechanical constitutive model and its numerical modelling for unsaturated soils', Computers and Geotechnics, 31, 155-167 (2004).

Xie Z., Dai Y., and Zeng O., 'An unsaturated soil water flow problem and its numerical simulation', LASG, Institute of Atmospheric Physics, Chinese Academy of Sciences (1999).

Xu C., Gong L., Jiang T., Chen D., and Singh V. P., 'Analysis of spatial distribution and temporal trend of reference evapotranspiration and pan evaporation in Changjiang (Yangtze River) catchment', J. Hydrol., 327, 81–93 (2006).

Yamanaka T., Takeda A., and Sugita F. 'A modified surface-resistance approach for representing bare-soil evaporation: Wind tunnel experiments under various atmospheric conditions', Water Resources Research, 33(9), 2117-2128 (1997).

Yanful E. K., 'Engineering soil covers for reactive tailing management: Theoretical concepts and laboratory development', MEND Proceedings, 461-585 (1991).

Yanful E. K., and Choo L. P., 'Measurement of evaporative fluxes from candidate cover soils', Can. Geotech. J., 34, 447-459 (1997).

Yanful E. K., and St-Arnaud L. C., 'Design, instrumentation and construction of engineered soil covers for reactive tailing management', Proceedings of the 2nd International Conference on Abatement of Acidic Drainage, Montreal Mine Environment Neutral Drainage (MEND) Program, Ottawa, 487-504 (1991).

Yanful E. K., and St-Arnaud L. C., 'Migration of acidic pore waters at the Waite Amulet tailings site near Rouyn-Noranda, Quebec, Canada', Canadian Geotechnical Journal, (29) 466-476 (1992).

Yanful E. K., and Mousavi S. M., 'Estimating falling rate evaporation from finite soil columns', The Science of the Total Environment', 313, 141-152 (2003).

Yanful, E. K., Mousavi S. M., and De Souza L. P., 'A numerical study of soil cover performance', Journal of Environmental Management, 81, 72-92 (2006).

Yang M., and Yanful E. K., 'Water balance during evaporation and drainage in cover soils under different water table conditions', Advances in Environmental Research, 6, 505-521 (2002).

Yu L., 'Global variations in oceanic evaporation (1958-2005): The role of the changing wind

speed', Journal of Climate, 20, (2007).

Zeng Y., Su Z., Wan L., and Wen J., 'A simulation analysis of the advective effect on evaporation using a two-phase heat and mass flow model', Water Resources Research, 47 (2011).

APPENDIX A

The terms of the matrix (Eq. 3.24) are as below:

$$[R_{uu}] = \int_{\Omega} B^T.D.B d\Omega$$

$$[R_{uT}] = \int_{\Omega} B^T.C.N d\Omega$$

$$[R_{uw}] = \int_{\Omega} B^T.F.N d\Omega$$

$$[R_{ua}] = \int_{\Omega} B^T.(m-F).N d\Omega$$

$$\{F_{\sigma}\} = \int N^T.\bar{\sigma}.d_{\Gamma} + \int N b_i d\Omega$$

The terms of thermal coupling:

$$[C_{TU}] = \int_{\Omega} N^T [D_{3U}] B d\Omega \qquad \text{with: } [D_{3U}] = \left[m^T [IV] + \underline{g}_1 [V] D \right]$$

$$[C_{TT}] = \int_{\Omega} N^T [D_{3T}] N d\Omega \qquad \text{with: } [D_{3T}] = \left[(g_3 - C\underline{g}_1)[V] + [VI] \right]$$

$$[C_{Tw}] = \int_{\Omega} N^T [D_{3w}] N d\Omega \qquad \text{with: } [D_{3w}] = \left[(\underline{g}_1 F - g_2)[V] \right]$$

$$[C_{Tg}] = \int_{\Omega} N^T [D_{3Pg}] N d\Omega \qquad \text{with: } [D_{3Pg}] = \left[\left(g_2 - F\underline{g}_1 \right)[V] \right]$$

$$[K_{TT}] = \int_{\Omega} (\nabla N)^T \left[\lambda + [fx1](T - T_0) + \rho_w D_{Tv} h_{fg} + \rho_v K_g \beta_{Pg} h_{fg} \right] \nabla N d\Omega$$

$$fx1 = \rho_w C_w D_{Tw} + \rho_w C_v D_{Tv} + \rho_g K_g \beta_{Pg} C_{pg}$$

$$\left[K_{Tw}\right]=\int_{\Omega}\left(\nabla N\right)^{T}\left[\left(\rho_{w}C_{w}D_{Pw}+\rho_{w}C_{v}D_{Pv}\right)\left(T-T_{0}\right)+\rho_{w}D_{Pv}h_{fg}\right]\nabla N d\Omega$$

$$\left[K_{Ta}\right]=\int_{\Omega}\left(\nabla N\right)^{T}\left[\left(C_{a}K_{a}\rho_{a}\left(T-T_{0}\right)+\rho_{v}K_{a}h_{fg}\right)\right]\nabla N d\Omega$$

The coupling terms corresponding to water:

$$\left[C_{wv}\right]=\int_{\Omega}N^{T}\left[Am^{T}+B'\underline{g}_{1}D\right][B]d\Omega$$

$$\left[C_{wT}\right]=\int_{\Omega}N^{T}\left[E+B'\left(g_{3}-\underline{g}_{1}C\right)+nS_{r}\beta_{T}\right]N d\Omega$$

$$\left[C_{ww}\right]=\int_{\Omega}N^{T}\left[B'\left(\underline{g}_{1}F-g_{2}\right)+nS_{r}\beta_{P}\right]N d\Omega$$

$$\left[C_{wa}\right]=\int_{\Omega}N^{T}\left[B'\left(g_{2}-\underline{g}_{1}F\right)\right]N d\Omega$$

$$\left[K_{wT}\right]=\int_{\Omega}\left(\nabla N\right)^{T}\left[D_{TT}\right]\nabla N d\Omega \qquad \text{with:} \quad D_{TT}=\rho_{w}\left(D_{Tv}+D_{Tw}\right)$$

$$\left[K_{ww}\right]=\int_{\Omega}\left(\nabla N\right)^{T}\left[D_{P}\right]\nabla N d\Omega \qquad \text{with:} \quad D_{P}=\rho_{w}\left(D_{Pv}+D_{Pw}\right)$$

And the coupling terms corresponding to air:

$$\left[C_{au}\right]=\int_{\Omega}N^{T}\left[D_{2u}\right][B]d\Omega \;;\; D_{2u}=\left[m^{T}\rho_{a}\left(1-S_{r}\left(1-H\right)\right)+\left[\alpha_{Sr}\underline{g}_{1}+\left(1-H\right)n\rho\underline{g}_{1}\right]D\right]$$

$$\left[C_{gT}\right]=\int_{\Omega}N^{T}\left[n(1-S_{r}(1-H))\alpha_{T}+(g_{3}-\underline{g}_{1}C)\left[\alpha_{Sr}-(1-H)n\rho_{g}\right]\right]N d\Omega$$

$$\left[C_{gw}\right]=\int_{\Omega}N^{T}\left[\left(\underline{g}_{1}F-g_{2}\right)\left(\alpha_{Sr}-\left(1-H\right)n\rho_{g}\right)\right]N d\Omega$$

$$\left[C_{gg}\right]=\int_{\Omega} N^{T}\left[n\left(1-S_{r}\left(1-H\right)\right)\alpha_{P}+\left(g_{2}-\underline{g}_{1}F\right)\left(\alpha_{Sr}-\left(1-H\right)n\rho_{g}\right)\right]NdΩ$$

$$\left[K_{aT}\right]=\int_{\Omega}\left(\nabla N^{T}\right)\left[\frac{-K_{a}\rho_{a}}{\gamma_{a}}\beta_{Pa}-H\rho_{a}D_{Tw}+\rho_{w}D_{Tv}\right]\nabla N d\Omega$$

$$\left[K_{aw}\right]=\int_{\Omega}\left(\nabla N\right)^{T}\left[\rho_{w}D_{Pv}-H\rho_{a}D_{\theta w}\right]\nabla N d\Omega$$

$$\left[K_{aa}\right]=\int_{\Omega}\left(\nabla N\right)^{T}\left[\frac{-K_{a}}{\gamma_{a}}\rho_{a}\right]\nabla N d\Omega$$

In which the following terms were used:

$F = DD_{s}^{-1}$ with $D_{s}^{-1} = \beta_{s} m$ in which $\beta_{s}=\frac{1}{1+e}\frac{\partial e}{\partial(p_{g}-p_{w})}$

and $m^{T}=\left[1 \quad 1 \quad 0\right]$

$C = DD_{t}^{-1}$ with $D_{t}^{-1} = \beta_{t} m$ in which $\beta_{t}=\frac{1}{1+e}\frac{\partial e}{\partial T}$

$$g_{1}=\frac{\partial S_{r}}{\partial\left(\sigma-P_{a}\right)}$$

$$g_{2}=\frac{\partial S_{r}}{\partial\left(P_{a}-P_{w}\right)}$$

$$g_{3}=\frac{\partial S_{r}}{\partial T}$$

$$\underline{g}_{1}=m_{1}^{T}.g_{1}=\left[0 \quad 1 \quad 0\right]g_{1}$$

$$\alpha_{T}=\frac{\rho_{a}}{T+273}$$

$$\alpha_P = \frac{\left(1 + \frac{HS_r}{1 - S_r}\right)}{R_g(T + 273)}$$

$$\alpha_{Sr} = \frac{P_a + P_{atm}}{R_g(T + 273)} \frac{H}{(1 - S_r)^2}$$

$$A = \rho_w S_r + \rho_v(1 - S_r) + nS_r(1 - S_r)A_n$$

$$B' = n(\rho_w - \rho_v) + n^2(1 - S_r)A_n$$

$$E = n(1 - S_r)(\rho_v A_0 - 4975.9nS_r A_n)$$

$$\beta_T = \left.\frac{\partial \rho_w}{\partial T}\right|_{P_w = cte} \quad , \quad \beta_P = \left.\frac{\partial \rho_w}{\partial P_w}\right|_{T = cte}$$

$$\rho_w = \rho_{w0}(1 + \beta_P \rho_w + \beta_T T)$$

$$I = S_r \rho_w C_{Pw} - \rho_s C_{Ps} + (1 - S_r)(\rho_v C_{Pv} + \rho_g C_{Pg}) + A_n S_r n(1 - S_r C_{Pv})$$

$$II = n\rho_w C_{Pw} - n(\rho_v C_{Pv} + C_{Pg}\rho_a) + A_n . n^2(1 - S_r)C_{Pv}$$

$$III = ((A_0 \rho_v - 4975.9nS_r A_n)n(1 - S_r)C_{Pv})$$

$$IV = I(T - T_0) + (1 - S_r)\rho_v h_{fg} + n(1 - S_r)h_{fg}A_n . S_r$$

$$V = II(T - T_0) - n\rho_v h_{fg} + n^2(1 - S_r)h_{fg} . A_n$$

$$VI = C_T + III(T - T_0) + n(1 - S_r)h_{fg}(A_0 \rho_v - 4975.9nS_r A_n)$$

$$A_0 = \frac{1}{\rho_0}\frac{d\rho_0}{dT}$$

$$A_n = \frac{1}{S_r}\frac{\partial \rho_v}{\partial n} = \frac{1}{n}\frac{\partial \rho_v}{\partial S_r}$$

APPENDIX B

Subroutines and functions of Program EVAP1

The following is a list of subroutines and functions of program EVAP1 and their functionality within the program and the tasks they accomplish. From total 64 subroutines and functions of EVAP1, the 31 Black written subroutines are intact subroutines of program θ-Stock. The 15 subroutines and functions that are written in red are the added ones. The 5 and 13 subroutines written in green and blue are modified and repeated subroutines, respectively.

Program EVAP1

It is a two-dimensional plane strain finite element program for the thermo-hydro-mechanical analysis of evaporation from unsaturated soils.

The program includes four-noded drained, saturated and unsaturated elements. Hyperbolic model is used for drained and saturated elements.

The state surface-hyperbolic model is used for unsaturated elements. The program considers hydraulic anisotropic soils and different boundary conditions considering state surface of void ratio and degree of saturation. It also considers element pressures (water and air) based on boundary values considering physical loading, air flow, water flow and heat flow conditions and atmospheric coupling.

Atmospheric parameters of air temperature, net radiation, wind speed, and humidity are used on daily based to calculate potential and actual evaporations.

Following is a list of subroutines and functions of the program.

ccno(0)

Main program

ccno(1)

subroutine Markaz(a,lmax)

This subroutine controls the program.

ccno(2)

subroutine nlchk(iconst,nload,itime,k,i)

This subroutine checks for loading step.

ccno(3)

subroutine checkpl(nelcam,icam)

This subroutine checks the occurrence of plasticity.

ccno(4)

subroutine dim1(l1,l2,l3,l4,l5,l6,l7,l8,l9,l10,l11,l12,l13,

*l14,l15,l16,l17,l18,l19,l20)

This subroutine reads basic and climate data and allocates

storage.

ccno(5)

subroutine input(ie4d,ie4c,ie4u,iconst,kodex,kodey,

*kodew,kodea,x,sm4d,sm4c,sm4u)

This subroutine reads mesh, material, boundary conditions

and loading data.

ccno(6)

subroutine dim2(ie4d,ie4c,ie4u,id,l20,l21,l22,l23,l24,l25,l26)

This subroutine further allocates dynamic storage

and determines degrees of freedom (id array).

ccno(7)

subroutine detna(ie4d,ie4c,ie4u,id,kodex,kodey,kodew,kodea,

*di,na)

This subroutine determines the na vector (this locates the diagonal coefficient for skyline storage) and the length of the stiffness vector.

ccno(8)

subroutine init1(ie4d,ie4c,ie4u,

*sig4d,sig4c,sig4u,dsig4d,dsig4c,dsig4u,

*r,rr,dt,iact)

This subroutine initializes stress and displacement arrays.

ccno(9)

subroutine init2(ie4d,ie4c,ie4u,x,sm4d,sm4c,sm4u,

*sig4d,sig4c,sig4u,dsig4d,dsig4c,dsig4u,r,rr,dt,id)

This subroutine performs initial calculation.

ccno(10)

subroutine init3(r,rr,di,dt,id)

This subroutine stores and prints initial stresses.

ccno(11)

subroutine build(ie4d,ie4c,ie4u,id,iconst,x,

*sm4d,sm4c,sm4u,sig4d,sig4c,sig4u,rr,iact,dt)

This subroutine determines the loading condition and calls the load routines.

ccno(12)

subroutine loadnode(x,id,rr)

This subroutine calculates nodal loads due to surface physical loads.

ccno(13)

subroutine flotnode(x,id,rr)

This subroutine calculates nodal heat loads due to surface heat flow.

ccno(14)

subroutine flotevapnode(x,id,rr)

This subroutine calculates nodal temperature loads due to evaporation in surface elements.

ccno(15)

subroutine flownode(x,id,rr)

This subroutine calculates nodal water loads due to surface water flow.

ccno(16)

subroutine flowevapnode(x,id,rr)

This subroutine calculates nodal water loads due to evaporation in surface elements.

ccno(17)

subroutine floanode(x,id,rr)

This subroutine calculates nodal loads due to surface air Flow.

ccno(18)

subroutine lstp(r,rr)

This subroutine adds the external loads to r.

ccno(19)

subroutine stiff(ie4d,ie4c,ie4u,id,x,sm4d,sm4c,sm4u,

* sig4d,sig4c,sig4u,dsig4d,dsig4c,dsig4u,

* r,rr,di,dt,na,iact,s1,s2)

This subroutine assembles the global stiffness matrix.

ccno(20)

subroutine shap4n(s,t,f,pfs,pft)

This subroutine calculates the shape functions and

their derivatives.

ccno(21)

subroutine bmat4n(xe,ye,f,pfs,pft,b,detj)

This subroutine calculates the strain displacement

matrix for a 4 noded soil element.

ccno(22)

subroutine body(m,mt,mb,xe,ye,q,gam)

This subroutine calculates body loads.

ccno(23)

subroutine stif4d(m,mt,qk,q,sige,dsige,xe,ye,sm4d,istop)

This subroutine calculates the stiffness matrix for

a 4 noded drained element.

ccno(24)

subroutine dmatd(m,mt,d,sige,dsige,sm4d,et,bt,sr)

This subroutine calls the appropriate soil model

and determines the stress for nonlinear analysis

for drained materials.

ccno(25)

subroutine dmatdh(m,mt,d,sstr,sm4d,et,bt,sr)

This subroutine calculates the d matrix

using the hyperbolic model for drained materials.

ccno(26)

subroutine stif4c(m,mt,qk,q,sige,dsige,xe,ye,sm4c,pw,istop)

This subroutine calculates the stiffness matrix for

a 4 noded saturated element.

ccno(27)

subroutine dmatc(m,mt,d,sige,dsige,sm4c,et,bt,sr,xkw,comp,sat

*,coef)

This subroutine calls the appropriate soil model

and determines the stress for nonlinear analysis

for saturated materials.

ccno(28)

subroutine dmatch(m,mt,d,sstr,sm4c,et,bt,sr,xkw,comp,sat,coef)

This subroutine calculates the d matrix

using the hyperbolic model for drained materials.

ccno(29)

subroutine perm(permws,xkw,coef,rw,tvisc,ev,vide,tt,pp)

This subroutine calculates the water permeability.

ccno(30)

subroutine stif4u(m,mt,qstif,q,sige,dsige,xe,ye,sm4u,pw,pa,

istop)

This subroutine calculates the stiffness matrix for

a 4 noded unsaturated element.

ccno(31)

subroutine dmatu(m,mt,d,dfs,ds,sige,dsige,sm4u,bt,et,permwu,
*xka,g1,g2,xm1,ev,sat,sr)

This subroutine calls the appropriate soil model and determines the stress for nonlinear analysis of unsaturated materials.

ccno(32)

subroutine dmatuh(m,mt,d,dfs,ds,sstr,sm4u,bt,et,permwu,xka,
*g1,g2,xm1,ev,sat,sr)

This subroutine calculates the d matrix for unsaturated soil using the hyperbolic model and also suction matrix.

ccno(33)

subroutine statevt(sy,tt,suc,a,b,c,d,ct,xm,sigb,ev,bt,
*xm1,xmt,s1,s3,ten,tamb)

This subroutine calculates the void ratio, bulk modulus and suction modulus from the new thermal void ratio state surface.

ccno(34)

subroutine statest(sy,tt,suc,a,b,c,d,sat,g1,g2,g3,tamb)

This subroutine calculates the saturation and gradients.

ccno(35)

subroutine perwt(a,sat,sru,al,ev,pm,tt,tamb,pp,rw,xkw)

This subroutine calculates the water permeability.

ccno(36)

subroutine pergt(b,sat,sru,bet,xmu,ev,pm,xkg)

This subroutine calculates the air permeability.

ccno(37)

subroutine strent(c,phi,s1,s3,sm,suc,sucm,succ,

*sucp1,sucp2,smax,tt)

This subroutine calculates the strength.

ccno(38)

subroutine condt(ev,sat,tlans,tlanw,tlana,tlan,hfg,tt,pg,rw

*,rv,rmix,drv0,rv0,humr,rg,crg,dov,dtv,dow,dtw,tamb,xkg,xkw,cps

*,cpw,cpv,cpg,betpg,alsr,alp,altt,cktt,cktw,cktg,fxt,cf4,cf5

*,cf6)

This subroutine calculates the heat conductivity, Dtv

and Dov, Dtw and Dow.

ccno(39)

subroutine solve(a,c,b,na,neq,isolv)

This subroutine solves for the global displacements and

pore pressures.

skyline solver for symmetric matrix (isolv=1)

skyline solver for unsymmetric matrix (isolv=3)

ccno(40)

subroutine stress(ie4d,ie4c,ie4u,id,x,sm4d,sm4c,sm4u,

*sig4d,sig4c,sig4u,dsig4d,dsig4c,dsig4u,r,rr,di,dt)

This subroutine calculates stress in the element.

ccno(41)

subroutine princp(sx,sy,sxy,s1,s3,theta)

This subroutine calculates principal stresses.

ccno(42)

subroutine str4nd(m,mt,xe,ye,du,sm4d,sige,dsige)

This subroutine calculates the stresses for drained elements at the centroid.

ccno(43)

subroutine str4nc(m,mt,xe,ye,du,sm4c,sige,dsige,pw,dpw)

This subroutine calculates the stresses for saturated elements at the centroid.

ccno(44)

subroutine str4nu(m,mt,xe,ye,du,sm4u,sige,dsige,pw,pa,dpw,dpa)

This subroutine calculates the stresses for unsaturated elements at the centroid.

ccno(45)

subroutine update(ie4d,ie4c,ie4u,id,iconst,sig4d,sig4c,sig4u,
*dsig4d,dsig4c,dsig4u,r,rr,di,dt)

This subroutine updates the displacements, stresses and pore pressures at the end of each time step.

ccno(46)

subroutine varup(i,mt,sm4c,ics,ingp,ncode,varpmc,pe,qt,
*pc0,psc,evs,evd,pc,pp,dgama1,dgama2,pinv0c)

This subroutine determines the current stress state at the end of the current increment.

ccno(47)

subroutine output(ie4d,ie4c,ie4u,id,x,sm4d,sm4c,sm4u,

*sig4d,sig4c,sig4u,dt,iact)

This subroutine prints out results of each

load step.

ccno(48)

subroutine rread(a,l5,l6,l17,l14)

This subroutine reads data for restart analysis(init=0).

ccno(49)

subroutine wwrite(a,l5,l6,l17,l23,l24)

This subroutine writes data for restart analysis.

ccno(50)

subroutine rread1(a,l23,l24)

This subroutine reads data for restart analysis.

ccno(51)

subroutine caldi(r,di)

This subroutine stores displacements and pore pressures in vector di.

ccno(52)

subroutine General_Climate_Data(surfacElemNo,evaporl

*,total_evap_length)

This subroutine calculates total length of evaporation surface.

ccno(53)

subroutine Calculate_Evap(csuction,ctemper,evaporlen,

*slpotOne,starQ,windNday,pvair,rhair,airtemperature,

*currentevap)

This subroutine calculates evaporation using suction, temperature

and atmospheric data.

ccno(54)

subroutine EVAP_FLUX (csuction, ctemper,slpotOne,starQ,

*windNday,pvair,rhair,airtemperature,evaporlen,VFLUX)

This subroutine calculates the surface flux and the potential evaporation based on suction and temperature.

ccno(55)

subroutine SET_INITIAL_SETTINGS(currentime,specif,DAYLENGth,

*TEMPeratureAIR,RHAIR,SLPOT,PVAIR,STARq)

This subroutine calculates the air temperature, the air relative humidity, the slope of the saturated vapor pressure function, and the net radiation, and saves the starting suctions and temperatures for the current time step.

ccno(56)

function Calc_AirRH(DayLeng,TimeScnds)

This function calculates a sin distribution for relative humidity.

ccno(57)

function Calc_RH(Suction,Temperature)

This function calculates Relative Humidity for given suction (kPa) and temperature (k).

ccno(58)

function Calc_AIRTemp(DayLeng,Timescnds)

This function calculates a sin distribution for temperature.

ccno(59)

function Calc_DAYLENG(N)

This function calculates the time (HR) of the DAYLENG.

ccno(60)

function Calc_NETRAD(Dayleng)

This function calculates a sin distribution for net radiation.

ccno(61)

function Calc_SatVp(Temp)

This function calculates the saturated vapor pressure given the temperature in Kelvin.

ccno(62)

function Calc_SoilTemp(TheWind,TheSpecified,minimumtemp)

This function calculates the soil temperature to be applied to the top node.

ccno(63)

function Calc_Vflux(RhSoil,slpotOne,starQ,windNday,pvair,rhair,
*airtemperature)

This function calculates the vertical flux to be applied to the top node.

ccno(64)

function Calc_Vfluxpen(rh1,slpotOne,starQ,windNday,pvair,rhair,
*airtemperature)

This function calculates the potential evaporation at the top Node.

SEYED MORTEZA MOUSAVI

HIGHLIGHTS OF QUALIFICATIONS

- 25 years experience in research
- 12 Years experience in teaching

SUMMARY OF ACCOMPLISHMENTS

RESEARCH, ANALYTICAL & DESIGN SKILLS

- Completed an interdisciplinary Ph.D. Thesis on Land Subsidence due to Groundwater Withdrawal (in the field of water resources, Groundwater, and Geotechnics)
- Developed an axisymmetric numerical finite element model to estimate land subsidence due to groundwater withdrawal using new concepts of unsaturated soil mechanics
- Planned and installed Global Positioning System (GPS) stations as a field work and analyzed land subsidence using the results of two monitoring
- Developing a 2-D numerical model for Thermo-Hydro-Mechanical (THM) analysis of soil covers used for waste management and protection of environment in Environmental Geotechnics

TEACHING SKILLS

- Taught Statics, Geotechnics, Groundwater Hydrology, Advanced Groundwater, Numerical methods
- instructed lab experiments in hydraulics laboratory

MANAGEMENT SKILLS

- Managed a Coastal Engineering Section in a research institute
- Headed a team of six engineers to develop a Coastal Engineering Dictionary
- Supervised some construction projects as a senior civil engineer
- Managed the central office of a consultant and construction company

COMPUTER SKILLS

- knowledge of software programs (MICROSOFT OFFICE, SAP90, MATHEMATICA, FESOL, BESOL, UDAM, USUB, SEEP/W, SOILCOVER,VADOSE/W, θ-Stock)
- Knowledge of numerical methods (FINITE ELEMENT)
  Knowledge of programming language (FORTRAN)

WORK EXPERIENCE

- **Assistant Professor** **2008-present**
  Department of Civil Engineering, KN Toosi University of Technology, Tehran, Iran
- **Research Associate** **2000-2005**
  Geotechnical Research Centre, Department of Civil and Environmental Engineering
  Western University, London, ON
- **Postdoctoral fellow** **1999 -2000**
  Geotechnical Research Centre, Department of Civil and Environmental Engineering
  Western University, London, ON
- **Ph. D. student** **1992 - 1999**
  Civil Engineering Department, Sharif University of Technology, Tehran, Iran
- **Manager and Supervisor** **1992 - 1996**
  Niktaraz Consultant Engineering Company, Tehran, Iran
- **Teaching Assistant** **1990 - 1999**
  Civil Engineering Department, Sharif University of Technology, Tehran, Iran

EDUCATION

- **Ph.D. Degree** in Civil Engineering (Water Resources) **1999**
  Sharif University of Technology, Tehran, Iran
- **M. A. Sc.** in Civil Engineering (Hydraulic structures) **1991**
  Sharif University of Technology
- **B. A. Sc.** In Civil Engineering **1986**
  Sharif University of Technology

HONOURS

- One of the two students having the highest rank in Iran in the examination for selection of the best M.Sc. graduates for Ph.D. studies (Civil Eng., Water Resources) at Sharif University of Technology, Tehran, Iran, 1993.

- The 14th rank in Iranian National Board for M. A. Sc. At Civil Engineering (Hydraulic Structures), Feb. 1989.

REFERENCES AVAILABLE UPON REQUEST

SEYED MORTEZA MOUSAVI

PUBLICATIONS

1. Ernest K. Yanful, S. Morteza Mousavi, Lin-Pei De Souza. **"A numerical study of soil cover performance"**, Journal of Environmental Management, 81 (2006) pp. 72–92.

2. Ernest K. Yanful, S. Morteza Mousavi, and Mingdi Yang. **"Modeling and measurement of evaporation in moisture retaining soil covers"**, Advances in Environmental research, 7 (2003) pp.783-801.

3. Ernest K. Yanful, and S. Morteza Mousavi, **"Estimating falling rate evaporation from finite soil columns"**, The Science of the Total Environment, 313 (2003) pp.141-152.

4. E K Yanful, and S. M Mousavi, **"Quantifying Evaporation From Soils Using Experimental and Mathematical Methods",** Proceedings of 6th International Conference ICARD, Australia, 2003, 1185-1193.

5. S. Morteza Mousavi, Abolfazl Shamsai, M. Hesham El Naggar, and Mashaallah Khamehchian. **"A GPS-based monitoring program of land subsidence due to groundwater withdrawal in Iran",** Canadian Journal of Civil Engineering, 28 (2001) pp.452-464.

6. S. Morteza Mousavi, Behrouz Gatmiri, Ali Pak, M. Hesham El Naggar, "Analysis of land subsidence due to groundwater withdrawal considering unsaturated layers", **Proceedings of 53rd Canadian Geotechnical Conference, Montreal, Quebec, Oct. 15-18, 2000, Vol. 2, 1153-1160.**

7. S. Morteza Mousavi, M Hesham El Naggar, and Abolfazl Shamsai, **"Application of GPS to evaluate land subsidence in Iran",** Proceedings of The Sixth International Symposium on Land Subsidence", Ravenna, Italy, September 2000, pp. 107-112.

8. S. Morteza Mousavi, M Hesham El Naggar, Abolfazl Shamsai, **"Evaluation of land subsidence using GPS",** 28th Annual Conference of Canadian Society for Civil Engineering, London, Canada, June 2000, pp. 440-447.

9. S. Morteza Musavi, Abolfazl Shamsai, Mashalah Khamehchian, **"Land Subsidence in Rafsanjan Plain, Iran",** Proceedings of Eighth International Congress, International Association for Engineering Geology and Environment, Vancouver, Canada, 1999, pp. 2395-2400.

10. S. Morteza Musavi, Abolfazl Shamsai, Mashalah Khamehchian,

"Land Subsidence Due to Ground Water Withdrawal in Rafsanjan, Iran", IWRE Symposium on Ground Water, The University of Memphis, USA, 1998, (Accepted for presentation)